Title
Identifying Novel Molecular Biomarkers and Therapeutic Targets for Prostate Cancer

Author
Shenoy, Tanushree

Publication Date
2017

Peer reviewed|Thesis/dissertation

UNIVERSITY OF CALIFORNIA

Los Angeles

Identifying Novel Molecular Biomarkers and Therapeutic Targets for Prostate Cancer

A dissertation submitted in partial satisfaction of the requirements for the degree Doctor of Philosophy in Molecular and Medical Pharmacology

by

Tanushree Ravi Shenoy

2017

ABSTRACT OF THE DISSERTATION

Identifying Novel Molecular Biomarkers and Therapeutic Targets for Prostate Cancer

by

Tanushree Ravi Shenoy

Doctor of Philosophy in Molecular and Medical Pharmacology

University of California, Los Angeles, 2017

Professor Owen N Witte, Co-Chair

Professor Hong Wu, Co-Chair

Prostate cancer is the most common malignancy in males, and the third leading cause of male cancer-related death in the Western world. Although most prostate cancers are diagnosed at an early and treatable stages, predicting the outcome of prostate cancer progression and treatment has proven to be challenging because of the heterogeneous nature of the disease. Recent cancer genome studies have identified novel alterations as well as the potential actionable targets. Among these novel alterations is chromodomain helicase DNA-binding protein 1 (CHD1).

CHD1 deletion occurs in as many as 20% of prostate cancers and may be associated with genomic instability. To validate the function of CHD1 in prostate cancer *in vivo*, we created the *Pb-Cre*$^{+}$*;Chd1*$^{L/L}$ mouse model, whereby *Chd1* is deleted in mouse prostate epithelial cells, and engineered CHD1-deleted prostate cancer cell lines. We found that while *Chd1* deletion alone does not induce prostate cancer *in vivo,* it confers DNA damage sensitivity and homologous

recombination impairment, making CHD1-deficient cells sensitive to PARP inhibitors and Platinum-based drugs. A metastatic castrate-resistant prostate cancer patient whose tumors had CHD1 deletion was responsive to carboplatin, suggesting that CHD1 status may be a biomarker for PARP inhibitor and platinum treatment responsiveness.

The dissertation of Tanushree Ravi Shenoy is approved.

Siavash K Kurdistani

Caius Gabriel Radu

Robert H Schiestl

Owen N Witte, Committee Co-Chair

Hong Wu, Committee Co-Chair

University of California, Los Angeles

2017

DEDICATION PAGE

For Shyaam, Mom, Dad, and Anoushka

Table of Contents

LIST OF FIGURES

ACKNOWLEDGEMENTS

I would like to thank my mentor, Dr. Hong Wu, for the opportunity to work in her lab. She always challenged me to become a better scientist and pushed me to address the scientific questions that inspired me. She has been a great role model and her guidance has played no small part in my scientific growth and future.

I would like to thank my committee members, Drs. Siavash Kurdistani, Caius Radu, Robert Schiestl, and Owen Witte, whose support and suggestions over the years helped focus my research and contributed to its success.

I would like to thank my labmates and friends, both past and present, for their support and help both scientifically, professionally, and personally.

Chapter 1 contains modified figures from the following articles with permission. Chapter 1, Figure 1 is modified from “The mutational landscape of prostate cancer” published in European Urology. Chapter 1, Figure 2 is modified from “ETS gene fusions in prostate cancer” published in Nature Reviews Urology. Chapter 1, Figure 3 is modified from “Cullin 3^{SPOP} ubiquitin E3 ligase promotes the poly-ubiquitination and degradation of HDAC6” published in Oncotarget. This work is licensed under the Creative Commons Attribution 3.0 Unported License. To view a copy of this license, visit http://creativecommons.org/licenses/by/3.0/ or send a letter to Creative Commons, PO Box 1866, Mountain View, CA 94042, USA. Chapter 1, Figure 5 is modified from “Base Excision Repair, a Pathway Regulated by Posttranslational Modifications” published in Molecular and Cellular Biology. Chapter 1, Figure 6 is modified from “Nucleotide excision repair and cancer” published in the Journal of Molecular Histology. Chapter 1, Figure 7 is modified from “Excision repair invades the territory of mismatch repair” published in Nature Genetics. Chapter 1, Figure 8 is modified from “Regulators of homologous recombination as novel targets for cancer treatment”

published in Frontiers in Genetics. This work is licensed under the Creative Commons Attribution 4.0 International License. To view a copy of this license, visit http://creativecommons.org/licenses/by/4.0/ or send a letter to Creative Commons, PO Box 1866, Mountain View, CA 94042, USA. Chapter 1, Figure 8 is modified from “The Elephant and the Blind Men: Making Sense of PARP Inhibitors in Homologous Recombination Deficient Tumor Cells” published in Frontiers in Oncology. This work is licensed under the Creative Commons Attribution 3.0 Unported License. To view a copy of this license, visit http://creativecommons.org/licenses/by/3.0/ or send a letter to Creative Commons, PO Box 1866, Mountain View, CA 94042, USA. Figure 1, Chapter 9 is modified from “Links between genome integrity and BRCA1 tumor suppression” published in Trends in Biochemical Sciences.

Chapter 2 is a version of “Shenoy, T.R., Boysen, G., Wang, M.Y., Xu, Q.Z., Guo, W., Koh, F.M., Wang, C., Zhang, L.Z., Wang, Y., Gil, V.*, et al.* (2017). CHD1 loss sensitizes prostate cancer to DNA damaging therapy by promoting error-prone double-strand break repair. Annals of Oncology *28*, 1495-1507.” H. Wu and J .de Bono were the PIs. TR Shenoy, G Boysen and H Wu contributed to the concept and design, the writing, reviewing, and revising of the manuscript. TR Shenoy, G Boysen and MY Wang contributed to the development of methodology, analysis and interpretation of the data. TR Shenoy, G Boysen, MY Wang, QZ Xu, W Guo, FM Koh, C Wang, LZ Zhang, Y Wang, V Gil, S Aziz, R Christova, DN Rodrigues, M Crepo, P Rescigno, N Tunariu, R Riisnaes, Z Zafeiriou, P Flohr, W Yuan, E Knight, A Swain, M Ramalho-Santos, and DY Xu contributed to the acquisition of the data.

Appendix A is a version of “Zou, Y.K., Qi, Z., Guo, W., Zhang L., Ruscetti M., Shenoy T.R., Liu N., and Wu H. Co-Targeting the Cell Intrinsic and Microenvironment Pathways of Prostate Cancer by PI3Kα/β/δ Inhibitor BAY 1082439. (Manuscript submitted for publication)” H Wu was

the PI. YK Zou, Z Qi and H Wu contributed to the concept and design, the development of the methodology, and the writing, reviewing, and submitting of the manuscript. YK Zou, Z Qi, W Guo, L Zhang, M Ruscetti, TR Shenoy, and N Liu contributed to the acquisition of the data. YK Zou and Z Qi contributed to the analysis and interpretation of the data.

VITA

Education

University of California-Los Angeles — Dec 2009
B.S., Molecular, Cell, and Developmental Biology
Minor: English

Research Experience

University of California-Los Angeles — Fall 2011—Present
Graduate Student Researcher — Los Angeles, CA

University of California-San Francisco — Feb 2010—Aug 2011
Staff Research Associate — San Francisco, CA
Advisor: Pui-Yan Kwok, M.D., Ph.D.

University of California-Los Angeles — Mar 2009—Dec 2009
Undergraduate Researcher — Los Angeles, CA
Advisor: Volker Hartenstein, Ph.D.

Natera, Inc — Jun 2008—Sep 2008
Researcher — Redwood City, CA

Pharmacofore, Inc — Jun 2008—Sep 2008
Researcher — Redwood City, CA

Aravasc Inc/Molecular Medicine Research Institute — Summers 2006, 2007
Researcher — Sunnyvale, CA

Peer-Reviewed Publications

Shenoy, T.R., et al. *CHD1 loss sensitizes prostate cancer to DNA damaging therapy by promoting error-prone double-strand break repair.* Annals of Oncology, 2017. In Press.
Editorial Review: Helleday, T. *CHD1, a new treatment biomarker for recombination deficiency in castration resistant prostate cancer?* Annals of Oncology, 2017. In Press.

Kvale, M.N., et al., *Genotyping Informatics and Quality Control for 100,000 Subjects in the Genetic Epidemiology Research on Adult Health and Aging (GERA) Cohort.* Genetics, 2015. 200(4): p. 1051-1060.

Hoffmann, T.J., et al., *Next generation genome-wide association tool: Design and coverage of a high-throughput European-optimized SNP array.* Genomics, 2011. 98(2): p. 79-89.

Oral Presentations

Prostate Cancer Foundation Young Investigators Working Group Meeting — January 18, 2017
Los Angeles, CA
CHD1 loss sensitizes prostate cancer to DNA damaging therapy by promoting error-prone double-strand break repair.

7th Annual NCI Tumor Microenvironment Junior Investigators Meeting — May 18, 2016
Bethesda, MD
Chd1 loss sensitizes prostate cancer to DNA damaging therapy.

Molecular and Medical Pharmacology Departmental Retreat 2015 — October 30, 2015
Huntington Beach, CA
The role of chromodomain helicase DNA-binding protein 1 (CHD1) in prostate cancer and DNA damage.

Southern California Biomedical Sciences Graduate Student Symposium — October 2, 2015, Los Angeles, CA
The role of chromodomain helicase DNA-binding protein 1 (CHD1) in prostate cancer.

6th Annual Tumor Microenvironment Junior Investigators Meeting — June 24, 2015, Los Angeles, CA
The role of CHD1 deficiency in prostate cancer.

Posters

23rd annual Prostate Cancer Foundation Scientific Retreat — October 28 2016, Carlsbad, CA
CHD1 loss sensitizes prostate cancer to DNA damaging therapy by promoting error-prone double-strand break repair.

Molecular and Medical Pharmacology Departmental Retreat 2014 — November 21, 2014, Huntington Beach, CA
Loss of CHD1 sensitizes cells to DNA damage.

2014 Broad Stem Cell Research Centers Tri-Institutional Retreat — April 15, 2014, Asilomar, CA
Loss of CHD1 contributes to prostate cancer through its role in DNA damage.

Molecular and Medical Pharmacology Departmental Retreat 2012 — November 17, 2012, Huntington Beach, CA
Differential responsiveness of in vivo prostate cancer models to PI3K/mTOR inhibitors.

Abstracts

Schlacher K, Shenoy T, Jasin M, Wu H. *DNA Replication and Repair Crossroads Reveal Distinct Protection Mechanisms by HR and Novel NHEJ Factors*. Environmental and Molecular Mutagenesis. 2013; 54 (Supplement 1): 21-25 September 2013; Monterey, California. Abstract #P23, pg S35.

Professional Memberships

American Association for Cancer Research — 2016-Present

Teaching Experience

University of California-Los Angeles — Spring Quarter 2013, Los Angeles, CA
Teaching Assistant, Introduction to Genetics
Prepared and delivered lectures
Facilitated class discussions
Designed and graded assignments and exams

University Service

University of California-Los Angeles — Dec 2013-Nov 2014, Los Angeles, CA
Graduate Student Representative, Molecular and Medical Pharmacology

Chapter 1: Molecular classifications of prostate cancer and the role of DNA damage repair in prostate cancer

Introduction

Prostate cancer is among the leading causes of cancer-related death for men in the United States (Siegel et al., 2017). Because of regular screenings of prostate specific antigen (PSA) levels in the blood, most men are diagnosed with prostate cancer at an early stage. In this case, many patients will have indolent disease that can either be treated with radical prostatectomy and radiation, or with active surveillance (Choo et al., 2002; Thomsen et al., 2014). While most patients respond to these treatments—or in the case of active surveillance do not progress to aggressive cancer—a subset are either diagnosed at a stage when tumor metastasis has already occurred, the cancer recurs despite initial treatment, or the indolent lesions develop into aggressive cancers. The most effective treatment for the progressive stage of the disease is depletion of androgens via surgical or chemical castration as prostate cancer cells depend on AR signaling for survival and proliferation (Heinlein and Chang, 2004). However, androgen deprivation therapy is not a curative treatment—most patients that initially respond to androgen deprivation therapy the disease eventually develop castrate-resistant prostate cancer (CRPC). The biological heterogeneity seen in prostate tumors—where many patients can live for decades with active surveillance with indolent prostate cancer, while others develop metastatic CRPC and die within a couple years of diagnosis—suggests an underlying genomic diversity.

Several groups in the past five years have published data from large-scale genomic studies with the hope of molecularly classifying tumors in terms of indolence or aggressiveness and to serve as a basis for developing targeted therapies. These studies have generated a large amount of information about the molecular basis of primary and metastatic prostate cancer which were either already well known or previously unknown. Among these studies, the cancer genome atlas (TCGA) characterized primary prostate carcinomas and identified subtypes based on mutations, copy-number alterations, mRNA expression, DNA methylation, and protein expression

(Abeshouse et al., 2015). These subtypes include tumors that contain ERG-, ETV1-, ETV4-, or FLI1-specific gene fusions, SPOP mutations, FOXA1 mutations, and IDH1 mutations.

These studies found that a significant number of both primary and metastatic prostate cancers have alterations in well-studied components of DNA damage repair pathways, such as BRCA1, BRCA2, and ATM (Beltran et al., 2013; Grasso et al., 2012a; Pritchard et al., 2016). These alterations show clinical relevance by conferring increased sensitivity to PARP inhibitors in patients with metastatic CRPC (Mateo et al., 2015a). A subset of patients did not contain alterations in known components of DNA damage response or repair, suggesting alterations either in DDR gene enhancer regions that are not covered by whole exome sequencing or alterations in novel genes with connections to DNA damage response and repair.

Among previously unknown genetic alterations, several studies found that CHD1 homozygous deletion frequently occurs in both primary and metastatic prostate cancer (Berger et al., 2011; Burkhardt et al., 2013a; Gao et al., 2014; Grasso et al., 2012a; Huang et al., 2012; Liu et al., 2012; Taylor et al., 2010a). CHD1 deletion co-occurs SPOP mutation and is mutually exclusive from ERG- and ETS-type translocations (Abeshouse et al., 2015). Additionally, these genomic studies found an association of CHD1 homozygous deletion with genomic instability and high levels of chromosomal rearrangements, suggesting a potential role of CHD1 in DNA repair (Baca et al., 2013a; Liu et al., 2012; Tereshchenko et al., 2014).

While these genomic studies provides a substantial backbone for understanding the molecular determinants important to prostate cancer development, detailed validation must be carried out for their utility in prognosis and treatment. These include (1) characterizing these genetic alterations and their roles in tumorigenesis, (2) determining the molecular impact of co-occurring

subtype-specific genomic alterations, and (3) pin-pointing actionable targets for therapeutic development.

The Molecular Classification of Primary and Castrate-Resistant Prostate Cancer

Population-wide prostate cancer screenings, such as blood testing of PSA levels, allow nearly 90% of prostate cancers to be detected that the clinically localized disease stage (Penney et al., 2013). However, the prognosis of these localized cancers is variable—while most men have indolent cancers that can be cured with first-line therapies such as prostatectomy or radiation, or are better off observed with active surveillance, a subset of men will develop aggressive cancer that leads to metastasis and death. Although several methods of stratification have been established—combining Gleason score, PSA level, and clinical and pathological staging—to distinguish indolent from aggressive prostate cancers, these tools are insufficient to accurately predict disease progression (Cooperberg et al., 2009; D'Amico et al., 1998; Kattan et al., 1998).

To this end, recent studies have created molecular classifications of prostate cancer whereby each group contains its own genomic, expression, and epigenetic diversity (Baca et al., 2013a; Barbieri et al., 2012; Berger et al., 2011; Kaffenberger and Barbieri, 2016; Lapointe et al., 2007; Pflueger et al., 2011; Taylor et al., 2010a; Tomlins et al., 2007; Wang et al., 2011). The main subgroup contains ETS fusions, with TMPRSS2-ERG translocations being the most frequent one. The 3 next frequent subgroups are defined by mutations in SPOP, FOXA1, or IDH1, respectively (Figure 1).

IDH1 mutations in prostate cancer

Isocitrate dehydrogenases (IDH) are a major enzyme component of cellular respiration in the tricarboxylic acid (TCA) cycle. Their main function is to catalyze the conversion of isocitrate to α-ketoglutarate and CO_2, using either NAD+ or NADP+ as their electron receptor (Bhagavan and

Ha, 2011). This class of enzymes is comprised of three subtypes, IDH1, IDH2, and IDH3, which differ in their cellular localization and their electron receptors (Dimitrov et al., 2015). IDH1 predominantly localizes to peroxisomes while IDH2 is mainly found in the mitochondria (Fujii et al., 2016). IDH1 and IDH2 rely on NADP+ as their electron receptor while IDH3, which predominantly localizes to the mitochondrial matrix, relies on NAD+ (Bzymek and Colman, 2007; Zeng et al., 2015).

IDH1 and IDH2 are among the most frequently mutated metabolic genes in cancer, including gliomas, acute myeloid leukemia (AML), thyroid carcinomas, cartilaginous tumors, intrahepatic cholangiocarcinoma, and prostate cancer (Yang et al., 2012). Within the IDH1 mutant prostate cancer subgroup, studies found that those tumors were SPOP WT, ETS fusion negative, had few genomic alterations, and had higher levels of DNA methylation, similar to AML and glioma. (Ghiam et al 2012, Kang et al, 2009, Hovelson et al 2015, Noushmehr 2010, Mardis 2009, Rohle 2013).

FOXA1 mutations in prostate cancer

Forkhead box A1 (FOXA1), also known as hepatocyte nuclear factor 3α (HNF-3α), regulates gene transcription by binding to the FKHD consensus sequence. It has been termed a pioneering transcription factor because of its ability to remodel compact chromatin, opening it up to allow nuclear hormone receptors such as androgen receptor (AR) and estrogen receptor (ER) to bind to their targets. In addition to its role in prostate tumorigenesis, FOXA1 controls AR-regulated signaling during prostate development—tissue recombination experiments show that *Foxa1*$^{-/-}$ prostatic tissue are deficient in prostate epithelial cell differentiation and have expansion of the surrounding smooth muscle (Gao et al., 2005; Gao et al., 2003).

Several papers have reported that FOXA1 mutations occur in around 3-5% of primary and metastatic tumors (Abeshouse et al., 2015; Barbieri et al., 2012; Grasso et al., 2012a). Most of the mutations found are missense mutations located in either the forkhead domain or C-terminal trans-activating domain and in residues that do not directly interact with DNA (Abeshouse et al., 2015). Currently, the molecular effect of these mutations is unknown. Interestingly, tumors with FOXA1 mutations displayed several similarities to SPOP-mutant tumors and were for the most part mutually exclusive. FOXA1 and SPOP-mutant tumors also had similar levels of DNA methylation and had the highest AR transcriptional activity of all molecular subtypes (Abeshouse et al., 2015).

ETS-type translocations in prostate cancer

ETS-type translocations in prostate cancer, which juxtapose an androgen-sensitive promoter and an ETS transcription factor are found in approximately 50% of prostate cancers (Figure 2) (Tomlins et al., 2005). Because of the high frequency of this class of genetic alterations, ETS-type gene fusions serve as the primary scaffold for creating molecular classifications of primary and metastatic prostate cancers. The majority of this class of genetic alterations involves fusions of the 5' end of the androgen-sensitive transmembrane protease, serine 2 (TMPRSS2) gene with ETS transcription factor family members including ERG, ETV1, ETV4, ETV5, and ELK4 (Rubin, 2012). The most common translocations in this class are TMPRSS2:ERG fusions, which account for approximately 90% of ETS-type translocations(Perner et al., 2006; Pettersson et al., 2012; Tomlins et al., 2009).

TMPRSS2:ETS fusions are considered an early driver of prostate cancer—approximately 20% of high-grade prostate intraepithelial neoplasias (hg-PINs) (Cerveira et al., 2006; Perner et al., 2007). ETS-type translocations have been found to be associated with both aggressive and

indolent disease, suggesting a heterogeneous molecular underpinning within this genetic subtype; however, evidence suggests that TMPRSS2:ETS-positive patients being treated with active surveillance had higher risk of death from prostate cancer (Attard et al., 2008; Demichelis et al., 2007; Pettersson et al., 2012; Tomlins et al., 2009).

In terms of molecular characteristics, ETS-type translocations display a variety of DNA methylation alterations, with about 30% comprising a hypermethylation group specific to ERG fusion-positive tumors (Abeshouse et al., 2015). Importantly, ETS-type translocations are enriched for other important genetic alterations, including PI3K pathway alterations, PTEN deletion, and TP53 alterations (Abeshouse et al., 2015; Taylor et al., 2010a). Furthermore, these translocations are mutually exclusive with SPOP mutations, CHD1 deletions, and FOXA1 mutations (Abeshouse et al., 2015; Barbieri et al., 2012; Blattner et al., 2014).

SPOP mutations in prostate cancer

Mutations of the Speckle-Type POZ Protein (SPOP) gene are the most common point mutations in prostate cancer, occurring in up to 15% of both primary and metastatic malignancies (Abeshouse et al., 2015; Barbieri et al., 2012; Blattner et al., 2014). The SPOP gene encodes the substrate-binding unit of a Cullin-based E3 ubiquitin ligase, and point mutations of the SPOP protein result in impaired proteasomal degradation of SPOP substrates (Zhuang et al., 2009).

E3 ubiquitin ligases selectively bind to a diverse set of substrates, targeting them for ubiquitination and subsequent proteasomal degradation. SPOP belongs to the largest subfamily of E3 ligases—Cullin-RING ligases (Zhuang et al., 2009). These multi-subunit enzymes are divided into 8 different subfamilies, each containing a different subunit—CUL1, CUL2, CUL3, CUL4A, CUL4B, CUL5, CUL7, and CUL9 (Duan and Pagano, 2015). These Cullin subunits function as a scaffold for substrate receptors. SPOP serves as a substrate receptor for CUL3, and contains two

domains—a C-terminal BTB (broad complex, tramtrack, bric-a-brac) domain which interacts with Cul3, and an N-terminal Meprin and TRAF Homology (MATH) domain that interacts with substrates (Zhuang et al., 2009).

Studies so far have found that most SPOP mutations prevalent in prostate cancer structurally affect the substrate-binding MATH domain, suggesting that SPOP's role in substrate recognition and proteasomal degradation serves as an important tumor suppression function (Figure 3) (Duan and Pagano, 2015). This notion is substantiated by more recent studies indicating several SPOP substrates that are well known to be involved in prostate cancer pathogenesis, including ERG and AR proteins (An et al., 2015; An et al., 2014; Gan et al., 2015). In the case of AR, wild-type SPOP recognizes a ser/thr-rich degron on the hinge domain of AR, resulting in the degradation of AR and inhibition of AR-regulated gene transcription. In cells with SPOP mutation or AR splice variants, AR degradation was inhibited (An et al., 2014). In addition to the indirect effect that SPOP has on ERG expression via its control of AR protein stability, SPOP can also directly interact with and promote the degradation of ERG proteins. Two studies so far have indicated that mutations of SPOP or fusions of ERG with other genes such as TMPRSS2 impaired their interaction and the subsequent degradation of ERG protein (An et al., 2015; Gan et al., 2015).

Interestingly, the SPOP-mutant subclass was found to be mutually exclusive with ETS-type translocations as well as with genomic alterations in the PI3K pathways (Abeshouse et al., 2015; Barbieri et al., 2012; Blattner et al., 2014). The functional overlap of TMPRSS2-ERG translocations and SPOP mutations in terms of their effect on ERG protein stability may in part explain why these two genomic aberrations are mutually exclusive. The mutual exclusivity seen between SPOP mutations and PI3K/mTOR pathway alterations may also be due to overlapping functions in tumorigenesis. SPOP mutation results in the coordinate activation of the PI3K/mTOR

pathway and upregulation of a network of AR-associated transcription factors and co-activators independent of the genomic status of AR or PI3K/mTOR pathway components (Blattner et al., 2017).

CHD1 deletions in prostate cancer

While mutually exclusive to ETS-type translocations, the SPOP mutation subclass co-occurs frequently with CHD1 deletion at chromosome 5q21 as well as deletion chromosomes 2q and 6q (Abeshouse et al., 2015; Baca et al., 2013a; Barbieri et al., 2012; Blattner et al., 2014). The SPOP-mutant/CHD1-deleted subtype, in addition to being mutually exclusive with TMPRSS-ERG translocations, is also characterized by increased genomic instability and higher levels in chromosomal rearrangements, indicating a role of either of these proteins in DNA repair (Baca et al., 2013a; Boysen et al., 2015; Liu et al., 2012; Tereshchenko et al., 2014). Indeed, both of these proteins have been implicated in DNA damage response and repair. SPOP has been found to impair homology-directed repair and promote non-homologous end-joining, and increase sensitivity of SPOP mutant cells to DNA damaging agents such as PARP inhibitors (Boysen et al., 2015). CHD1 has also been implicated in DNA repair, whereby loss of CHD1 impairs homologous recombination and increases sensitivity to PARP inhibitors (Kari et al., 2016; Shenoy et al., 2017). Kari et al indicated that loss of CHD1 inhibits the recruitment of CtIP, a protein needed for end resection of double stranded breaks, to DNA, thereby inhibiting homologous recombination repair (Kari et al., 2016). A study by our group suggests a similar impairment of homologous recombination, but through the increased proficiency of non-homologous end-joining promoted by increased levels of 53BP1 (Figure 4) (Shenoy et al., 2017). Overall, these data suggest that SPOP-mutation and CHD1 deletion may serve as clinically relevant biomarkers for PARP inhibitor and DNA damage sensitivity in their subclass of prostate cancers. Ongoing studies

are being performed to evaluate the robustness of SPOP mutations and CHD1 deletions in prostate cancers as biomarkers for PARP inhibitor sensitivity.

In addition to sharing a role in DNA damage response and repair, SPOP and CHD1 have both been shown to share a role in altering AR transcriptional output. As described earlier, the SPOP mutant subclass of prostate cancers has higher levels of AR transcriptional signaling, and SPOP mutation has been shown to result in increased AR signaling because of impaired degradation of AR (Abeshouse et al., 2015; An et al., 2014). In addition, SPOP mutation decouples AR signaling and PI3K/mTOR signaling, resulting in a coordinate increase in both signaling pathways. Previous studies indicate that CHD1 regulates AR transcriptional signaling by mediating the binding of AR to its target promoters (Burkhardt et al., 2013a; Metzger et al., 2016a). However, our group's data indicate that loss of CHD1 does not affect AR or AR transcriptional output (Shenoy et al., 2017). One explanation for this contradictory data is that CHD1 only affects AR recruitment in the context of other genetic or signaling pathway alterations, although studies have to be performed to confirm this hypothesis.

While several studies have investigated the role of SPOP mutation and CHD1 deletion alone in prostate cancer, there have been no studies published so far that analyze the collaboration of CHD1 and SPOP mutation together in prostate cancer initiation and progression. However, several studies have been performed indicating the role that CHD1 plays in the context of other genomic alterations. Coordinate loss of CHD1 and MAP3K7 promotes prostate cancer progression by altering prostatic differentiation and a loss of E-cadherin (Rodrigues et al., 2015). In addition, tumor cells with PTEN deficiency enhances the stabilization of CHD1, which binds to H3K4me3 to activate the transcription of the pro-tumorigenic TNF-NF-κB transcriptional program; co-deletion of PTEN and CHD1 causes synthetic lethality in these cells (Zhao et al., 2017). In

addition, our group's preliminary data shows that prostate-specific deletion of *Pten* and *Chd1* leads to increased cell death compared to prostates with *Pten* deletion alone. However, kinetic analysis in compound mutant prostates indicates increase prostate tumor by 10 weeks of age, with large amounts of cell death beginning to occur by 6 months of age. This enhanced synthetic lethality seen in CHD1 and PTEN co-deleted cells substantiates genomic data indicating an enrichment of PTEN deletions in ETS translocation positive cells, which are mutually exclusive with SPOP mutations and CHD1 deletions (Abeshouse et al., 2015; Taylor et al., 2010a). In addition, our data along with other studies suggest both cell-intrinsic and cell-extrinsic or immune-based mechanisms of synthetic lethality *in vivo*. Future directions in our lab include investigating the mechanism of cell-extrinsic cell death in compound mutant cells, as well as analysis the interaction of cell-intrinsic and cell-extrinsic mechanism of cell death.

Molecular investigations of CHD1 function have found that it's a highly conserved chromatin remodeler that contains a SNF2-related ATPase/helicase domain and an additional C-terminal DNA-binding domain (Marfella and Imbalzano, 2007). It regulates chromatin assembly and active transcription by binding to H3K4me3 and other elongation (Simic et al., 2003b; Sims et al., 2005; Stokes et al., 1996) factors. Interestingly, KMT2C, the histone lysine transferase responsible for H3K4 methylation, is also mutated in 4% and 12% of primary and metastatic castration resistant prostate cancer samples, respectively (Robinson et al., 2015) (Abeshouse et al., 2015), suggesting that chromatin modifiers may indeed be involved in prostate cancer development. In addition, CHD1 has also been shown to play a role in regulating DNA replication and pre-mRNA splicing (Biswas et al., 2008; Sims et al., 2005). Loss of CHD1 leads to increased heterochromatin formation in murine embryonic stem cells and to embryonic lethality (Gaspar-Maia et al., 2009; Guzman-Ayala et al., 2015).

Other members of the CHD family have been reported to play important roles in both the DNA damage response and in cancer pathogenesis. ATM-dependent KAP1 phosphorylation can interfere with CHD3-KAP1 interaction and trigger heterochomatin decondensation and allow DNA repair (Sulli et al., 2012). CHD4 loss has been found to sensitize cells to IR-induced DSBs and reduced efficiency of DNA repair via HR (Larsen et al., 2010; Polo et al., 2010), and CHD4 depletion sensitizes breast cancer cells to PARP inhibition (Pan et al., 2012). CHD5 is also known to be a tumor suppressor that controls cell proliferation, apoptosis, and senescence via the p19(Arf)/p53 pathway (Bagchi et al., 2007). CHD2, the closest relative to CHD1, was found to be a tumor suppressor whose haploinsufficiency results in lymphomas (Nagarajan et al., 2009). Mouse embryonic fibroblasts derived from *Chd2*$^{-/-}$ mice displayed higher basal levels of DSBs and an inability to resolve DSBs after IR (Nagarajan et al., 2009). However, the molecular mechanisms underlying CHD1 and CHD2 function in DSB repair may be different. A recent study demonstrated that CHD2 is required for PARP1-mediated chromatin expansion and recruitment of NHEJ components to the damage loci while CHD2 loss influences NHEJ without affecting HR (Luijsterburg et al., 2016), which contrasts our results showing that CHD1 complexes with NHEJ components and modulates 53BP1 degradation.

While structurally similar, several lines of evidences suggest that CHD1 and CHD2 may play different roles in modulating chromatin structure and DNA damage response. Studying genome-wide nucleosome specificity and function of CHD family in mESC demonstrates that mammalian CHD1 and CHD2 have very different distributions: while CHD2 is similar to yeast Chd1 whose associated nucleosomes are enriched in entire transcript and correlate with H3K36me3, CHD1 is highly enriched near the 5' ends of genes and only enriched at the H3K4me3 class (de Dieuleveult et al., 2016). While *CHD2* alterations were found in approximately 1-2% of primary and metastatic adenocarcinomas, both *CHD1* and H3K4 methyltransferases, such as *KMT2C* and *KMT2D*, are

more commonly mutated in primary and mCRPC samples (Abeshouse et al., 2015; Robinson et al., 2015), underlying the role of *CHD1* as prostate-specific tumor suppressor. This tissue-specific role is also highlighted by previous studies, suggesting that these two proteins may perform distinct functions in DNA damage response, chromatin remodeling, and transcriptional activation in non-prostate backgrounds (de Dieuleveult et al., 2016; Luijsterburg et al., 2016; Siggens et al., 2015).

DNA Damage Repair in Cancer

Almost 20 years ago Hanahan and Weinberg published the seminal “Hallmarks of Cancer” paper, in which they proposed 6 key cellular processes that characterize cancerous cells—the ability to sustain proliferation, to evade growth suppressors, resist cell death, induce angiogenesis, enable replicative immortality, and activate invasion and metastasis (Hanahan and Weinberg, 2000). A follow-up 10 years later suggested that the acquisition of these hallmarks were due to an underlying genomic instability in tumor cells (Hanahan and Weinberg, 2011). Under normal circumstances, cells are equipped with extensive mechanisms to protect DNA from damage by environmental agents or spontaneous events that occur in the cell itself (Ciccia and Elledge, 2010). However, tumor cells develop genetic and epigenetic alterations in DNA damage response and repair components, leading to genomic instability that allows these cells to more quickly evolve and adapt to changing tumor environments.

A large number of the alterations found to cause genomic instability in cancers are in genes that promote DNA repair. These genes encode proteins that are involved DNA repair mechanisms, major ones of which are base excision repair (BER), nucleotide excision repair (NER), mismatch repair (MMR), non-homologous end-joining (NHEJ), and homologous recombination (HR). While there is significant heterogeneity in terms of genomic aberrations and the alterations of different

mechanisms of repair in cancer, several examples exist indicating a link between dysfunction in DNA damage repair and tumorigenesis. These mechanisms of DNA damage repair and their dysfunction in cancer will be discussed below.

Base Excision Repair

BER is normally activated at the site of oxidative lesions, alkylation, and single-stranded breaks on DNA (Wallace et al., 2012). During the process of BER, DNA glycosylases identify and remove damaged bases by hydrolysis of the bond that links the base to the phosphate backbone (Markkanen et al., 2015). AP-endonuclease 1 (APE1) then cleaves the backbone, creating a single-stranded break (SSB), which is then repaired by the addition of a newly synthesized DNA molecule by a complex containing DNA polymerase β (POLβ), XRCC1, and DNA Ligase IIIa (Figure 5) (Markkanen et al., 2015).

Alterations in components of the BER pathway have been implicated in tumorigenesis. Haploinsufficiency of XRCC1 increases the development of precancerous lesions in mice treated with carcinogenic substances (McNeill et al., 2011). Increased levels of APE1 were found in prostatic intraepithelial neoplasia (PIN) lesions and cancerous regions of human prostate cancer (Kelley et al., 2001). Elevated levels of POLβ were found in breast, colon, and prostate adenocarcinomas compared to normal tissue (Srivastava et al., 1999). Other studies have indicated that the link between increased levels of POLβ and cancer may be due to the lower fidelity of DNA POLβ compared to the replicative DNA polymerases, resulting in a mutator phenotype (Starcevic et al., 2004) (Canitrot et al., 1998).

Nucleotide Excision Repair

NER is normally activated when larger lesions and bulky adducts, such as those caused by ultraviolet light, are created and thus distort the double helix structure of DNA (Leibeling et al.,

2006). NER is a complex process, in which the lesions is detected by a protein complex containing the XPC, HHR23B, and centrin 2 (de Boer and Hoeijmakers, 2000) (Emmert et al., 2000) (Khan et al., 2000; Khan et al., 2006). This complex then recruits downstream components of NER which incises the single stranded oligonucleotide containing the lesion. This process requires two endonucleases, ERCC1 and XPG (Emmert et al., 2001; Emmert et al., 2002). Finally, the lesion is then removed and replaced with new nucleotides using DNA polymerase δ, ε, or η (Figure 6) (Emmert et al., 2006).

Xeroderma pigmentosum is an autosomal-recessive heritable disease caused by defective genes involved in NER (Lehmann et al., 2011). The main symptoms of xeroderma pigmentosum include increased risk of sunburn and early onset of skin cancers (Lehmann et al., 2011). Additional studies have indicated an accumulation of inactivating mutations in NER genes in prostate cancer (Dietlein et al., 2014).

Mismatch Repair

Mismatch repair occurs when dNTPs are misincorporated because of noncomplementary matching to their base pair during DNA replication (Fukui, 2010). These mismatches distort the double helix structure of DNA and result in the removal of these lesions and the resynthesis of this DNA lesion. The main proteins involved in this process are *MSH1*, *MSH2*, and *MLH1* (Figure 7) (Jiricny, 2006).

Mutations in components of NER can result in an abnormal shortening or lengthening of dinucleotide repeat sequences known as microsatellite instability (Jiricny, 2006). This pattern of genomic instability occurs in around 12% of sporadic colorectal cancers and is caused by epigenetic silencing of the *MLH1* (Boland and Goel, 2010). Another 3% of colorectal cancers display microsatellite instability due to Lynch syndrome, which causes hereditary non-polyposis

colorectal cancer (HNPCC), an inherited disorder resulting from inactivating mutations in NER genes (Jiricny, 2006). Microsatellite instability has also been observed in prostate cancer patients, and men with Lynch syndrome have a higher risk of developing prostate cancer (Nghiem et al., 2016) (Dominguez-Valentin et al., 2016).

Non-homologous End-Joining

NHEJ is one of two main mechanisms used by the cell to resolve DNA double stranded breaks, the other being HR. In contrast to HR, which is generally limited to the S and G2 phases of the cell cycle, NHEJ occurs throughout the cell cycle (Davis and Chen, 2013). The first step in NHEJ is the recognition of the DSB by Ku70 and Ku80, which together form a heterodimer complex. This complex then serves as a scaffold to recruit downstream components of NHEJ such as DNA-PK, which bridge the DNA ends and promote end stability. The complex then recruits the XRCC4-DNA-Ligase IV to mediate ligation of the DSB (Figure 8) (Davis and Chen, 2013).

Genetic studies in mice have indicated the importance of NHEJ components in maintaining genomic stability (Bunting and Nussenzweig, 2013). In addition, mice with knockout of Ku80, XRCC4, or DNA Ligase IV in a p53-deficient background developed pro-B cell lymphomas (Difilippantonio et al., 2000; Nussenzweig et al., 1997) (Frank et al., 2000). Scid mice with knockout of p53 and inactivating mutation of DNA-PK developed lymphomas and leukemias (Guidos et al., 1996). However, next generation sequencing studies of human prostate cancer so far has not identified alterations in components of NHEJ (Abeshouse et al., 2015) (Grasso et al., 2012a).

Homologous Recombination

The other mechanism to repair DNA DSBs HR, which uses the homologous chromatid to serve as a template for repair of the damaged area and thus is restricted to the S and G2 phases of the

cell cycle. Because of the use of a homologous template, HR is generally considered less error-prone compared to NHEJ (Cerbinskaite et al., 2012). In the absence or downregulation of HR due to genetic or epigenetic inactivation of components of this repair pathway, cells either apoptose or compensate with other error-prone mechanisms of repair, such as NHEJ, thus causing genomic instability (Moynahan et al., 2001a; Moynahan et al., 2001b) (Tutt et al., 2001). During this process, one DNA strand of the DSB is resected using the Mre11-Rad50-Nbs1 (MRN) complex. The single stranded overhang is protected from processing by RPA, after which RAD51 is recruited and replaces RPA. This single stranded overhang bound by RAD51 then invades the homologous sequence on a sister chromatid, followed by DNA synthesis strand of the double stranded break, and subsequent resolution of the DSB (Figure 8) (Sung and Klein, 2006).

Several studies have implicated mutation or loss of function of HR genes to neoplasia. BRCA1 and BRCA2 were first identified as responsible for a significant proportion of familial breast cancers (Futreal et al., 1994; Miki et al., 1994; Tavtigian et al., 1996). More recently, alterations in other HR genes, including PALB2, ATM, RAD51C, and RAD51D have been implicated in hereditary forms of breast, ovarian, and pancreatic cancers (Lord and Ashworth, 2012). HR defects are also prevalent in spontaneous cancers, with about 50% of high-grade serous ovarian adenocarcinomas containing somatic and germline alterations in HR genes (Bell et al., 2011). Furthermore, defects in HR genes such as BRCA1, BRCA2, and ATM occur in approximately 20% of castrate resistant prostate cancers (Mateo et al., 2015a).

Targeting DNA Damage Repair Defects in Cancer

Before understanding the biological mechanism underlying the efficacy of platinum salts, clinics have historically used this class of drugs to exploit DNA damage repair defects in ovarian cancer. These drugs cause DNA inter- and intra-strand crosslinks that must be repaired by components

of NER and HR. More recent evidence indicates that because ovarian cancers frequently have defects in HR, platinum salts such as carboplatin and cisplatin cause damage in these tumors that require HR to repair; in tumors with HR defects, these drugs cause synthetic lethality (Lord and Ashworth, 2012; Turner et al., 2004).

More recently, PARP inhibitors are being investigated as targeted therapies that exploit defects in HR in certain cancer types such as breast, ovarian, and prostate cancer. These drugs target PARP1 and PARP2, which are members of the PARP protein superfamily. PARP1 has been well studied to function in BER-based DNA single-stranded break repair. During this process, PARP1 detects and binds single-stranded breaks in DNA, initiating damage response pathways to repair these breaks; when PARP1 is inhibited, single-stranded break repair is inhibited (Figure 9) (Rouleau et al., 2010), (Lord and Ashworth, 2012).

The role of PARP inhibitors as targeted therapies to induce synthetic lethality in tumors with HR deficiencies was in 2005 when it was found that PARP inhibitors could inhibit the growth of cells with defects in the BRCA1 or BRCA2 genes (Farmer et al., 2005) (Bryant et al., 2005). PARP inhibition works on these HR-deficient cells by preventing the repair of single stranded breaks or by inhibiting PARP release from a DNA break. These lesions then cause stalled or collapsed replication forks during S and G2 phases of the cell cycle, which need to be repaired by components of HR. In cells without HR deficiency, the repair of these stalled or collapsed forks is efficient; however, in cells with defects in genes involved in HR, these DNA defects cannot be repaired, and cell death is induced.

The studies investigating synthetic lethality between PARP inhibitors and BRCA1- and BRCA2-deficient cells served as a starting point for more the more recent discovery of several other gene defects that can cause synthetic lethality with PARP inhibitors, most of which are involved in HR.

These genes include RAD51, ATRX, SHFM1, RPA1, NBN, ATR, ATM, CHEK1, CHEK2, miR-182, CDK1, SWI5-SFR1, USP1/UAF1, and several Fanconi anemia proteins (Akamatsu and Jasin, 2010; Johnson et al., 2011; McCabe et al., 2006; Moskwa et al., 2011; Murai et al., 2011; Peasland et al., 2011). These defects have been proven to be clinically relevant where genomic studies found somatic mutations in homologous recombination genes in a significant subset of high-grade serous ovarian carcinoma (Bell et al., 2011), advanced prostate cancer (Mateo et al., 2015a), and pancreatic cancer (Carnevale and Ashworth, 2015; Waddell et al., 2015). In the context of prostate cancer, PARP inhibitor clinical trials have shown that about 30% of metastatic castrate resistant prostate cancer patients showed a response to olaparib, with approximately half of those responders having BRCA2 or ATM defects (Mateo et al., 2015a). In addition, other studies have shown that PARP inhibitor sensitivity can occur in patients with defects in genes previously unknown to be involved in HR. For example, two studies showed that homozygous deletion of CHD1, which is frequently altered in both primary and metastatic prostate cancer, caused deficiency in homologous recombination and synthetic lethality to PARP inhibitors (Kari et al., 2016; Shenoy et al., 2017). In addition, a metastatic castrate resistant prostate cancer patient with homozygous deletion was more sensitive to carboplatin, suggesting potential responsiveness to PARP inhibitors. Further clinical studies are needed to confirm the increased responsiveness of prostate cancer patients with homozygous deletion of CHD1 to PARP inhibitors (Shenoy et al., 2017).

Figure 1

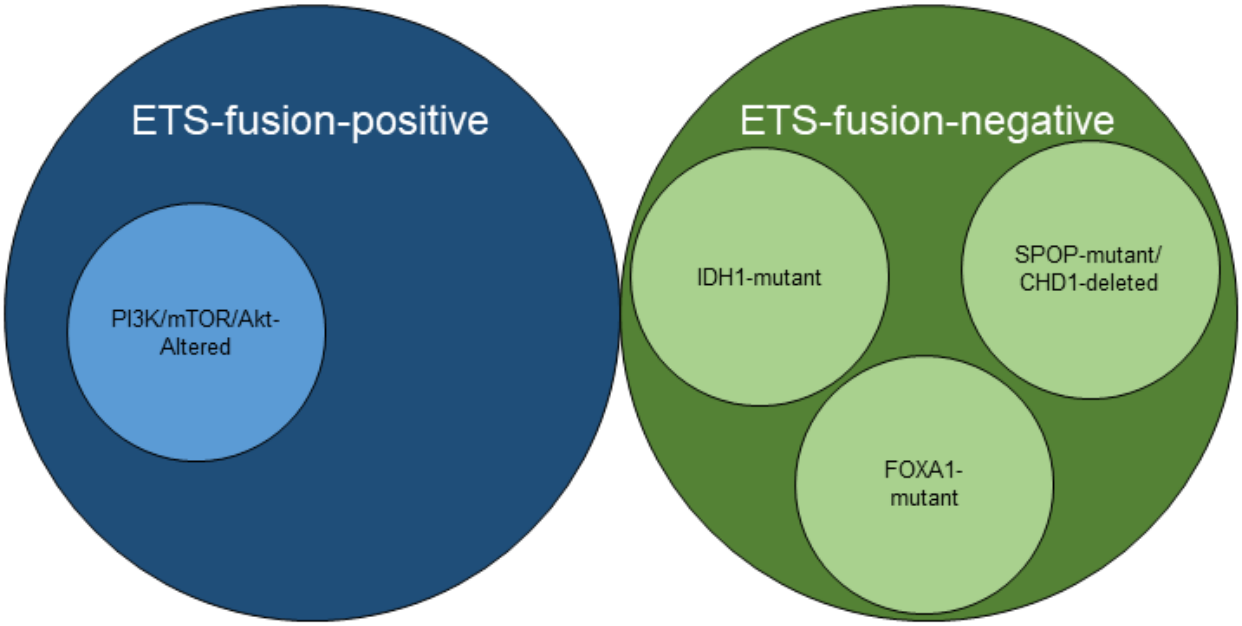

Figure 1. Molecular subclasses of prostate cancer. Prostate cancers can be classified into those with or those without ETS-type fusions.

ETS-fusion-positive cancers (left) are enriched for PI3K/mTOR/AKT pathway alterations. On the other had, ETS-fusion negative cancers (right) are comprised of IDH1-mutant, FOXA1-mutant, and SPOP-mutant/CHD1-deleted cancers. Adapted and modified from (Barbieri et al., 2013) with kind permission from Elesvier Publishing.

Figure 2

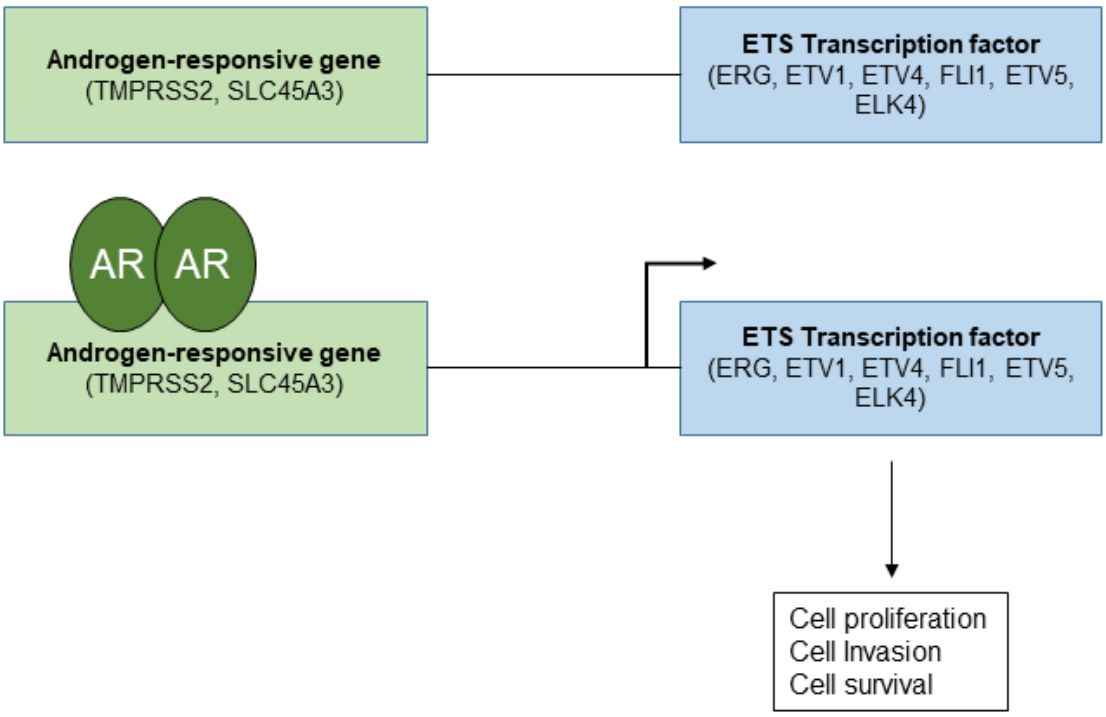

Figure 2. ETS fusions in prostate cancer.

A gene fusion event occurs between AR responsive genes such as TMPRSS2 and SLC45A3, and an ETS transcription factor such as ERG, ETV1, ETV4, ETV5, and ELK4. After this fusion, the 5' promoter of the androgen responsive gene activations the expression of the ETS genes. The overexpression of ETS transcription factors in prostates results in oncogenesis, causing increased proliferation, invasion, and survival in tumors with this fusion. Adapted and modified from (Clark and Cooper, 2009) with kind permission from Nature Publishing Group.

Figure 3

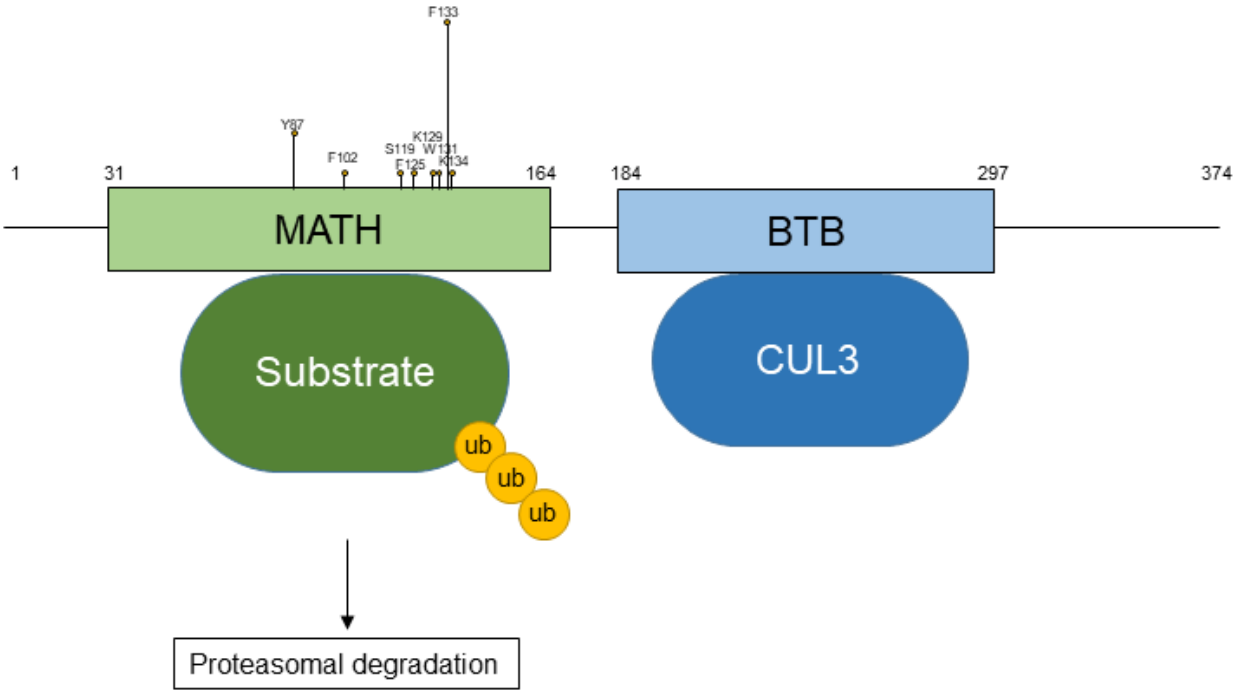

Figure 3. Schematic representation of the SPOP gene.

The distribution of the most common mutations in prostate cancer, and domain binding partners. These recurrent mutations are clustered to the N-terminal MATH domain, which is the substrate-binding domain. Mutations in the MATH domain prevent binding and ubiquitination of its substrate binding partners. Adapted and modified (Tan et al., 2017) under the Creative Commons Attribution 3.0 Unported License.

Figure 4

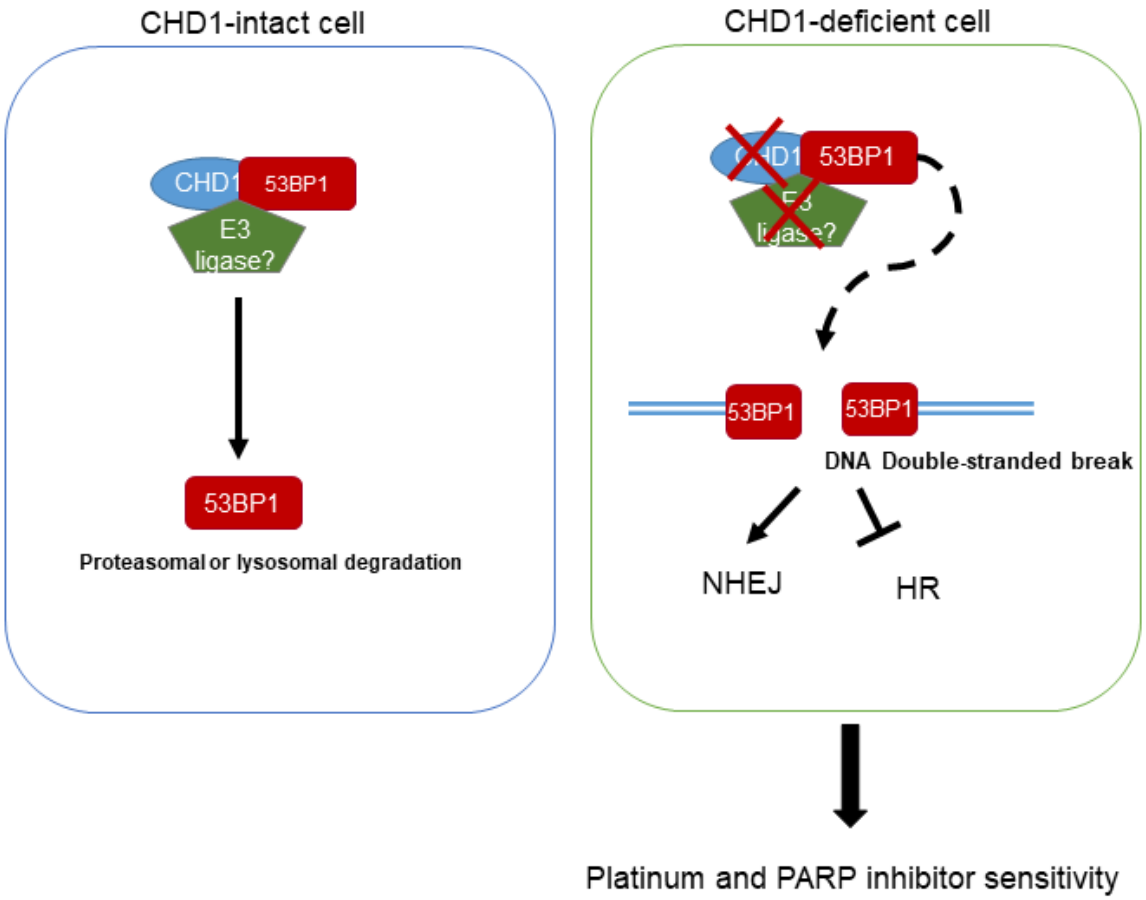

Figure 4. Schematic of CHD1 function in PARP inhibitor sensitivity.

In a CHD1-intact cell, CHD1 and 53BP1 bind, which recruits a yet unknown E3 ligase complex, promoting the degradation of 53BP1. Without CHD1, this E3 ligase isn't recruited, resulting in excess 53BP1. After the induction of double-stranded breaks, there is excess 53BP1 that binds to this damage, which inhibits homologous recombination and promotes non-homologous end-joining. This inhibition of homologous recombination thus causes platinum and PARP inhibitor sensitivity.

Figure 5

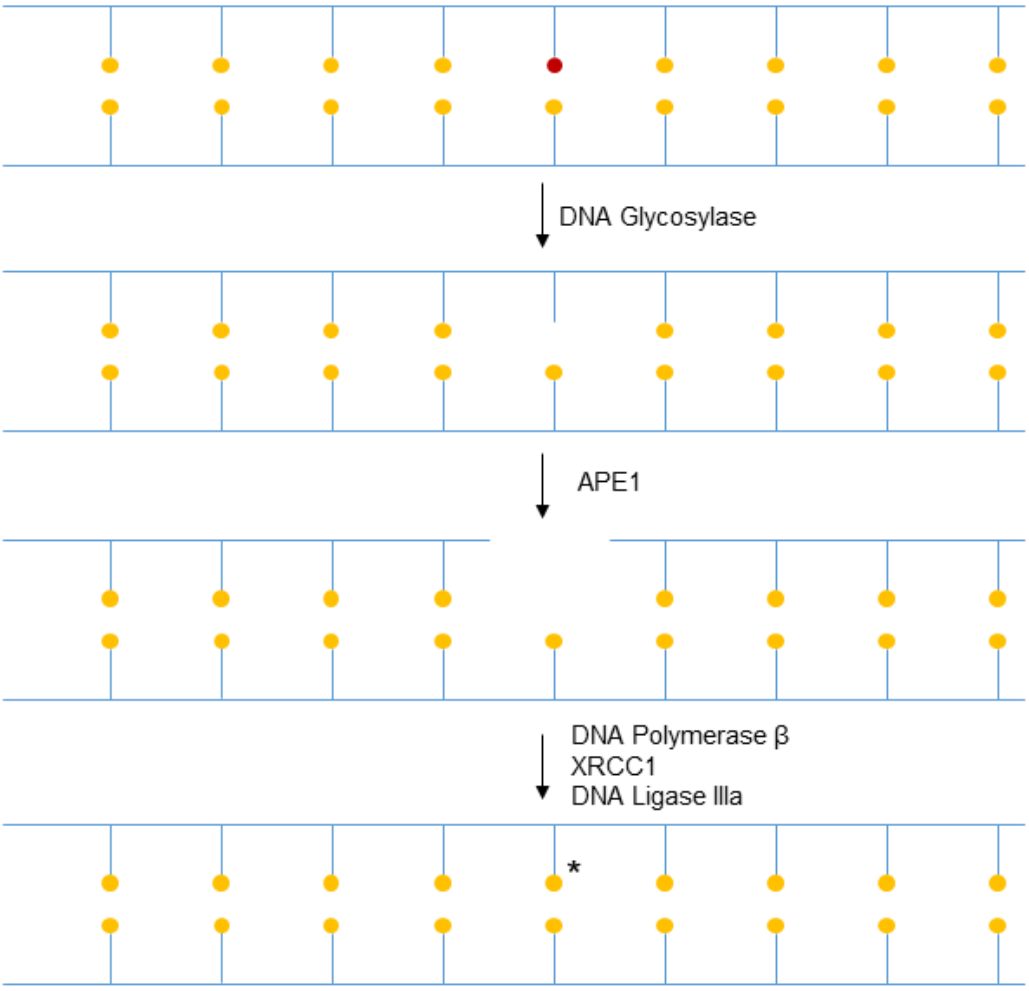

Figure 5. Schematic of the Base Excision Repair Pathway.

During BER, DNA glycosylases identify and remove damaged bases to create an a basic site. This site is the cut by APE1 to create a sing-stranded break. Finally, DNA Pol β adds a single correct nucleotide and the single stranded break is repaired by the XRCC1-DNA Ligase IIIa complex. Adapted and modified from (Carter and Parsons, 2016) with kind permission from the American Society for Microbiology Publishing.

Figure 6

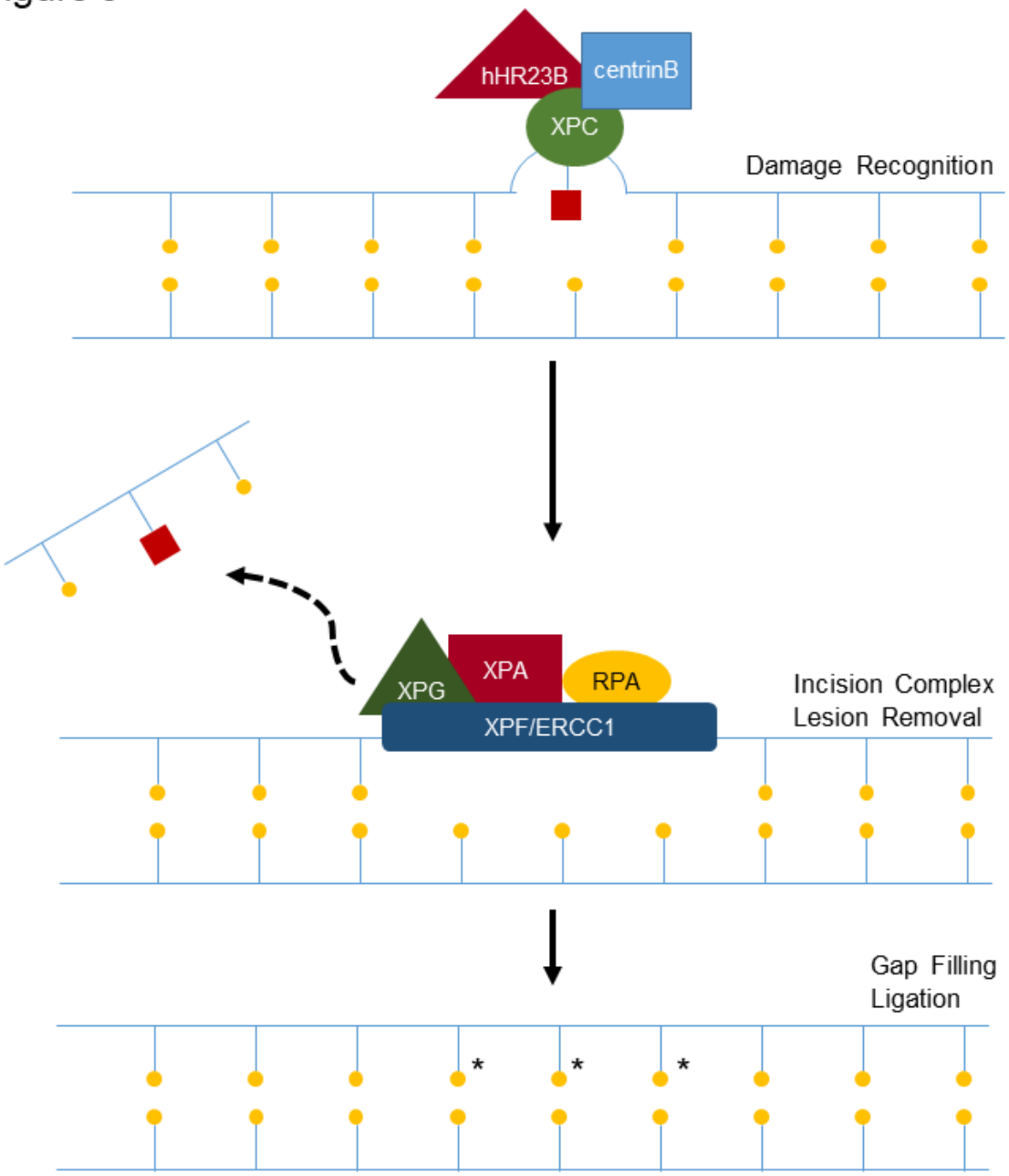

Figure 6. Schematic of the Nucleotide Excision Pathway.

During NER, the XPC/hHR23B/centrin B complex recognizes the DNA lesion. This complex then recruits XPA, RPA, XPG, and XPF/ERCC1, which enables the removal of the damage-containing oligonucleotide. Finally, DNA polymerase δ, ε, or η fills in the gap, and the nick is sealed by DNA

ligase I. Adapted and modified from (Leibeling et al., 2006) with kind permission from Springer Publishing.

Figure 7

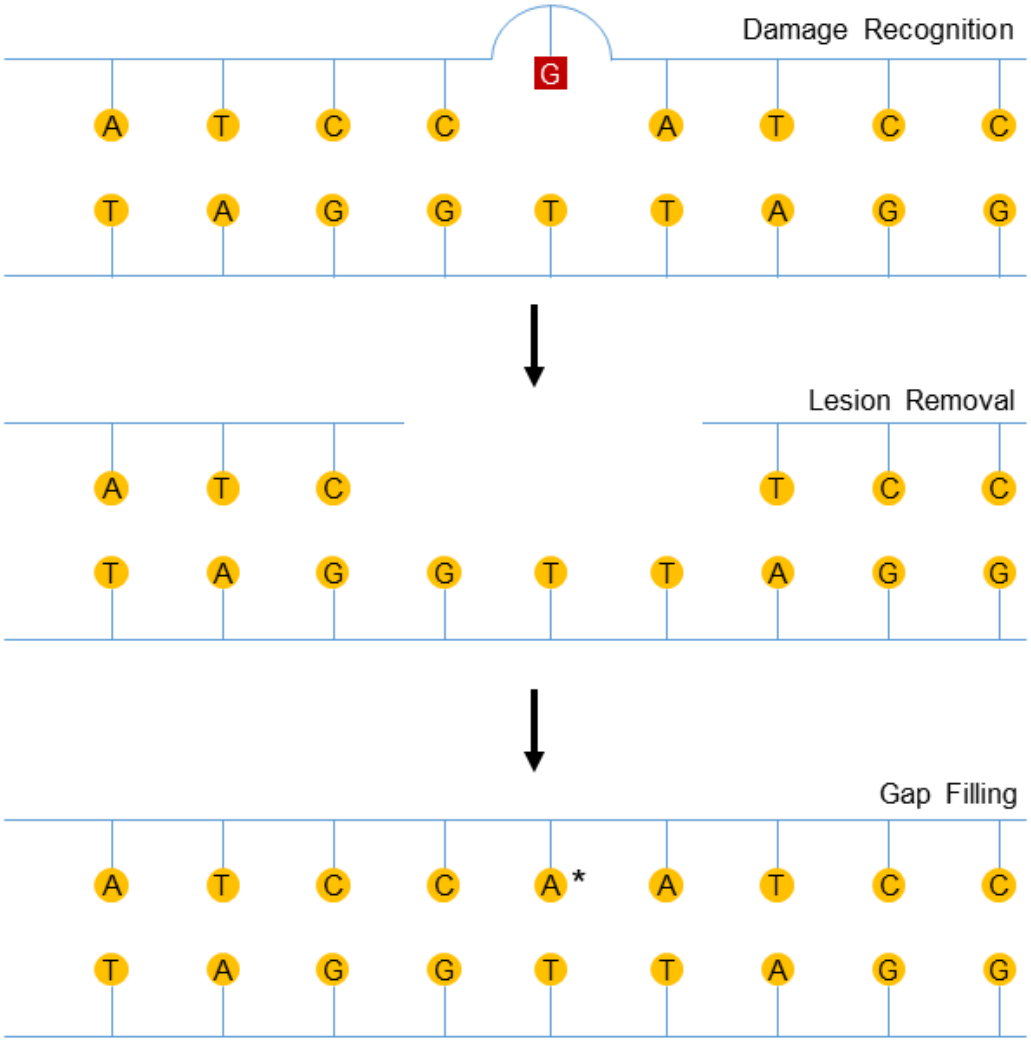

Figure 7. Schematic of the Mismatch Repair Pathway.

Repair occurs when nucleotide base-pairing mistakes occur during DNA replication. This mistake causes a kink in the double helix. During this process, the mismatch is recognized, one DNA oligonucleotide containing the lesion is removed. Finally, the gap is filled by DNA polymerase. Adapted and modified from (Sancar, 1999) with kind permission from Nature Publishing Group.

Figure 9

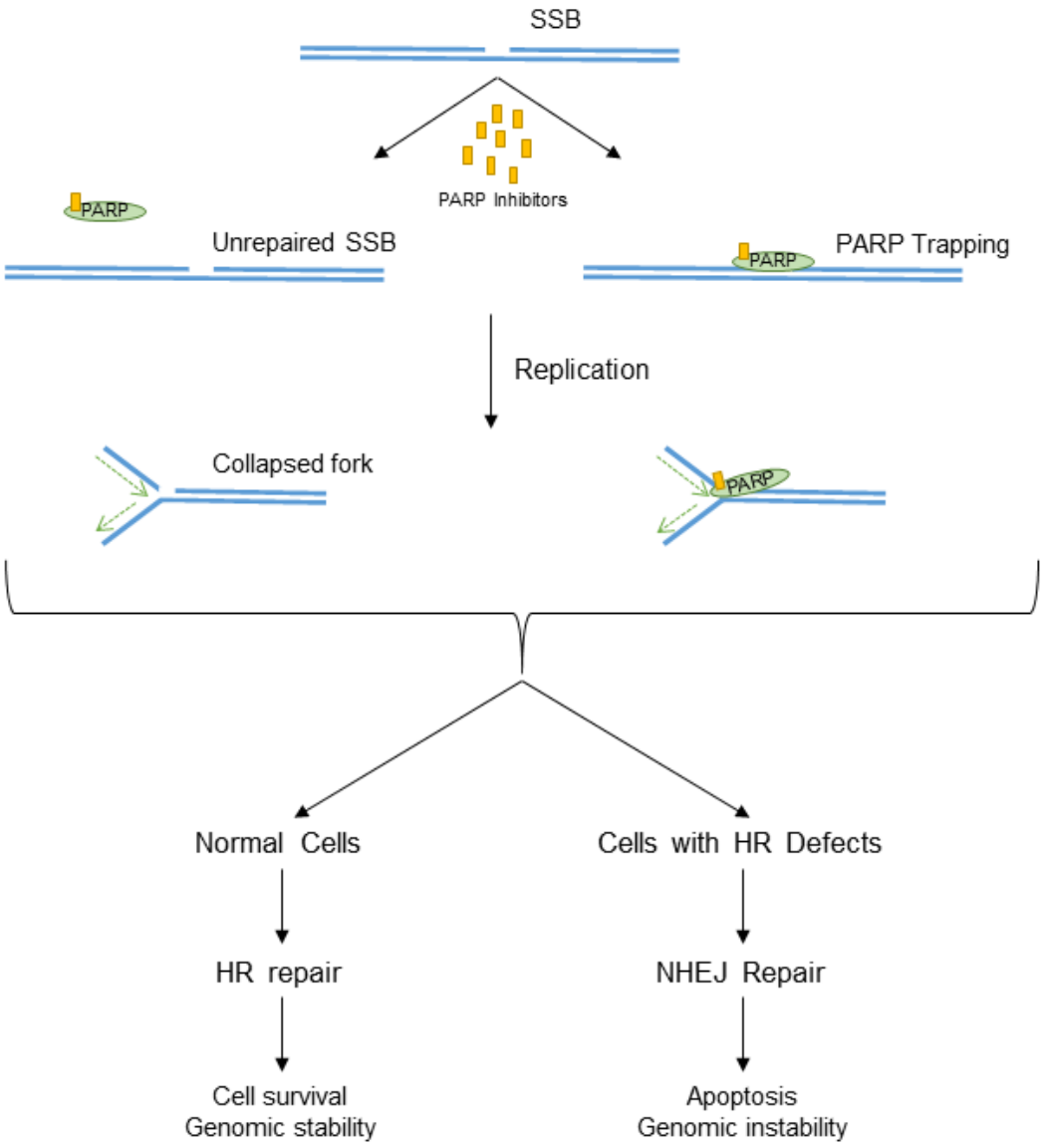

Figure 8. Double-Stranded Break Repair Pathways.

Double-stranded breaks can be repaired throughout the cell cycle by non-homologous end-joining while repair by homologous recombination is restricted to the G2 and S phases of the cell cycle. During NHEJ (left), the ku70/ku80 heterodimers recognizes and binds the double-stranded break. This complex then recruits DNA-PK which bridges the break and promotes the ligation of the two broken ends by the XRCC4/DNA Ligase IV complex. During HR (right), the Mre11/Rad50/Nbs1

complex binds and resects one strand of the break, creating a single-stranded overhang. RPA binds the single-stranded overhang, protecting this strand from resection, and recruiting RAD51, which forms a nucleoprotein filament that invades a homologous DNA duplex, normally the sister chromatid. DNA polymerase then uses this homologous template to repair the resected DNA. Adapted and modified from (Krajewska et al., 2015) under the Creative Commons Attribution 4.0 International License. Adapted and modified from (De Lorenzo et al., 2013) under the Creative Commons Attribution 3.0 Unported License.

Figure 9

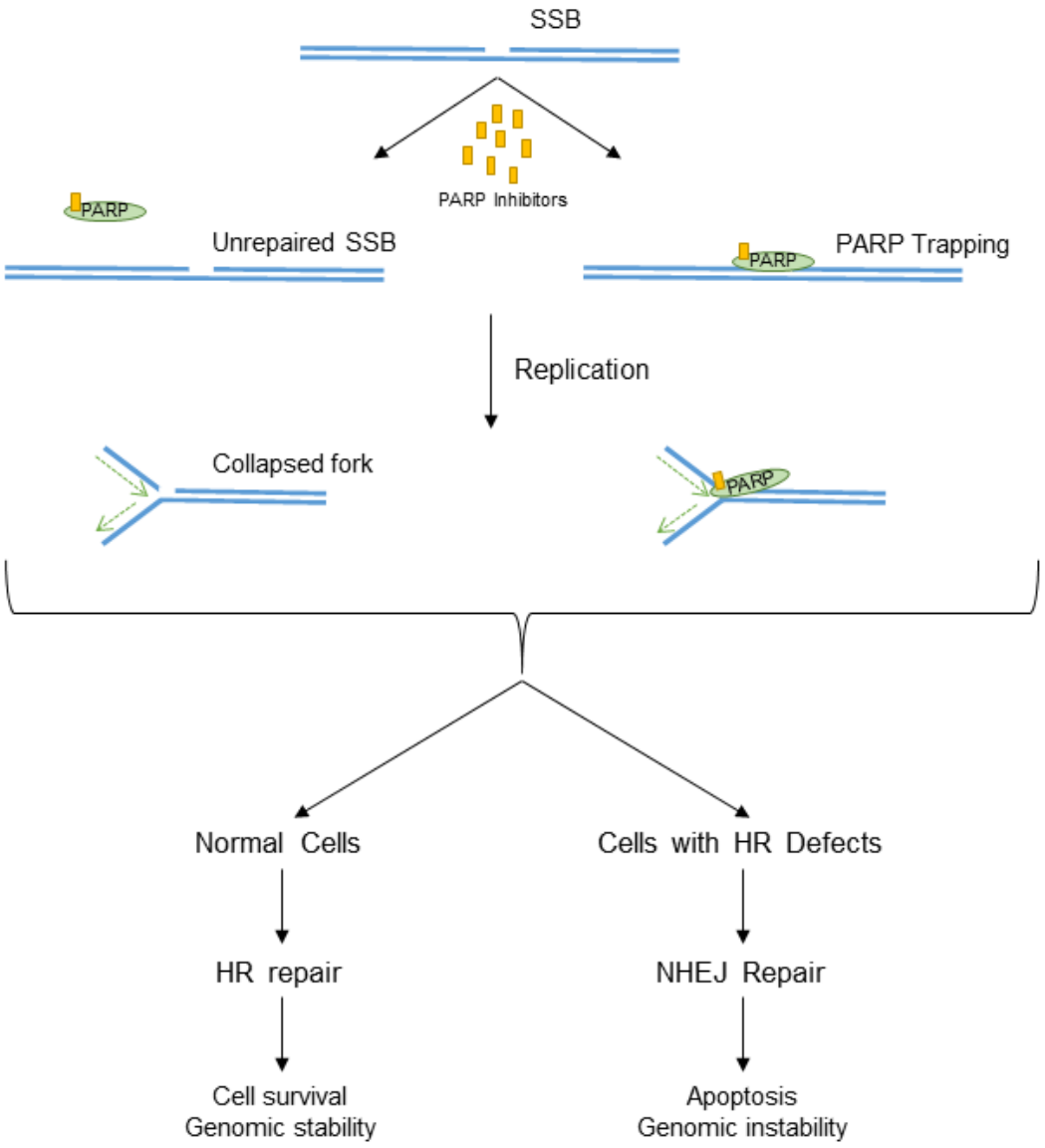

Figure 9. PARP inhibitors and HR defects.

In normal cells, PARP1 can bind that promote the repair of single-stranded breaks in DNA. When cells are treated with PARP inhibitors, cells cannot repair these single-stranded breaks. When these single-stranded breaks meet a replication fork during DNA replication, they become double-stranded breaks that muct be repaired by homologous recombination. Normal cells with no HR deficiency can repair these double-stranded breaks at the replication fork. However, when cells

have a deficiency in HR repair, such as BRCA1 or BRCA2 deficiencies, cells are forced to repair the fork by NHEJ, causing genomic instability or resulting in cell death. Adapted and modified from (Li and Greenberg, 2012) with kind permission from Elesvier Publishing.

References

Abeshouse, A., Ahn, J., Akbani, R., Ally, A., Amin, S., Andry, C.D., Annala, M., Aprikian, A., Armenia, J., Arora, A.*, et al.* (2015). The Molecular Taxonomy of Primary Prostate Cancer. Cell *163*, 1011-1025.

Akamatsu, Y., and Jasin, M. (2010). Role for the Mammalian Swi5-Sfr1 Complex in DNA Strand Break Repair through Homologous Recombination. Plos Genet *6*.

An, J., Ren, S., Murphy, S.J., Dalangood, S., Chang, C., Pang, X., Cui, Y., Wang, L., Pan, Y., Zhang, X.*, et al.* (2015). Truncated ERG Oncoproteins from TMPRSS2-ERG Fusions Are Resistant to SPOP-Mediated Proteasome Degradation. Mol Cell *59*, 904-916.

An, J., Wang, C., Deng, Y., Yu, L., and Huang, H. (2014). Destruction of full-length androgen receptor by wild-type SPOP, but not prostate-cancer-associated mutants. Cell Rep *6*, 657-669.

Attard, G., Clark, J., Ambroisine, L., Fisher, G., Kovacs, G., Flohr, P., Berney, D., Foster, C.S., Fletcher, A., Gerald, W.L.*, et al.* (2008). Duplication of the fusion of TMPRSS2 to ERG sequences identifies fatal human prostate cancer. Oncogene *27*, 253-263.

Baca, S.C., Prandi, D., Lawrence, M.S., Mosquera, J.M., Romanel, A., Drier, Y., Park, K., Kitabayashi, N., MacDonald, T.Y., Ghandi, M.*, et al.* (2013). Punctuated evolution of prostate cancer genomes. Cell *153*, 666-677.

Bagchi, A., Papazoglu, C., Wu, Y., Capurso, D., Brodt, M., Francis, D., Bredel, M., Vogel, H., and Mills, A.A. (2007). CHD5 is a tumor suppressor at human 1p36. Cell *128*, 459-475.

Barbieri, C.E., Baca, S.C., Lawrence, M.S., Demichelis, F., Blattner, M., Theurillat, J.P., White, T.A., Stojanov, P., Van Allen, E., Stransky, N.*, et al.* (2012). Exome sequencing identifies recurrent SPOP, FOXA1 and MED12 mutations in prostate cancer. Nat Genet *44*, 685-689.

Bell, D., Berchuck, A., Birrer, M., Chien, J., Cramer, D.W., Dao, F., Dhir, R., DiSaia, P., Gabra, H., Glenn, P.*, et al.* (2011). Integrated genomic analyses of ovarian carcinoma. Nature *474*, 609-615.

Beltran, H., Yelensky, R., Frampton, G.M., Park, K., Downing, S.R., MacDonald, T.Y., Jarosz, M., Lipson, D., Tagawa, S.T., Nanus, D.M.*, et al.* (2013). Targeted next-generation sequencing of advanced prostate cancer identifies potential therapeutic targets and disease heterogeneity. Eur Urol *63*, 920-926.

Berger, M.F., Lawrence, M.S., Demichelis, F., Drier, Y., Cibulskis, K., Sivachenko, A.Y., Sboner, A., Esgueva, R., Pflueger, D., Sougnez, C.*, et al.* (2011). The genomic complexity of primary human prostate cancer. Nature *470*, 214-220.

Bhagavan, N.V., and Ha, C.-E. (2011). Essentials of medical biochemistry : with clinical cases, 1st edn (Amsterdam ; Boston: Elsevier/Academic Press).

Biswas, D., Takahata, S., Xin, H., Dutta-Biswas, R., Yu, Y., Formosa, T., and Stillman, D.J. (2008). A role for Chd1 and Set2 in negatively regulating DNA replication in Saccharomyces cerevisiae. Genetics *178*, 649-659.

Blattner, M., Lee, D.J., O'Reilly, C., Park, K., MacDonald, T.Y., Khani, F., Turner, K.R., Chiu, Y.L., Wild, P.J., Dolgalev, I.*, et al.* (2014). SPOP mutations in prostate cancer across demographically diverse patient cohorts. Neoplasia *16*, 14-20.

Blattner, M., Liu, D., Robinson, B.D., Huang, D., Poliakov, A., Gao, D., Nataraj, S., Deonarine, L.D., Augello, M.A., Sailer, V.*, et al.* (2017). SPOP Mutation Drives Prostate Tumorigenesis In Vivo through Coordinate Regulation of PI3K/mTOR and AR Signaling. Cancer Cell *31*, 436-451.

Boland, C.R., and Goel, A. (2010). Microsatellite instability in colorectal cancer. Gastroenterology *138*, 2073-2087 e2073.

Boysen, G., Barbieri, C.E., Prandi, D., Blattner, M., Chae, S.S., Dahija, A., Nataraj, S., Huang, D., Marotz, C., Xu, L.*, et al.* (2015). SPOP mutation leads to genomic instability in prostate cancer. Elife *4*.

Bryant, H.E., Schultz, N., Thomas, H.D., Parker, K.M., Flower, D., Lopez, E., Kyle, S., Meuth, M., Curtin, N.J., and Helleday, T. (2005). Specific killing of BRCA2-deficient tumours with inhibitors of poly(ADP-ribose) polymerase. Nature *434*, 913-917.

Bunting, S.F., and Nussenzweig, A. (2013). End-joining, translocations and cancer. Nature Reviews Cancer *13*, 443-454.

Burkhardt, L., Fuchs, S., Krohn, A., Masser, S., Mader, M., Kluth, M., Bachmann, F., Huland, H., Steuber, T., Graefen, M.*, et al.* (2013). CHD1 is a 5q21 tumor suppressor required for ERG rearrangement in prostate cancer. Cancer Res *73*, 2795-2805.

Bzymek, K.P., and Colman, R.F. (2007). Role of alpha-Asp181, beta-Asp192, and gamma-Asp190 in the distinctive subunits of human NAD-specific isocitrate dehydrogenase. Biochemistry *46*, 5391-5397.

Canitrot, Y., Cazaux, C., Frechet, M., Bouayadi, K., Lesca, C., Salles, B., and Hoffmann, J.S. (1998). Overexpression of DNA polymerase beta in cell results in a mutator phenotype and a decreased sensitivity to anticancer drugs. Proc Natl Acad Sci U S A *95*, 12586-12590.

Carnevale, J., and Ashworth, A. (2015). Assessing the Significance of BRCA1 and BRCA2 Mutations in Pancreatic Cancer. J Clin Oncol *33*, 3080-+.

Cerbinskaite, A., Mukhopadhyay, A., Plummer, E.R., Curtin, N.J., and Edmondson, R.J. (2012). Defective homologous recombination in human cancers. Cancer Treat Rev *38*, 89-100.

Cerveira, N., Ribeiro, F.R., Peixoto, A., Costa, V., Henrique, R., Jeronimo, C., and Teixeira, M.R. (2006). TMPRSS2-ERG gene fusion causing ERG overexpression precedes chromosome copy number changes in prostate carcinomas and paired HGPIN lesions. Neoplasia *8*, 826-832.

Choo, R., Klotz, L., Danjoux, C., Morton, G.C., DeBoer, G., Szumacher, E., Fleshner, N., Bunting, P., and Hruby, G. (2002). Feasibility study: watchful waiting for localized low to intermediate grade prostate carcinoma with selective delayed intervention based on prostate specific antigen, histological and/or clinical progression. J Urol *167*, 1664-1669.

Ciccia, A., and Elledge, S.J. (2010). The DNA damage response: making it safe to play with knives. Mol Cell *40*, 179-204.

Cooperberg, M.R., Broering, J.M., and Carroll, P.R. (2009). Risk assessment for prostate cancer metastasis and mortality at the time of diagnosis. J Natl Cancer Inst *101*, 878-887.

D'Amico, A.V., Whittington, R., Malkowicz, S.B., Schultz, D., Blank, K., Broderick, G.A., Tomaszewski, J.E., Renshaw, A.A., Kaplan, I., Beard, C.J.*, et al.* (1998). Biochemical outcome after radical prostatectomy, external beam radiation therapy, or interstitial radiation therapy for clinically localized prostate cancer. JAMA *280*, 969-974.

Davis, A.J., and Chen, D.J. (2013). DNA double strand break repair via non-homologous end-joining. Transl Cancer Res *2*, 130-143.

de Boer, J., and Hoeijmakers, J.H. (2000). Nucleotide excision repair and human syndromes. Carcinogenesis *21*, 453-460.

de Dieuleveult, M., Yen, K., Hmitou, I., Depaux, A., Boussouar, F., Bou Dargham, D., Jounier, S., Humbertclaude, H., Ribierre, F., Baulard, C.*, et al.* (2016). Genome-wide nucleosome specificity and function of chromatin remodellers in ES cells. Nature *530*, 113-116.

Demichelis, F., Fall, K., Perner, S., Andren, O., Schmidt, F., Setlur, S.R., Hoshida, Y., Mosquera, J.M., Pawitan, Y., Lee, C.*, et al.* (2007). TMPRSS2:ERG gene fusion associated with lethal prostate cancer in a watchful waiting cohort. Oncogene *26*, 4596-4599.

Dietlein, F., Thelen, L., and Reinhardt, H.C. (2014). Cancer-specific defects in DNA repair pathways as targets for personalized therapeutic approaches. Trends Genet *30*, 326-339.

Difilippantonio, M.J., Zhu, J., Chen, H.T., Meffre, E., Nussenzweig, M.C., Max, E.E., Ried, T., and Nussenzweig, A. (2000). DNA repair protein Ku80 suppresses chromosomal aberrations and malignant transformation. Nature *404*, 510-514.

Dimitrov, L., Hong, C.S., Yang, C., Zhuang, Z., and Heiss, J.D. (2015). New developments in the pathogenesis and therapeutic targeting of the IDH1 mutation in glioma. Int J Med Sci *12*, 201-213.

Dominguez-Valentin, M., Joost, P., Therkildsen, C., Jonsson, M., Rambech, E., and Nilbert, M. (2016). Frequent mismatch-repair defects link prostate cancer to Lynch syndrome. Bmc Urol *16*.

Duan, S., and Pagano, M. (2015). SPOP Mutations or ERG Rearrangements Result in Enhanced Levels of ERG to Promote Cell Invasion in Prostate Cancer. Mol Cell *59*, 883-884.

Emmert, S., Kobayashi, N., Khan, S.G., and Kraemer, K.H. (2000). The xeroderma pigmentosum group C gene leads to selective repair of cyclobutane pyrimidine dimers rather than 6-4 photoproducts. Proc Natl Acad Sci U S A *97*, 2151-2156.

Emmert, S., Leibeling, D., and Runger, T.M. (2006). Syndromes with genetic instability: model diseases for (skin) cancerogenesis. J Dtsch Dermatol Ges *4*, 721-731.

Emmert, S., Schneider, T.D., Khan, S.G., and Kraemer, K.H. (2001). The human XPG gene: gene architecture, alternative splicing and single nucleotide polymorphisms. Nucleic Acids Res *29*, 1443-1452.

Emmert, S., Slor, H., Busch, D.B., Batko, S., Albert, R.B., Coleman, D., Khan, S.G., Abu-Libdeh, B., DiGiovanna, J.J., Cunningham, B.B.*, et al.* (2002). Relationship of neurologic degeneration to genotype in three xeroderma pigmentosum group G patients. J Invest Dermatol *118*, 972-982.

Farmer, H., McCabe, N., Lord, C.J., Tutt, A.N.J., Johnson, D.A., Richardson, T.B., Santarosa, M., Dillon, K.J., Hickson, I., Knights, C.*, et al.* (2005). Targeting the DNA repair defect in BRCA mutant cells as a therapeutic strategy. Nature *434*, 917-921.

Frank, K.M., Sharpless, N.E., Gao, Y.J., Sekiguchi, J.M., Ferguson, D.O., Zhu, C.M., Manis, J.P., Horner, J., DePinho, R.A., and Alt, F.W. (2000). DNA ligase IV deficiency in mice leads to defective neurogenesis and embryonic lethality via the p53 pathway. Molecular Cell *5*, 993-1002.

Fujii, T., Khawaja, M.R., DiNardo, C.D., Atkins, J.T., and Janku, F. (2016). Targeting isocitrate dehydrogenase (IDH) in cancer. Discov Med *21*, 373-380.

Fukui, K. (2010). DNA mismatch repair in eukaryotes and bacteria. J Nucleic Acids *2010*.

Futreal, P.A., Liu, Q.Y., Shattuckeidens, D., Cochran, C., Harshman, K., Tavtigian, S., Bennett, L.M., Haugenstrano, A., Swensen, J., Miki, Y.*, et al.* (1994). Brca1 Mutations in Primary Breast and Ovarian Carcinomas. Science *266*, 120-122.

Gan, W., Dai, X., Lunardi, A., Li, Z., Inuzuka, H., Liu, P., Varmeh, S., Zhang, J., Cheng, L., Sun, Y.*, et al.* (2015). SPOP Promotes Ubiquitination and Degradation of the ERG Oncoprotein to Suppress Prostate Cancer Progression. Mol Cell *59*, 917-930.

Gao, D., Vela, I., Sboner, A., Iaquinta, P.J., Karthaus, W.R., Gopalan, A., Dowling, C., Wanjala, J.N., Undvall, E.A., Arora, V.K.*, et al.* (2014). Organoid cultures derived from patients with advanced prostate cancer. Cell *159*, 176-187.

Gao, N., Ishii, K., Mirosevich, J., Kuwajima, S., Oppenheimer, S.R., Roberts, R.L., Jiang, M., Yu, X., Shappell, S.B., Caprioli, R.M.*, et al.* (2005). Forkhead box A1 regulates prostate ductal morphogenesis and promotes epithelial cell maturation. Development *132*, 3431-3443.

Gao, N., Zhang, J., Rao, M.A., Case, T.C., Mirosevich, J., Wang, Y., Jin, R., Gupta, A., Rennie, P.S., and Matusik, R.J. (2003). The role of hepatocyte nuclear factor-3 alpha (Forkhead Box A1) and androgen receptor in transcriptional regulation of prostatic genes. Mol Endocrinol *17*, 1484-1507.

Gaspar-Maia, A., Alajem, A., Polesso, F., Sridharan, R., Mason, M.J., Heidersbach, A., Ramalho-Santos, J., McManus, M.T., Plath, K., Meshorer, E.*, et al.* (2009). Chd1 regulates open chromatin and pluripotency of embryonic stem cells. Nature *460*, 863-868.

Grasso, C.S., Wu, Y.M., Robinson, D.R., Cao, X., Dhanasekaran, S.M., Khan, A.P., Quist, M.J., Jing, X., Lonigro, R.J., Brenner, J.C.*, et al.* (2012). The mutational landscape of lethal castration-resistant prostate cancer. Nature *487*, 239-243.

Guidos, C.J., Williams, C.J., Grandal, I., Knowles, G., Huang, M.T.F., and Danska, J.S. (1996). V(D)J recombination activates a p53-dependent DNA damage checkpoint in scid lymphocyte precursors. Gene Dev *10*, 2038-2054.

Guzman-Ayala, M., Sachs, M., Koh, F.M., Onodera, C., Bulut-Karslioglu, A., Lin, C.J., Wong, P., Nitta, R., Song, J.S., and Ramalho-Santos, M. (2015). Chd1 is essential for the high transcriptional output and rapid growth of the mouse epiblast. Development *142*, 118-127.

Han, B., Mehra, R., Lonigro, R.J., Wang, L., Suleman, K., Menon, A., Palanisamy, N., Tomlins, S.A., Chinnaiyan, A.M., and Shah, R.B. (2009). Fluorescence in situ hybridization study shows association of PTEN deletion with ERG rearrangement during prostate cancer progression. Mod Pathol *22*, 1083-1093.

Hanahan, D., and Weinberg, R.A. (2000). The hallmarks of cancer. Cell *100*, 57-70.

Hanahan, D., and Weinberg, R.A. (2011). Hallmarks of cancer: the next generation. Cell *144*, 646-674.

Heinlein, C.A., and Chang, C. (2004). Androgen receptor in prostate cancer. Endocr Rev *25*, 276-308.

Huang, S., Gulzar, Z.G., Salari, K., Lapointe, J., Brooks, J.D., and Pollack, J.R. (2012). Recurrent deletion of CHD1 in prostate cancer with relevance to cell invasiveness. Oncogene *31*, 4164-4170.

Jiricny, J. (2006). The multifaceted mismatch-repair system. Nat Rev Mol Cell Biol *7*, 335-346.

Johnson, N., Li, Y.C., Walton, Z.E., Cheng, K.A., Li, D.A., Rodig, S.J., Moreau, L.A., Unitt, C., Bronson, R.T., Thomas, H.D.*, et al.* (2011). Compromised CDK1 activity sensitizes BRCA-proficient cancers to PARP inhibition. Nat Med *17*, 875-U257.

Kaffenberger, S.D., and Barbieri, C.E. (2016). Molecular subtyping of prostate cancer. Curr Opin Urol *26*, 213-218.

Kari, V., Mansour, W.Y., Raul, S.K., Baumgart, S.J., Mund, A., Grade, M., Sirma, H., Simon, R., Will, H., Dobbelstein, M.*, et al.* (2016). Loss of CHD1 causes DNA repair defects and enhances prostate cancer therapeutic responsiveness. EMBO Rep *17*, 1609-1623.

Kattan, M.W., Eastham, J.A., Stapleton, A.M., Wheeler, T.M., and Scardino, P.T. (1998). A preoperative nomogram for disease recurrence following radical prostatectomy for prostate cancer. J Natl Cancer Inst *90*, 766-771.

Kelley, M.R., Cheng, L., Foster, R., Tritt, R., Jiang, J., Broshears, J., and Koch, M. (2001). Elevated and altered expression of the multifunctional DNA base excision repair and redox enzyme Ape1/ref-1 in prostate cancer. Clin Cancer Res *7*, 824-830.

Khan, S.G., Metter, E.J., Tarone, R.E., Bohr, V.A., Grossman, L., Hedayati, M., Bale, S.J., Emmert, S., and Kraemer, K.H. (2000). A new xeroderma pigmentosum group C poly(AT) insertion/deletion polymorphism. Carcinogenesis *21*, 1821-1825.

Khan, S.G., Oh, K.S., Shahlavi, T., Ueda, T., Busch, D.B., Inui, H., Emmert, S., Imoto, K., Muniz-Medina, V., Baker, C.C.*, et al.* (2006). Reduced XPC DNA repair gene mRNA levels in clinically normal parents of xeroderma pigmentosum patients. Carcinogenesis *27*, 84-94.

Lapointe, J., Li, C., Giacomini, C.P., Salari, K., Huang, S., Wang, P., Ferrari, M., Hernandez-Boussard, T., Brooks, J.D., and Pollack, J.R. (2007). Genomic profiling reveals alternative genetic pathways of prostate tumorigenesis. Cancer Res *67*, 8504-8510.

Larsen, D.H., Poinsignon, C., Gudjonsson, T., Dinant, C., Payne, M.R., Hari, F.J., Rendtlew Danielsen, J.M., Menard, P., Sand, J.C., Stucki, M.*, et al.* (2010). The chromatin-remodeling factor CHD4 coordinates signaling and repair after DNA damage. J Cell Biol *190*, 731-740.

Lehmann, A.R., McGibbon, D., and Stefanini, M. (2011). Xeroderma pigmentosum. Orphanet J Rare Dis *6*, 70.

Leibeling, D., Laspe, P., and Emmert, S. (2006). Nucleotide excision repair and cancer. J Mol Histol *37*, 225-238.

Liu, W., Lindberg, J., Sui, G., Luo, J., Egevad, L., Li, T., Xie, C., Wan, M., Kim, S.T., Wang, Z.*, et al.* (2012). Identification of novel CHD1-associated collaborative alterations of genomic structure and functional assessment of CHD1 in prostate cancer. Oncogene *31*, 3939-3948.

Lord, C.J., and Ashworth, A. (2012). The DNA damage response and cancer therapy. Nature *481*, 287-294.

Luijsterburg, M.S., de Krijger, I., Wiegant, W.W., Shah, R.G., Smeenk, G., de Groot, A.J., Pines, A., Vertegaal, A.C., Jacobs, J.J., Shah, G.M.*, et al.* (2016). PARP1 Links CHD2-Mediated Chromatin Expansion and H3.3 Deposition to DNA Repair by Non-homologous End-Joining. Mol Cell *61*, 547-562.

Marfella, C.G., and Imbalzano, A.N. (2007). The Chd family of chromatin remodelers. Mutat Res *618*, 30-40.

Markkanen, E., Fischer, R., Ledentcova, M., Kessler, B.M., and Dianov, G.L. (2015). Cells deficient in base-excision repair reveal cancer hallmarks originating from adjustments to genetic instability. Nucleic Acids Res *43*, 3667-3679.

Mateo, J., Carreira, S., Sandhu, S., Miranda, S., Mossop, H., Perez-Lopez, R., Nava Rodrigues, D., Robinson, D., Omlin, A., Tunariu, N.*, et al.* (2015). DNA-Repair Defects and Olaparib in Metastatic Prostate Cancer. N Engl J Med *373*, 1697-1708.

McCabe, N., Turner, N.C., Lord, C.J., Kluzek, K., Bialkowska, A., Swift, S., Giavara, S., O'Connor, M.J., Tutt, A.N., Zdzienicka, M.Z*., et al.* (2006). Deficiency in the repair of DNA damage by homologous recombination and sensitivity to poly(ADP-ribose) polymerase inhibition. Cancer Research *66*, 8109-8115.

McNeill, D.R., Lin, P.C., Miller, M.G., Pistell, P.J., de Souza-Pinto, N.C., Fishbein, K.W., Spencer, R.G., Liu, Y., Pettan-Brewer, C., Ladiges, W.C*., et al.* (2011). XRCC1 haploinsufficiency in mice has little effect on aging, but adversely modifies exposure-dependent susceptibility. Nucleic Acids Res *39*, 7992-8004.

Metzger, E., Willmann, D., McMillan, J., Forne, I., Metzger, P., Gerhardt, S., Petroll, K., von Maessenhausen, A., Urban, S., Schott, A.K*., et al.* (2016). Assembly of methylated KDM1A and CHD1 drives androgen receptor-dependent transcription and translocation. Nat Struct Mol Biol *23*, 132-139.

Miki, Y., Swensen, J., Shattuckeidens, D., Futreal, P.A., Harshman, K., Tavtigian, S., Liu, Q.Y., Cochran, C., Bennett, L.M., Ding, W*., et al.* (1994). A Strong Candidate for the Breast and Ovarian-Cancer Susceptibility Gene Brca1. Science *266*, 66-71.

Moskwa, P., Buffa, F.M., Pan, Y.F., Panchakshari, R., Gottipati, P., Muschel, R.J., Beech, J., Kulshrestha, R., Abdelmohsen, K., Weinstock, D.M*., et al.* (2011). miR-182-Mediated Downregulation of BRCA1 Impacts DNA Repair and Sensitivity to PARP Inhibitors. Molecular Cell *41*, 210-220.

Moynahan, M.E., Cui, T.Y., and Jasin, M. (2001a). Homology-directed DNA repair, mitomycin-C resistance, and chromosome stability is restored with correction of a Brca1 mutation. Cancer Research *61*, 4842-4850.

Moynahan, M.E., Pierce, A.J., and Jasin, M. (2001b). BRCA2 is required for homology-directed repair of chromosomal breaks. Molecular Cell *7*, 263-272.

Murai, J., Yang, K.L., Dejsuphong, D., Hirota, K., Takeda, S., and D'Andrea, A.D. (2011). The USP1/UAF1 Complex Promotes Double-Strand Break Repair through Homologous Recombination. Mol Cell Biol *31*, 2462-2469.

Nagarajan, P., Onami, T.M., Rajagopalan, S., Kania, S., Donnell, R., and Venkatachalam, S. (2009). Role of chromodomain helicase DNA-binding protein 2 in DNA damage response signaling and tumorigenesis. Oncogene *28*, 1053-1062.

Nghiem, B., Zhang, X.T., Lam, H.M., True, L.D., Coleman, I., Higano, C.S., Nelson, P.S., Pritchard, C.C., and Morrissey, C. (2016). Mismatch repair enzyme expression in primary and castrate resistant prostate cancer. Asian J Urol *3*, 223-228.

Nussenzweig, A., Sokol, K., Burgman, P., Li, L.G., and Li, G.C. (1997). Hypersensitivity of Ku80-deficient cell lines and mice to DNA damage: The effects of ionizing radiation on growth, survival, and development. P Natl Acad Sci USA *94*, 13588-13593.

Pan, M.R., Hsieh, H.J., Dai, H., Hung, W.C., Li, K., Peng, G., and Lin, S.Y. (2012). Chromodomain helicase DNA-binding protein 4 (CHD4) regulates homologous recombination DNA repair, and its deficiency sensitizes cells to poly(ADP-ribose) polymerase (PARP) inhibitor treatment. J Biol Chem *287*, 6764-6772.

Peasland, A., Wang, L.Z., Rowling, E., Kyle, S., Chen, T., Hopkins, A., Cliby, W.A., Sarkaria, J., Beale, G., Edmondson, R.J*., et al.* (2011). Identification and evaluation of a potent novel ATR inhibitor, NU6027, in breast and ovarian cancer cell lines. Brit J Cancer *105*, 372-381.

Penney, K.L., Stampfer, M.J., Jahn, J.L., Sinnott, J.A., Flavin, R., Rider, J.R., Finn, S., Giovannucci, E., Sesso, H.D., Loda, M*., et al.* (2013). Gleason grade progression is uncommon. Cancer Res *73*, 5163-5168.

Perner, S., Demichelis, F., Beroukhim, R., Schmidt, F.H., Mosquera, J.M., Setlur, S., Tchinda, J., Tomlins, S.A., Hofer, M.D., Pienta, K.G.*, et al.* (2006). TMPRSS2:ERG fusion-associated deletions provide insight into the heterogeneity of prostate cancer. Cancer Res *66*, 8337-8341.

Perner, S., Mosquera, J.M., Demichelis, F., Hofer, M.D., Paris, P.L., Simko, J., Collins, C., Bismar, T.A., Chinnaiyan, A.M., De Marzo, A.M.*, et al.* (2007). TMPRSS2-ERG fusion prostate cancer: an early molecular event associated with invasion. Am J Surg Pathol *31*, 882-888.

Pettersson, A., Graff, R.E., Bauer, S.R., Pitt, M.J., Lis, R.T., Stack, E.C., Martin, N.E., Kunz, L., Penney, K.L., Ligon, A.H.*, et al.* (2012). The TMPRSS2:ERG rearrangement, ERG expression, and prostate cancer outcomes: a cohort study and meta-analysis. Cancer Epidemiol Biomarkers Prev *21*, 1497-1509.

Pflueger, D., Terry, S., Sboner, A., Habegger, L., Esgueva, R., Lin, P.C., Svensson, M.A., Kitabayashi, N., Moss, B.J., MacDonald, T.Y.*, et al.* (2011). Discovery of non-ETS gene fusions in human prostate cancer using next-generation RNA sequencing. Genome Res *21*, 56-67.

Polo, S.E., Kaidi, A., Baskcomb, L., Galanty, Y., and Jackson, S.P. (2010). Regulation of DNA-damage responses and cell-cycle progression by the chromatin remodelling factor CHD4. EMBO J *29*, 3130-3139.

Pritchard, C.C., Mateo, J., Walsh, M.F., De Sarkar, N., Abida, W., Beltran, H., Garofalo, A., Gulati, R., Carreira, S., Eeles, R.*, et al.* (2016). Inherited DNA-Repair Gene Mutations in Men with Metastatic Prostate Cancer. N Engl J Med *375*, 443-453.

Robinson, D., Van Allen, E.M., Wu, Y.M., Schultz, N., Lonigro, R.J., Mosquera, J.M., Montgomery, B., Taplin, M.E., Pritchard, C.C., Attard, G.*, et al.* (2015). Integrative clinical genomics of advanced prostate cancer. Cell *161*, 1215-1228.

Rodrigues, L.U., Rider, L., Nieto, C., Romero, L., Karimpour-Fard, A., Loda, M., Lucia, M.S., Wu, M., Shi, L., Cimic, A.*, et al.* (2015). Coordinate loss of MAP3K7 and CHD1 promotes aggressive prostate cancer. Cancer Res *75*, 1021-1034.

Rouleau, M., Patel, A., Hendzel, M.J., Kaufmann, S.H., and Poirier, G.G. (2010). PARP inhibition: PARP1 and beyond. Nature Reviews Cancer *10*, 293-301.

Rubin, M.A. (2012). ETS rearrangements in prostate cancer. Asian J Androl *14*, 393-399.

Shenoy, T.R., Boysen, G., Wang, M.Y., Xu, Q.Z., Guo, W., Koh, F.M., Wang, C., Zhang, L.Z., Wang, Y., Gil, V.*, et al.* (2017). CHD1 loss sensitizes prostate cancer to DNA damaging therapy by promoting error-prone double-strand break repair. Ann Oncol *28*, 1495-1507.

Siegel, R.L., Miller, K.D., and Jemal, A. (2017). Cancer Statistics, 2017. CA Cancer J Clin *67*, 7-30.

Siggens, L., Cordeddu, L., Ronnerblad, M., Lennartsson, A., and Ekwall, K. (2015). Transcription-coupled recruitment of human CHD1 and CHD2 influences chromatin accessibility and histone H3 and H3.3 occupancy at active chromatin regions. Epigenetics Chromatin *8*, 4.

Simic, R., Lindstrom, D.L., Tran, H.G., Roinick, K.L., Costa, P.J., Johnson, A.D., Hartzog, G.A., and Arndt, K.M. (2003). Chromatin remodeling protein Chd1 interacts with transcription elongation factors and localizes to transcribed genes. EMBO J *22*, 1846-1856.

Sims, R.J., 3rd, Chen, C.F., Santos-Rosa, H., Kouzarides, T., Patel, S.S., and Reinberg, D. (2005). Human but not yeast CHD1 binds directly and selectively to histone H3 methylated at lysine 4 via its tandem chromodomains. J Biol Chem *280*, 41789-41792.

Srivastava, D.K., Husain, I., Arteaga, C.L., and Wilson, S.H. (1999). DNA polymerase beta expression differences in selected human tumors and cell lines. Carcinogenesis *20*, 1049-1054.

Starcevic, D., Dalal, S., and Sweasy, J.B. (2004). Is there a link between DNA polymerase beta and cancer? Cell Cycle *3*, 998-1001.

Stokes, D.G., Tartof, K.D., and Perry, R.P. (1996). CHD1 is concentrated in interbands and puffed regions of Drosophila polytene chromosomes. Proc Natl Acad Sci U S A *93*, 7137-7142.

Sulli, G., Di Micco, R., and d'Adda di Fagagna, F. (2012). Crosstalk between chromatin state and DNA damage response in cellular senescence and cancer. Nat Rev Cancer *12*, 709-720.

Sung, P., and Klein, H. (2006). Mechanism of homologous recombination: mediators and helicases take on regulatory functions. Nat Rev Mol Cell Bio *7*, 739-750.

Suzuki, H., Freije, D., Nusskern, D.R., Okami, K., Cairns, P., Sidransky, D., Isaacs, W.B., and Bova, G.S. (1998). Interfocal heterogeneity of PTEN/MMAC1 gene alterations in multiple metastatic prostate cancer tissues. Cancer Res *58*, 204-209.

Tavtigian, S.V., Simard, J., Rommens, J., Couch, F., ShattuckEidens, D., Neuhausen, S., Merajver, S., Thorlacius, S., Offit, K., StoppaLyonnet, D*., et al.* (1996). The complete BRCA2 gene and mutations in chromosome 13q-linked kindreds. Nature Genetics *12*, 333-337.

Taylor, B.S., Schultz, N., Hieronymus, H., Gopalan, A., Xiao, Y., Carver, B.S., Arora, V.K., Kaushik, P., Cerami, E., Reva, B*., et al.* (2010). Integrative genomic profiling of human prostate cancer. Cancer Cell *18*, 11-22.

Tereshchenko, I.V., Zhong, H., Chekmareva, M.A., Kane-Goldsmith, N., Santanam, U., Petrosky, W., Stein, M.N., Ganesan, S., Singer, E.A., Moore, D*., et al.* (2014). ERG and CHD1 heterogeneity in prostate cancer: use of confocal microscopy in assessment of microscopic foci. Prostate *74*, 1551-1559.

Thomsen, F.B., Brasso, K., Klotz, L.H., Roder, M.A., Berg, K.D., and Iversen, P. (2014). Active surveillance for clinically localized prostate cancer--a systematic review. J Surg Oncol *109*, 830-835.

Tomlins, S.A., Bjartell, A., Chinnaiyan, A.M., Jenster, G., Nam, R.K., Rubin, M.A., and Schalken, J.A. (2009). ETS gene fusions in prostate cancer: from discovery to daily clinical practice. Eur Urol *56*, 275-286.

Tomlins, S.A., Laxman, B., Dhanasekaran, S.M., Helgeson, B.E., Cao, X., Morris, D.S., Menon, A., Jing, X., Cao, Q., Han, B.*, et al.* (2007). Distinct classes of chromosomal rearrangements create oncogenic ETS gene fusions in prostate cancer. Nature *448*, 595-599.

Tomlins, S.A., Rhodes, D.R., Perner, S., Dhanasekaran, S.M., Mehra, R., Sun, X.W., Varambally, S., Cao, X., Tchinda, J., Kuefer, R.*, et al.* (2005). Recurrent fusion of TMPRSS2 and ETS transcription factor genes in prostate cancer. Science *310*, 644-648.

Turner, N., Tutt, A., and Ashworth, A. (2004). Hallmarks of 'BRCAness' in sporadic cancers. Nature Reviews Cancer *4*, 814-819.

Tutt, A., Bertwistle, D., Valentine, J., Gabriel, A., Swift, S., Ross, G., Griffin, C., Thacker, J., and Ashworth, A. (2001). Mutation in Brca2 stimulates error-prone homology-directed repair of DNA double-strand breaks occurring between repeated sequences. Embo Journal *20*, 4704-4716.

Waddell, N., Pajic, M., Patch, A.M., Chang, D.K., Kassahn, K.S., Bailey, P., Johns, A.L., Miller, D., Nones, K., Quek, K.*, et al.* (2015). Whole genomes redefine the mutational landscape of pancreatic cancer. Nature *518*, 495-501.

Wallace, S.S., Murphy, D.L., and Sweasy, J.B. (2012). Base excision repair and cancer. Cancer Lett *327*, 73-89.

Wang, X.S., Shankar, S., Dhanasekaran, S.M., Ateeq, B., Sasaki, A.T., Jing, X., Robinson, D., Cao, Q., Prensner, J.R., Yocum, A.K.*, et al.* (2011). Characterization of KRAS rearrangements in metastatic prostate cancer. Cancer Discov *1*, 35-43.

Yang, H., Ye, D., Guan, K.L., and Xiong, Y. (2012). IDH1 and IDH2 mutations in tumorigenesis: mechanistic insights and clinical perspectives. Clin Cancer Res *18*, 5562-5571.

Zeng, L., Morinibu, A., Kobayashi, M., Zhu, Y., Wang, X., Goto, Y., Yeom, C.J., Zhao, T., Hirota, K., Shinomiya, K.*, et al.* (2015). Aberrant IDH3alpha expression promotes malignant tumor growth by inducing HIF-1-mediated metabolic reprogramming and angiogenesis. Oncogene *34*, 4758-4766.

Zhao, D., Lu, X., Wang, G., Lan, Z., Liao, W., Li, J., Liang, X., Chen, J.R., Shah, S., Shang, X.*, et al.* (2017). Synthetic essentiality of chromatin remodelling factor CHD1 in PTEN-deficient cancer. Nature *542*, 484-488.

Zhuang, M., Calabrese, M.F., Liu, J., Waddell, M.B., Nourse, A., Hammel, M., Miller, D.J., Walden, H., Duda, D.M., Seyedin, S.N.*, et al.* (2009). Structures of SPOP-substrate complexes: insights into molecular architectures of BTB-Cul3 ubiquitin ligases. Mol Cell *36*, 39-50.

Chapter 2: CHD1 loss sensitizes prostate cancer to DNA damaging therapy by promoting error-prone double-strand break repair

Original Article

CHD1 loss sensitizes prostate cancer to DNA damaging therapy by promoting error-prone double-strand break repair

T.R. Shenoy[1^], G. Boysen[3^], M.Y. Wang[2^] Q.Z. Xu[2], W. Guo[2], F. M. Koh[5@], C. Wang[1], L.Z. Zhang[2], Y. Wang[1], V. Gil[3], S. Aziz[3], R. Christova[3], D.N. Rodrigues[3,4], M. Crespo[3,4], P. Rescigno[4], N. Tunariu[4], R. Riisnaes[3,4], Z. Zafeiriou[4], P. Flohr[3,4], W. Yuan[3], E. Knight[3], A. Swain[3], M. Ramalho-Santos[5], D.Y. Xu[2], J. de Bono[3,4*] and H. Wu[1,2*]

1 Department of Molecular and Medical Pharmacology, University of California, Los Angeles, CA 90095, USA; 2 The MOE Key Laboratory of Cell Proliferation and Differentiation, School of Life Sciences, Peking-Tsinghua Center for Life Sciences, Peking University, Beijing 100871, China; 3 The Institute of Cancer Research, 123 Old Brompton Road, London, UK; 4 Prostate Cancer Targeted Therapy Group and Drug Development Unit, The Royal Marsden NHS Foundation Trust; 5 Eli and Edythe Broad Center of Regeneration Medicine and Stem Cell Research and Center for Reproductive Sciences, Department of Obstetrics, Gynecology and Reproductive Sciences, 35 Medical Center Way, University of California, San Francisco, CA 94143, USA.

Abstract

Background: Deletion of the chromatin remodeler *CHD1* is a common genomic alteration found in human prostate cancers (PCas). CHD1 loss represents a distinct PCa subtype characterized by *SPOP* mutation and higher genomic instability (Baca et al., 2013a; Burkhardt et al., 2013b; Liu et al., 2012). However, the role of CHD1 in PCa development *in vivo* and its clinical utility remain unclear.

Design: To study the role of CHD1 in PCa development and its loss in clinical management, we generated a genetically engineered mouse model with prostate-specific deletion of murine *Chd1* as well as isogenic *CHD1* WT and homozygous deleted human benign and PCa lines. We also developed patient-derived organoid cultures and screened patients with metastatic PCa for *CHD1* loss.

Results: We demonstrate that CHD1 loss sensitizes cells to DNA damage and causes a synthetic lethal response to DNA damaging therapy *in vivo*, *ex vivo* and in a patient with metastatic PCa. Mechanistically, CHD1 loss leads to decreased error-free homologous recombination (HR) repair, which is compensated by increased error-prone non-homologous end joining (NHEJ) repair for DNA double-strand break (DSB) repair.

Conclusions: Our study provides the first *in vivo* and in patient evidence supporting the role of CHD1 in DSB repair and in response to DNA damaging therapy. We uncover mechanistic insights that CHD1 modulates the choice between HR and NHEJ and suggest that CHD1 loss may contribute to genomic instability seen in this subset of PCa patients.

Key Words: Chromatin Remodeler CHD1, PCa, DDR, homologous recombination, non-homologous end joining, synthetic lethality

Key Message: Homozygous deletion of *CHD1* represents a distinct molecular subtype of PCa with genomic instability. CHD1 loss causes DDR defects and sensitizes cells to drugs such as olaparib (PARPi) and carboplatin (Pt) in preclinical models, patient-derived organoids and a metastatic PCa patient. Clinical trials are now needed to evaluate *CHD1* deletion as a predictive biomarker for Pt and PARPi treatment.

Introduction

Genomic profiling of human localized and metastatic prostate cancers (PCa) identified chromodomain helicase DNA binding protein 1 (*CHD1*) as a homozygously deleted putative tumor suppressor gene (Burkhardt et al., 2013b; Gao et al., 2014; Grasso et al., 2012b; Huang et al., 2012; Liu et al., 2012). CHD1 deficient PCas comprise a genetic subtype that typically presents mutations in the *SPOP* gene but lacks *TMPRSS-ERG* translocations and *PTEN* deletions, the most common genomic alteration found in human PCas (Abeshouse et al., 2015). Furthermore, the *CHD1*-loss or *SPOP*-mutant/*CHD1*-loss subtype is characterized by increased genomic instability and high levels of chromosomal rearrangements, suggesting a potential defect in DNA damage repair (Baca et al., 2013b; Boysen et al., 2015; Liu et al., 2012). Indeed, a recent in vitro study has linked CHD1 function with DNA double-strand break repair (Kari et al., 2016).

CHD1 is an evolutionarily highly conserved chromatin remodeler containing a chromodomain, a SNF2-related ATPase/helicase domain and a C-terminal DNA-binding domain (Lusser et al., 2005). CHD1 regulates chromatin assembly (Konev et al., 2007; Lusser et al., 2005) and active transcription by binding to H3K4me3 and elongation factors (Lin et al., 2011; Simic et al., 2003a; Sims et al., 2007). Loss of CHD1 leads to increased heterochromatin formation in murine embryonic stem cells (mESC) (Gaspar-Maia et al., 2009) and embryonic lethality (Guzman-Ayala et al., 2015).

Recent studies indicate that DNA repair genes, including BRCA2, ATM, CDK12, FANCA and RAD51C, are frequently inactivated in primary and metastatic castration resistant PCas (mCRPC) (Abeshouse et al., 2015; Mateo et al., 2015b; Robinson et al., 2015). Although some of these genetic defects sensitize mCRPC to Poly ADP-ribose (PARP) inhibitor treatment, these genomic aberrations do not explain all responders (Mateo et al., 2015b), suggesting that other

unidentified molecular and genetic events may control the responsiveness of some PCas to DNA damage related treatment.

So far, there are no genetically engineered *in vivo* models bearing prostate-specific deletion of *CHD1*. Furthermore, the existing *in vitro* models with stable *CHD1* deletion were either not prostate-derived or did not reflect the genetic characteristics of the CHD1 loss subtype (Burkhardt et al., 2013b). To study the role of CHD1 in PCa development, we generated a murine *Chd1* prostate conditional knockout model, human prostate *CHD1* knockout cell lines as well as human PCa-derived organoids with and without *CHD1* deletion. Here we show that in preclinical models closely reflecting the genetic background of this disease subtype, CHD1 functions by orchestrating DSB repair independent of AR activity. Loss of *CHD1* sensitizes prostatic epithelial cells to DNA damaging treatments, including irradiation and drugs such as carboplatin and PARP inhibitors. Mechanistically, loss of *CHD1* stabilizes 53BP1, increases error-prone NHEJ activity and decreases error-free HR DSB repair. Therefore, CHD1 status may be used to stratify human PCa for effective treatments.

Results

Pb-Cre^{+};Chd1$^{L/L}$ mice do not develop PCa

To determine the impact of *CHD1* deletions on PCa development, we deleted *Chd1* in murine prostate epithelial cells *in vivo* by crossing *Chd1$^{L/L}$* conditional knockout females (Guzman-Ayala et al., 2015; Koh et al., 2015b) with probasin (Pb)-Cre transgenic males (Wu et al., 2001). *Pb-Cre^{+};Chd1$^{L/+}$* and *Pb-Cre^{+};Chd1$^{L/L}$* mice were born with normal Mendelian distributions (data not shown). *Pb-Cre^{+};Chd1$^{L/L}$* prostates showed hyperplasia and prostatic intraepithelial neoplasia (PIN) lesions while *Pb-Cre^{+};Chd1$^{L/+}$* prostates were comparable to that of *Pb-Cre^{-}* WT control mice (Figure 1A; Figure S1 and data not shown). We therefore focused our analysis on the *Pb-Cre^{+};Chd1$^{L/L}$* prostate (*Chd1*-null hereafter).

Previous *in vitro* studies have implied that CHD1 controls cell invasion (Huang et al., 2012; Liu et al., 2012). However, homozygous deletion of *Chd1 in vivo* showed no invasive adenocarcinoma in mice up to one year of age, as evidenced by well-maintained smooth muscle actin staining around acini (SMA; Figure 1B). In addition, *Chd1*-null mouse prostates showed no significant differences in cell proliferation and cell survival (Figure 1A, middle and lower panels).

In order to relate the data from our mouse model study with human PCa (Abeshouse et al., 2015), we also generated isogenic *CHD1* knockout clones in 22Rv1 and RWPE cells using the CRISPR/Cas9 approach. RWPE is a benign prostate epithelial line, while 22Rv1 is one of few human advanced PCa lines wild-type for *PTEN* with functional *p53*, which are known to regulate the DNA damage response (DDR) (Pearl et al., 2015). 22Rv1 cells are also *TMPRSS2-ERG* fusion negative and express AR, which best mimics the genetic background found in advanced human PCas with *CHD1* loss(Abeshouse et al., 2015).

CHD1 loss was confirmed by Western blot and immunohistochemistry (IHC) analyses (*CHD1*$^{-/-}$ hereafter) (Figure 1C). Similar to the *in vivo* mouse model, CHD1 loss did not change cell cycle profile (Figure 1D) or *in vivo* xenograft tumor formation and growth (Figure 1E). These data suggest that CHD1 loss does not drive PCa in an otherwise unaltered genetic background.

Loss of CHD1 leads to increased sensitivity to ionizing radiation

Since *CHD1* loss is associated with genomic instability and a major increase in intrachromosomal rearrangements in human PCas (Baca et al., 2013b; Boysen et al., 2015; Liu et al., 2012), we tested the potential function of CHD1 in DDR *in vivo*. We treated WT and *Chd1* null mice between 12-16 weeks of age with a single dose of 10Gy of ionizing radiation (IR) and collected the prostates 24 hours after IR (Brown and Warren, 1978). Compared to WT prostates, *Chd1*-null prostates were more sensitive to IR as evidenced by increased γH2AX-positivity (Figure 2A**,** lower panel and quantified in graph on right).

To study the molecular mechanisms underlying the CHD1-regulated DDR, we needed experimental systems which minimize potentially confounding variables such as genomic alterations in DDR genes, which are frequently found in PCa cell lines (Taylor et al., 2010b). Given CHD1's ubiquitous expression pattern, isogenic mouse ES cell lines (mESCs) (Gaspar-Maia et al., 2009; Koh et al., 2015a) offer a clean genetic system for our mechanistic studies. Similar to our isogenic *CHD1* WT and *CHD1*$^{-/-}$ 22Rv1 and RWPE human PCa cell lines, *Chd1*$^{-/-}$ *mESCs* have a cell cycle profile comparable to that of WT mESCs (Figure S2A), but are more sensitive to IR at all doses tested (0.5-6Gy; Figure 2B), suggesting a conserved role for CHD1 in regulating DSB repair response. Neutral comet analysis showed that *Chd1*$^{-/-}$ mESCs have higher basal levels of DNA damage and increased comet tail length 1 and 4 hours after irradiation (Figure 2C and Figure S2B). We further quantified γH2AX foci formation to monitor DSB formation and

resolution after IR and found that *Chd1*$^{-/-}$ mESCs have higher γH2AX foci formation and slower resolution (Figure 2D and quantified in Figure 2E), confirming the data from the comet assay. Western blot analysis showed that ATM-dependent phosphorylation of histone H2A and p53 at serine 139 (γH2AX) and serine 15 (p53), respectively, were also increased in *Chd1*$^{-/-}$ mESCs (Figure 2F) and failed to decrease 6 hours post irradiation, suggesting slower repair kinetics in *Chd1*$^{-/-}$ mESCs (Figure 2F). Similarly, *Chd1*$^{-/-}$ mESCs showed higher levels of the apoptotic response marker cleaved PARP with delayed reappearance of the mitosis marker phospho-H3 (Figure 2F). Together these results suggest that CHD1 plays an important role in DSB recognition and repair.

Loss of CHD1 leads to defect in error-free but increased error-prone DSB repair

Homologous recombination (HR) and non-homologous end joining (NHEJ) are the two major DSB repair mechanisms in response to DSB (Chapman et al., 2012). A recent published work by Kari et al. demonstrated *in vitro* that CHD1 loss specifically affects HR-mediated DNA repair but not NHEJ(Kari et al., 2016). Since some of the major conclusions from this report were based on PC3 and VCaP cells, which are *PTEN/p53* null and *TMPRSS2-ERG* fusion positive, respectively, we investigated the nature of CHD1-mediated DSB repair in our isogenic systems, which lack these alterations.

We first generated HDRGFP-*Chd1*$^{+/+}$ and HDRGFP-*Chd1*$^{-/-}$ lines by knocking-in the previously described HDRGFP construct (Pierce et al., 1999) into the endogenous *Hprt* locus in *Chd1*$^{+/+}$ and *Chd1*$^{-/-}$ mESCs. This system enabled us to quantitatively compare the proficiency of these cells to repair DSBs by HR (Weinstock et al., 2006). HR deficient HDRGFP-*Brca1*$^{-/-}$ mESCs were used as a control. HDRGFP-*Chd1*$^{-/-}$ cells showed an at least 3-fold reduction in HR competence compared to HDRGFP-*Chd1*$^{+/+}$ *WT* cells (Figure 3A; an average of 5 independent clones were

quantified in Figure 3B). Consistent with this finding, we also observed S-G2/M blockage after IR (Figure S3A). We examined RAD51 and BRCA1 foci, specific markers for HR repair (Chapman et al., 2012) in *CHD1*-null 22Rv1 and RWPE cells and found decreased BRCA1 and RAD51 recruitment to DSBs after irradiation (Figure 3C, Figure S3B, S3C). Therefore our results, based on three independent isogenic cell lines further demonstrate the important role of CHD1 in modulating HR-mediated DSB repair.

However, when quantifying total DDR as well as NHEJ repair proficiency using the well-established HDRGFP reporter assay (Weinstock et al., 2006), we found that NHEJ repair was significantly increased in HDRGFP-*Chd1*$^{-/-}$ cells compared to HDRGFP-*Chd1*$^{+/+}$ cells, whereas the total repair competence in all clones was similar (Figure 3D). Increased NHEJ in *Chd1*$^{-/-}$ mESCs could be further confirmed using 53BP1 foci quantification, a commonly used indicator for NHEJ repair (Figure 3F and Figure S3D). Consistently, CHD1 loss in 22Rv1 and RWPE cells also led to increased 53BP1 foci (Figure 3E, Figure S3B and S3E). These results demonstrate that loss of CHD1 impairs the proficiency of HR repair, which is compensated by error-prone NHEJ repair.

CHD1 regulates DDR independent of AR signaling pathway

Previous studies demonstrated that inhibition of AR signaling sensitizes PCa cells to IR (Goodwin et al., 2013; Polkinghorn et al., 2013; Tarish et al., 2015). Mechanistically, AR signaling regulates the expression of genes related to DDR and promotes classical NHEJ repair (Goodwin et al., 2013; Polkinghorn et al., 2013; Tarish et al., 2015). Since CHD1 loss could impair AR-dependent transcription *in vitro* (Burkhardt et al., 2013b; Metzger et al., 2016b), it could also affect AR-regulated DNA repair gene expression, leading to altered NHEJ repair pathway. We therefore studied the impact of CHD1 loss on AR signaling in our preclinical models and publicly available prostate cancer datasets (Grasso et al., 2012b).

We first investigated whether AR transcriptional activity is altered by CHD1 loss in 22Rv1 cells by calculating their AR activity scores, which is based on the expression of established AR target genes (Abeshouse et al., 2015; Hieronymus et al., 2006; Kumar et al., 2016; Nelson et al., 2002). As shown in Figure 4A, there was no difference between *WT* and *CHD1*-deleted 22Rv1 cells. Similar results were also obtained when comparing the expression levels of these AR target genes in *WT* and *Chd1*-null prostates (Figure 4B and Figure S4A). We also analyzed the expression levels of AR-regulated DNA repair genes, such as *PRKDC* (encoding for DNAPKcs), *XRCC2*, *XRCC3* and *XRCC4* (Goodwin et al., 2013; Polkinghorn et al., 2013) and found no significant differences between WT and *CHD1*-null human PCa patients (Grasso et al., 2012b), PCa cell lines, and our murine model (Figure 4C, 4D, and Figure S4B).

To further evaluate whether CHD1 regulates AR function, we castrated WT and *Chd1*-null animals at 6 weeks-of-age and evaluated prostate involution by H&E staining, Ki67 (for androgen-independent growth) and γH2AX (for castration-induced DDR) IHC analyses 3 days and 1, 2, 4, and 8 weeks post-castration (Supplemental Figure 4C) (Kyprianou and Isaacs, 1988; Mulholland et al., 2011; Wang et al., 2003). We did not observe any significant differences in the kinetics/extent of prostatic involution when we compared WT and *Chd1*-null castrated prostates at these time points, nor in the number of Ki67 positive cells (Figure S4C and data not shown), indicating that CHD1 loss does not influence AR-dependent cell proliferation, which is very different from our previous studies of the *Pten*-null PCa model (Mulholland et al., 2011; Wang et al., 2003). Both WT and *Chd1* null prostates have comparable AR levels before castration (Figure 4E) and responded similarly to castration-induced DNA damage as evidenced by the numbers of γH2AX positive cells (Figure 4F and data not shown). These *in vivo* results further support the notion that CHD1 does not play a major role in regulating AR pathway or AR-targeted DDR genes.

CHD1 complexes with NHEJ components

To understand how CHD1 regulates HR-mediated DSB repair, we investigated CHD1 interacting proteins. Gel filtration analysis indicated that endogenous CHD1 is in a high molecular weight complex (approximately 1100kD; Figure 5A), overlapping with several NHEJ components, such as 53BP1, RIF1 and Ku70 (Figure 5A). RAD51, on the other hand, was more evenly distributed (Figure 5A), indicating that it may not be in the same complex. To confirm the physical association of endogenous CHD1 with NHEJ components, we also conducted immunoprecipitation and Western blot analyses on 22Rv1 human PCa cells and mESCs. As shown in Figure 5B, CHD1 physically associates with multiple endogenous NHEJ components, including 53BP1, RIF1 and Ku70, but not RAD51 (Figure 5B and Figure S5A).

To further investigate the impact of CHD1 loss on NHEJ components, we focused on 53BP1. 53BP1 is a major DDR protein and its levels are critical for DSB pathway choice, as higher levels of 53BP1 inhibit end resection of breaks, thus preventing HR (Bunting et al., 2010). Compared with WT 22Rv1 cells, *CHD1*$^{-/-}$ 22Rv1 cells have increased 53BP1 protein levels *in vitro* and *in vivo* (Figure 5C and S5B); this was replicated in mESCs where *Chd1*$^{-/-}$ mESCs have significantly increased total 53BP1 (T-53BP1) with or without irradiation, but virtually no difference in RAD51 protein in the same setting (Figure 5D and Figure S5C). Total 53BP1 levels were also significantly increased in the *in vivo Chd1*-null mouse model (Figure S5D). On the other hand, 53BP1 mRNA levels were not changed in either our pre-clinical models or human PCa (Figure S5E), suggesting that CHD1 may modulate 53BP1 protein levels.

CHD1 regulates 53BP1 stability

To investigate whether the role of CHD1 in DSB pathway choice are mediated through 53BP1, we depleted 53BP1 in *CHD1*$^{-/-}$ 22Rv1 cells (Figure S5F). We show that 53BP1 knockdown can

revert the HR deficiency seen in *CHD1*$^{-/-}$ 22Rv1 cells but have no obvious effect on HR-competent WT 22Rv1 cells (Figure 5E). This is consistent with previous studies showing that even a 50% reduction of 53BP1 expression could significantly rescue HR deficiency in *BRCA1*$^{-/-}$ cells (Johnson et al., 2013).

53BP1 protein levels are regulated by post-translational mechanisms, i.e. degradation via either ubiquitin/proteasome- or cathepsin-L endosome/lysosome-mediated pathways (Gonzalez-Suarez et al., 2011; Han et al., 2014; Hu et al., 2014; Mallette and Richard, 2012). To analyse whether 53BP1 protein stability is altered due to loss of CHD1, we treated mESCs with cycloheximide (CHX, 50ug/mL, 15 min) prior to IR to block new protein synthesis (Figure 5F, top panel). We then calculated 53BP1 half-life based on Western blot and densitometry. This analysis indicates that loss of CHD1 in mESCs leads to a four-fold increase of 53BP1 half-life (from 2 to 8 hours) (Figure 5G). Furthermore, 53BP1 degradation was effectively blocked by either MG132 or Z-FY-CHO treatment, the proteasome and cathepsin-L inhibitors, respectively, similar to previous reports (Figure 5H; Figure S5G) (Gonzalez-Suarez et al., 2011; Han et al., 2014; Hu et al., 2014; Mallette and Richard, 2012), while the TP53 control was more strongly regulated by the ubiquitin/proteasome-mediated pathway (Figures 5H and S5G). Taken together, our analyses demonstrate that CHD1 forms a complex with NHEJ components and negatively regulates 53BP1 stability and half-life, thereby modulating DSB repair choices.

Loss of CHD1 leads to hypersensitivity to PARP inhibition and DNA damaging agents

Tumors with defective HR repair, such as those with BRCA1 mutations, are sensitive to PARP inhibitors (Bryant et al., 2005). We treated *WT* and *Chd1*$^{-/-}$ mESCs with the PARP inhibitor olaparib, or the DNA cross-linking agents mitomycin C and carboplatin and found that *Chd1*$^{-/-}$

mESCs were more sensitive to all three drugs as single agents when compared to *WT* cells, although not as sensitive as *Brca1*-null mESCs (Figure 6A and Figure S6A).

To further confirm the hypersensitivity of *Chd1* deficient cells to olaparib and carboplatin *in vivo*, we inoculated equal numbers of isogenic *Chd1* WT and null mESCs into the bilateral flanks of the NSG mice (Figure 6B). When tumors became palpable, we treated the animals with olaparib (100mg/kg) or carboplatin (50mg/kg) for two weeks. While wildtype and *Chd1*$^{-/-}$ mESC-derived tumors grew at similar rates in the absence of any treatment, *Chd1*$^{-/-}$ mESC-derived tumors were more sensitive to both olaparib and carboplatin (Figure 6B). Taken together our study demonstrates that similar to BRCA1, CHD1 loss sensitizes cells to olaparib and carboplatin treatment *in vitro* and *in vivo*.

mCRPC with homozygous CHD1 *loss is sensitive to olaparib and carboplatin ex vivo and in vivo.*

To investigate the relevance of our findings in the clinical setting, we generated organoids from mCRPC biopsies (Gao et al., 2014). Patient-derived mCRPC organoids with homozygous deletion of *CHD1,* which was confirmed by digital droplet PCR (ddPCR), immunohistochemistry (Figure 7A and Figure S7A) and FISH (Figure S7B), were more sensitive to olaparib compared to those organoids with normal CHD1 copy number (Figure 7B).

One of the patients, from whom CHD1 loss mCRPC organoids were derived (V5272), had rapidly progressing disease, fatigue, worsening performance status and liver function and rapidly rising LDH and ALP levels (Figure S7C). CT scanning revealed extensive liver and thoracic lymph-nodes metastasis (Figure 7D, left and middle panels). He also had a rapidly increasing circulating tumor cell count (CTC, Figure S7D) and PSA (Figure S7E) when his biopsy was taken for organoid culture. The patient had previously received castration, radical prostate

radiotherapy (74Gy), abiraterone and docetaxel (Figure 7C). Since he was too unwell to be treated on a PARPi clinical trial, he received intravenous carboplatin treatment (700mg, AUC 6, 3 weekly). After two carboplatin doses, his symptoms had fully resolved, his CT scan indicated a major response, his CTC count had decreased from 1157 to 30 cells in 7.5ml of blood, and his PSA had dropped from 1300 to 806µg/L (Figure 7D, right panels; Figures S7C, S7D, S7E). His liver enzymes, ALP and LDH also normalized (Figure S7C). After 4 cycles of carboplatin, the patient continued to respond in lymph nodes and had a mixed response in the liver metastasis. However, the patient was discontinued due to progressing of the bone disease and clinical deterioration. These clinical data support our preclinical evidence and suggest that *CHD1* status may be a predictive biomarker for DNA damaging agents such as carboplatin or PARPi for mCRPC.

Discussion

By generating a murine *Chd1* prostate conditional knockout model, isogenic human prostate and PCa *CHD1* WT and deleted lines, as well as human PCa-derived organoids with and without *CHD1* deletion, we evaluated the function of CHD1 *in vitro* and *in vivo* in: (a) DNA damage repair in a genetic background reflecting this subtype of PCa, and (b) during PCa development. Our results indicate that: (1) Homozygous deletion of *Chd1* causes PIN lesions without a significant impact on cell proliferation and survival; (2) CHD1 is involved in modulating the stability of 53BP1; (3) CHD1 loss results in increased NHEJ activity and decreased HR which can be reversed by 53BP1 knockdown (4) CHD1 deficient cells are hypersensitive to DNA damage by radiation, carboplatin and mitomycin C, as well as PARPi treatment. We also report for the first time clinical evidence that advanced PCa with CHD1 loss is sensitive to carboplatin therapy, further validating these data. Overall, our study provides a rationale to evaluate whether CHD1 status predicts treatment outcome in prospective clinical trials of DNA damaging agents such as carboplatin or PARPi.

In contrast to our previous studies of the *Pten* prostate conditional deletion model, which produces highly invasive adenocarcinomas (Wang et al., 2003), homozygous deletion of *Chd1* causes only low-grade PIN lesions (Figure 1A, 1B, and Figure S1B). Similarly, we did not observe significant growth differences *in vitro* and *in vivo* in isogenic *CHD1*-WT and *CHD1*$^{-/-}$ 22Rv1 human PCa cell lines (Figure 1D and Figure 1E), similar to a recent report (Zhao et al., 2017). Our data suggest that loss of CHD1 alone is not sufficient to cause aggressive adenocarcinoma. Therefore *CHD1* is a new addition to the list of tumor suppressor genes associated with human PCas, such *p53*, *Rb*, *Brca2* and *NKX3.1,* whose loss alone in mice does not cause an aggressive phenotype but

only hyperplasia and PIN lesions (Bhatia-Gaur et al., 1999; Chen et al., 2005; Francis et al., 2010; Maddison et al., 2004; Zhou et al., 2006). Similar to the role of CHD1 in DNA damage repair, which we are describing here (Figure 2), many of these tumor suppressors also fulfill a critical role in the DDR.

Our results provide a mechanistic explanation for the increased genomic instability observed in PCas with homozygous deletion of *CHD1* (Baca et al., 2013a; Boysen et al., 2015; Liu et al., 2012). We demonstrate that CHD1 loss suppresses error-free HR DSB repair while promoting error-prone NHEJ (Figure 3). Thus CHD1 may function as a molecular switch between HR and NHEJ. Loss of CHD1 sensitizes cells to olaparib, carboplatin and mitomycin C (Figure 6), very similar to BRCA1 deleted cells. However, CHD1 may regulate HR upstream of BRCA1 by a) recruiting CtIP to sites of DSB as demonstrated in the previous report (Kari et al., 2016) and/or b) modulating the stability of 53BP1 and enhancing NHEJ as shown in our study (Figure 5).

Genetic studies in mice have indicated the importance of NHEJ components in maintaining genomic stability (Bunting and Nussenzweig, 2013). However, next generation sequencing studies of human PCas have so far not identified alterations in components of canonical NHEJ (Abeshouse et al., 2015; Grasso et al., 2012b). On the other hand, several genes that are frequently altered in PCa are required for maintaining genomic stability, particularly via deregulation of DSB repair. For example, we have shown that *SPOP* mutations are associated with increased genomic instability in PCa by inhibiting HR and promoting NHEJ (Boysen et al., 2015), similar to what we have reported here. Although a molecular link between SPOP mutation and CHD1 loss in NHEJ has not yet been established, it is possible that in patients with combined *CHD1* homozygous deletion and *SPOP* mutations, an additive effect of these alterations may

further sensitize cells to carboplatin or olaparib. Further studies are now needed to answer this question functionally and clinically.

Previous studies indicated that CHD1 regulates AR transcriptional signaling by mediating the binding of AR to its target promoters (Burkhardt et al., 2013b; Metzger et al., 2016a), while other studies found that antagonizing AR signaling by ADT sensitizes cells to IR by inhibiting NHEJ without impacting HR DSB repair (Al-Ubaidi et al., 2013; Goodwin et al., 2013; Polkinghorn et al., 2013; Tarish et al., 2015). This would suggest that loss of CHD1 sensitizes cancer cells to IR by reducing AR signaling, consequently decreasing NHEJ repair. However, in our models, loss of CHD1 does not affect AR transcriptional output, although our studies could not rule out paracrine AR signaling from stromal prostate cells (Figure 4)(Cunha, 1973). The fact that loss of CHD1 promotes NHEJ and suppresses HR without affecting AR function or AR target expression suggests that AR blockage might further sensitize this PCa subtype to radiotherapy.

The protein stability of DNA-repair proteins is tightly controlled to ensure timely and spatially restricted activity. 53BP1 protein half-life ranges from 0.5 to 2 hours in the context of DNA damage induction (Hu et al., 2014). We show here that CHD1 contributes to the regulation of 53BP1 stability (Figure 5) although the exact mechanism remains to be resolved. Based on our analyses and those published, both ubiquitin/proteasome and endosome/lysosome pathways are likely to play roles.

In summary, we report that the loss of CHD1 leads to changes in DDR. Using functional genetic approaches, we report that CHD1 loss decreases HR-mediated DSB repair and increases error-prone NHEJ activity. Importantly, CHD1 loss is associated with an increased sensitivity to PARP inhibition and anti-cancer drugs that induce DNA intercross-strand links including carboplatin. These observations may provide a mechanistic explanation for the high number of chromosomal

rearrangements observed in PCas with *CHD1* homozygous deletion. Our data provide a rationale for treating patients bearing tumors with *CHD1* deletion in prospective clinical trials of PARP inhibitors or DNA damaging agents such as carboplatin to evaluate their potential clinical benefit in this subclass of PCa.

Figure 1

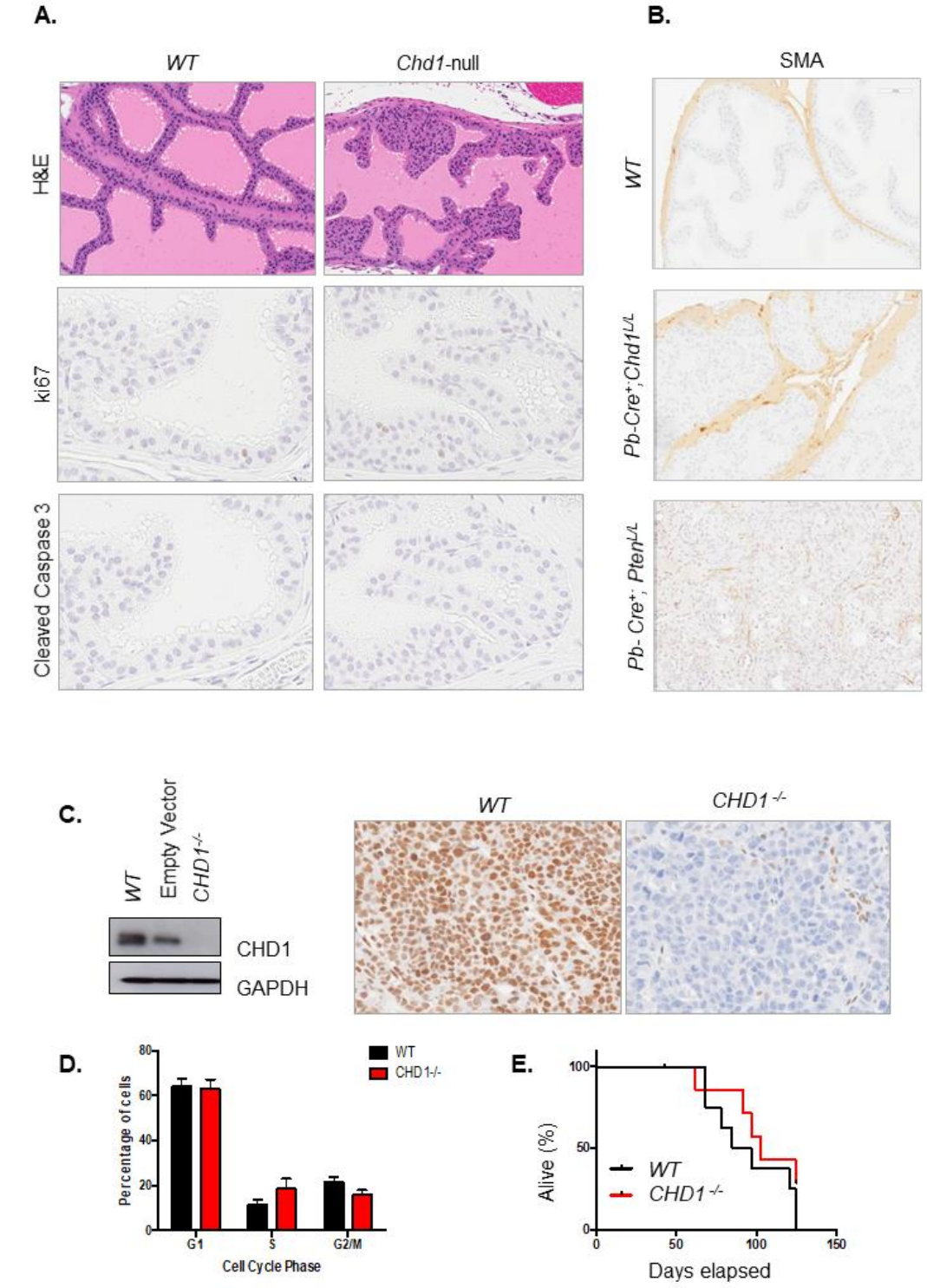

Figure 1: Loss of CHD1 induces prostatic intraepithelial neoplasia in mice.

A) Knockout of *Chd1* leads to PIN lesions. Representative IHC section images of hematoxylin and eosin (top panel), ki67 (middle panel), and cleaved caspase 3 (bottom panel) in the anterior lobe of *Pb-Cre*$^{-}$*;Chd1*$^{L/L}$ *and Pb-Cre*$^{+}$*;Chd1*$^{L/L}$ 6 week old mice. (see also Figure S1). B) Representative IHC sections of smooth muscle actin (SMA) in the anterior lobe of *Pb-Cre*$^{-}$*;Chd1*$^{L/L}$*, Pb-Cre*$^{+}$*;Chd1*$^{L/L}$, and *Pb-Cre*$^{+}$*;Pten*$^{L/L}$ 10 week old mice. C) (Left panel) Western Blot analyzing CHD1 levels in wild-type (WT), empty vector, and *CHD1*$^{-/-}$ isogenic 22Rv1 cells. (Right Panel) Representative IHC section images of CHD1 staining in 22Rv1 xenograft tumors. D) Cell cycle distribution of isogenic 22Rv1 cells with and without CHD1. Propidium iodide-based quantification of the percentage of WT and *CHD1*$^{-/-}$ isogenic 22Rv1 cells in G1, S, or G2/M phases of the cell cycle. Mean +/- s.e.m. (n=3). E) The growth of isogenic 22Rv1 xenograft tumors with (black line) or without (red line) CHD1. Survival was determined when the xenograft tumor reached 1000 mm^3, the maximal size allowance per institution guideline (n=3).

Figure 2

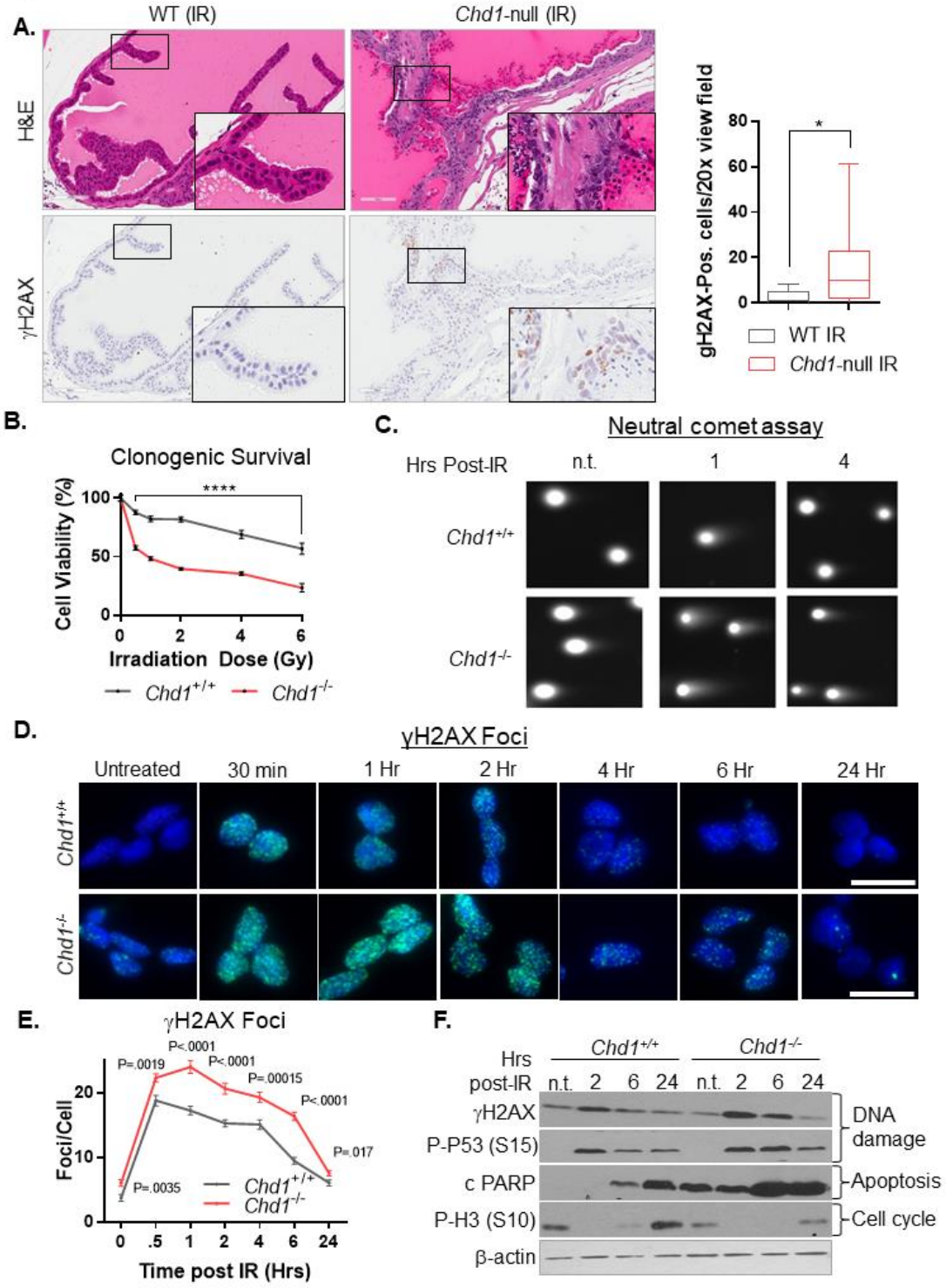

Figure 2: Loss of CHD1 leads to increased sensitivity to ionizing radiation

A) (Left Panel) Representative images of the anterior lobe of 16 week old mice that were treated with 10Gy of whole body irradiation and collected 24 hours later. Upper panels, H&E; lower, IHC for γH2AX; inserts, higher power images.bar=100mM. (Right Panel) Quantification of γH2AX-positive cells per 20x view field in the anterior lobes of WT and *Chd1*-null mice and 16 weeks of age. Mean +/- s.e.m (n=10). B) Clonogenic survival of $Chd1^{+/+}$ and $Chd1^{-/-}$ mESCs treated with the indicated doses of ionizing radiation. Mean +/- s.e.m. (n=4).C) Representative images from neutral comet assay of WT and *Chd1*-null mESCs, treated with 5Gy of irradiation and collected at the indicated time points. Quantified in Figure S2B. D) Representative images of γH2AX foci of $Chd1^{+/+}$ and $Chd1^{-/-}$ mESCs treated with 5Gy IR and collected at the indicated times. Bar=20 μm. E) Quantification of γH2AX foci/nucleus in $Chd1^{+/+}$ and $Chd1^{-/-}$ mESCs treated with 5Gy of IR and analyzed at the indicated time points. More than 100 cells were analyzed per time point for each of 3 independent experiments. Mean +/- s.e.m. (n=3). F) Western blot shows the levels of γH2AX (Ser 139), P-P53 (Ser15), cleaved PARP, and P-H3 (Ser10) in $Chd1^{+/+}$ and $Chd1^{-/-}$ mESCs treated with 5Gy of IR and analyzed at the indicated times.

Figure 3

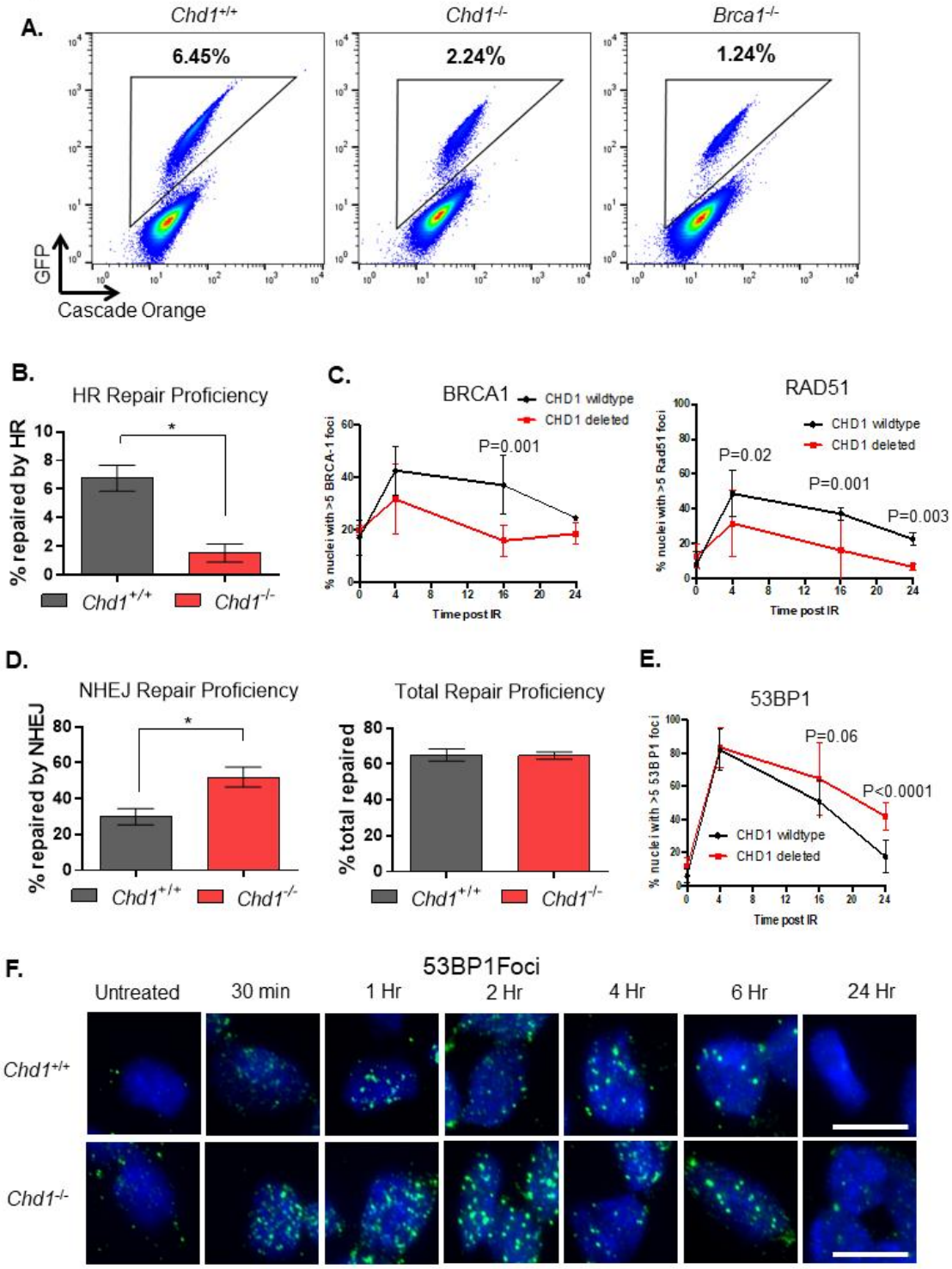

Figure 3: CHD1 regulates DSB repair pathway choices.

A) Representative FACS analysis of DRGFP-*Chd1*$^{+/+}$, DRGFP-*Chd1*$^{-/-}$, and DR-GFP-*Brca1*$^{-/-}$ mESCs 96 hours after electroporation of I-SceI plasmid. Triangular gates represent GFP-positive cells that have repaired I-SceI mediated DSBs with HR. B) HR repair proficiency in HPRT-DRGFP clones derived from *Chd1*$^{+/+}$ and *Chd1*$^{-/-}$ mESCs. Mean +/- s.e.m. (n = 5). *, P<0.05.C) BRCA1 (Left), and RAD51 (right) foci formation and resolution after irradiation-mediated DNA double-strand break induction (5Gy) in isogenic 22Rv1 cells with or without *CHD1*. Mean +/- s.e.m. (n=3). (See also Figure S3B) D) NHEJ and total repair proficiency in HPRT-DRGFP clones derived from *Chd1*$^{+/+}$ and *Chd1*$^{-/-}$ mESCs. Mean +/- s.e.m. (n = 5). *, P<0.05. E) 53BP1 foci formation and resolution after irradiation-mediated DNA double-strand break induction (5Gy) in isogenic 22Rv1 cells with or without *CHD1*. Mean +/- s.e.m. (n=3). (See also Figure S3B). F) Representative images of P-53BP1 foci quantified in Figure S3F, in *Chd1*$^{+/+}$ and *Chd1*$^{-/-}$ mESCs treated with 5Gy ionizing radiation and collected at the indicated times. Scale bar represents 20μm. (See also Figure S3D)

Figure 4

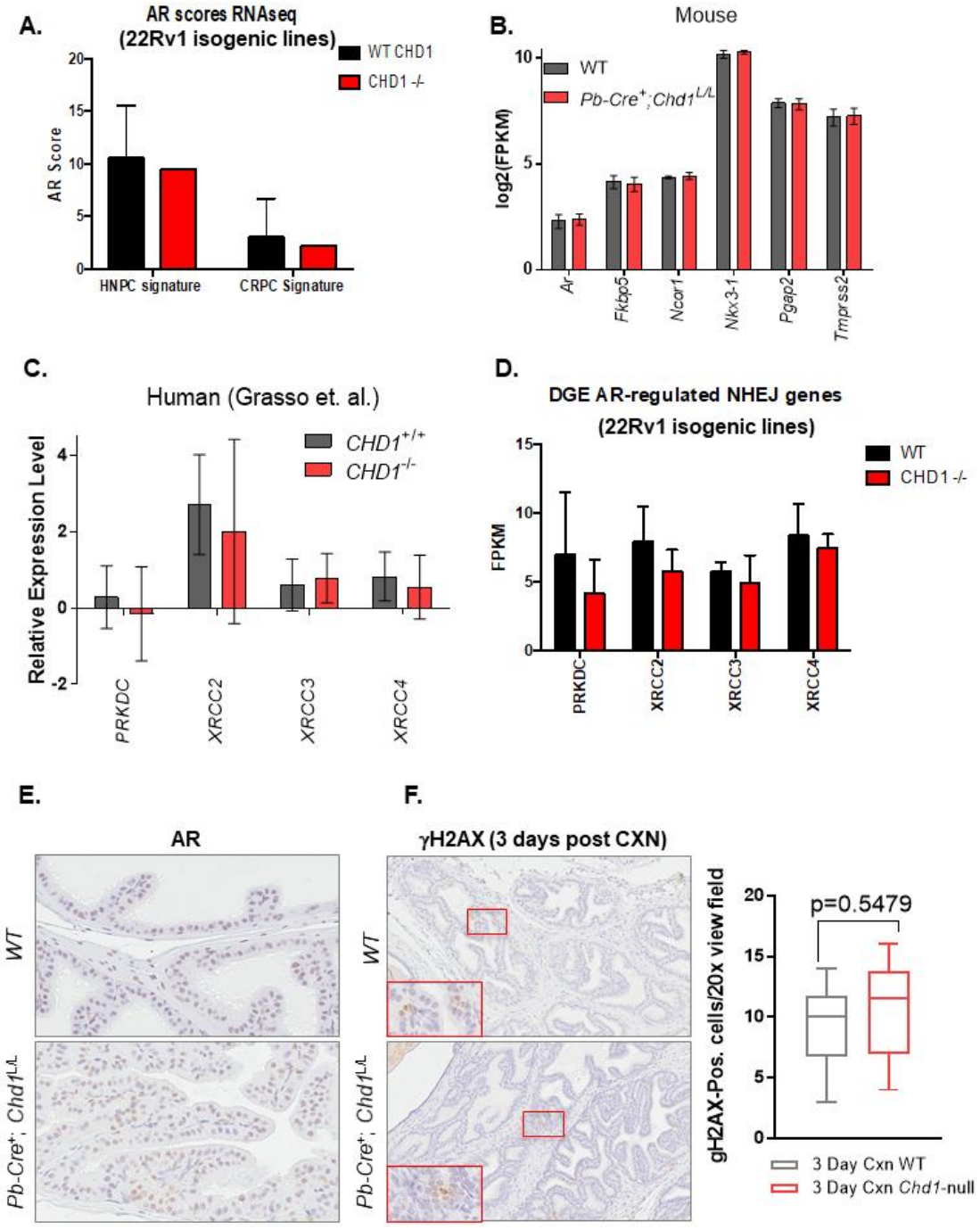

Figure 4: CHD1 regulates DDR independent of AR signaling pathway

A) AR transcriptional activity is not altered by loss of CHD1 in 22Rv1 cells. The AR activity score was calculated based on AR target gene expression using a signature from hormone-sensitive PCa cells based on 27 AR-regulated genes defined in LnCaP cells after DHT stimulation (HNPC signature) (Hieronymus et al., 2006) and castrate-resistant PCa patients based on 21 AR-regulated genes defined in 171 metastatic prostate tumors (CRPC signature) (Kumar et al., 2016). Mean +/- s.e.m. B) RNA expression levels of AR target genes in prostate derived from 10-week old WT (n=6) or *Pb-Cre*$^{+}$;*Chd1*$^{L/L}$ (n=5) mice. Mean +/- s.e.m. C) No significant difference in the expression of DDR genes under AR control. Data from Grasso et. al. (Grasso et al., 2012). Relative expression levels are presented as Mean +/- s.e.m.D) No significant difference in the expression of DDR genes under AR control. Data from 22Rv1 cells with or without knockout of *CHD1* (n=3). Relative expression levels are quantified as FPKM and presented as Mean +/- s.e.m. (See also Figure 4B). E) Representative IHC images of androgen receptor (AR) in the anterior lobe of age-matched, uncastrated WT (top) and *Chd1*-null (bottom) mice at 6 weeks of age. F) Representative IHC images of γH2AX in the anterior lobe of age-matched WT (top) and *Chd1*-null (bottom) mice 3 days post-castration (CXN). (right graph) Quantification of γH2AX-positive cells per 20x view-field in the anterior lobes of 3 day post-castrated WT and *Chd1*-null mice (n=6).

Figure 5

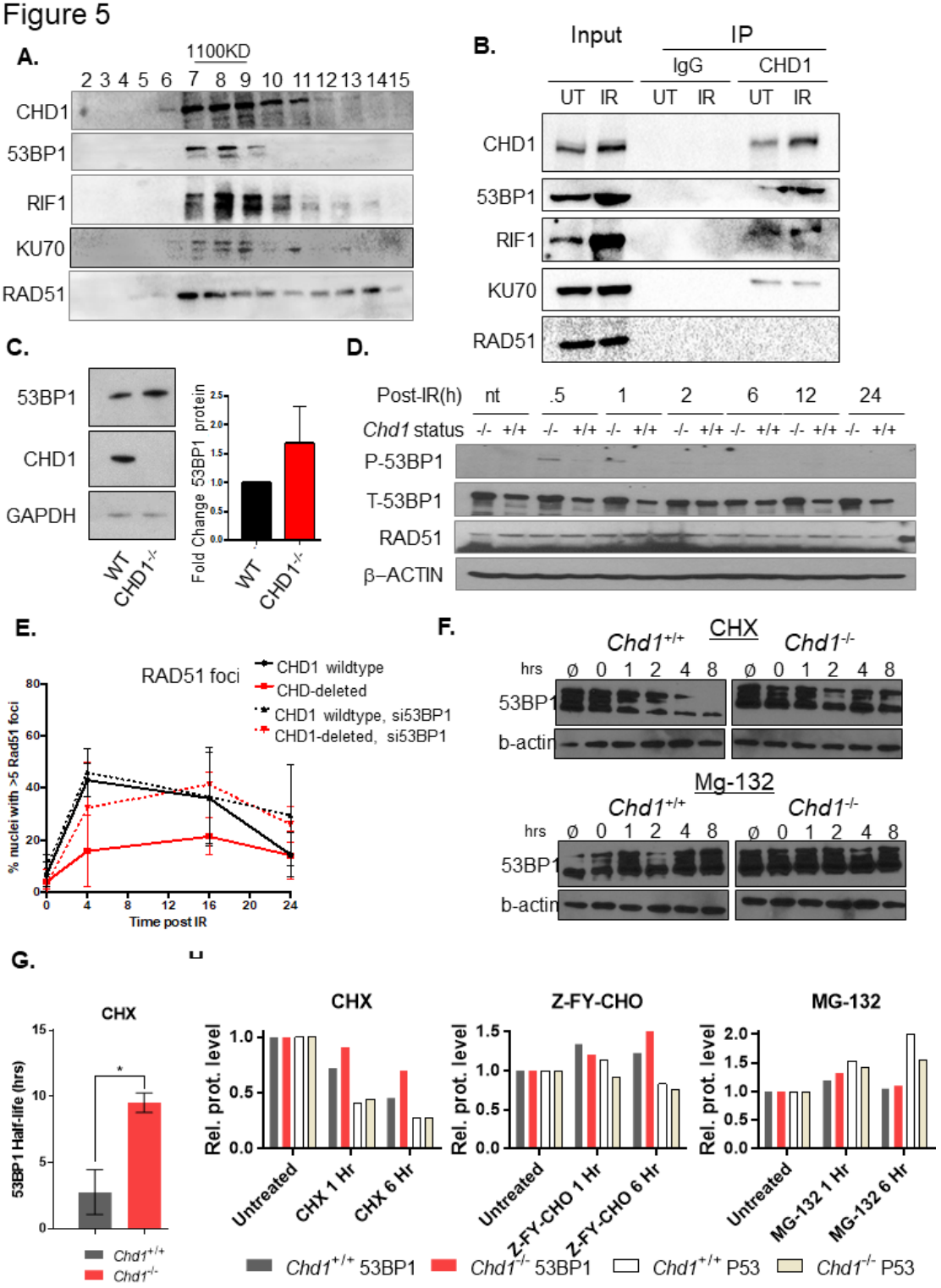

Figure 5: CHD1 interacts with components of NHEJ and stabilizes 53BP1

A) Proteins from *Chd1*$^{+/+}$ mESCs were run through a gel filtration column. Fractions were collected and immunoblotted with anti-CHD1, 53BP1, RIF1, KU70 and RAD51 antibodies. Fractions 7-9 represent complexes of approximately 1100 kD.B) Proteins from *Chd1*$^{+/+}$ mESCs were immunoprecipitated with anti-CHD1 antibody and immunoblotted with anti-53BP1, KU70, and RAD51 antibodies. (See also Figure S5A). C) (Left) Western blot analysis of 53BP1 protein level in isogenic 22Rv1 cells with and without *CHD1* deletion. (Right) Densitometry of western blots to quantify 53BP1 level. N=3. Mean+/- s.e.m. D) Western blot analysis of P-53BP1, T-53BP1, and RAD51 levels in WT and *Chd1*-null mESCs treated with 5Gy of irradiation and collected at the indicated time points. (See also Figures S5C). E) Quantification of HR activity in 22Rv1 cells with or without *CHD1* based on RAD51 recruitment to DNA DSBs. Isogenic 22Rv1 cells were treated with control siRNA or siRNA targeting 53BP1. N=3. Mean +/- s.e.m. F) Western blot analysis of total 53BP1 and β-actin protein levels in *Chd1*$^{+/+}$ and *Chd1*$^{-/-}$ mESCs treated with 50μg/mL of cycloheximide (CHX, top panel) or 10μM Mg-132 (bottom panel) for various amounts of time after 5Gy irradiation and continuous drug treatment. G) 53BP1 half-life was measured by western blot densitometry. WT and *Chd1*-null mESCs were treated with 5Gy of irradiation 15 minutes after pre-treatment with 50μg/mL cycloheximide (CHX). Mean +/- s.e.m (n=3, *$p<0.05$). (H) Quantification or total 53BP1 and P53 levels in WT and *Chd1*-null mESCs treated with 50μg/mL cycloheximide (CHX), 10 μM ZY-F-CHO, or 10 μM MG-132 and analyzed 1 hour and 6 hours after continuous treatment. 53BP1 levels were normalized to vinculin and P53 levels were normalized to β-actin. (See also Figure S5G).

Figure 6

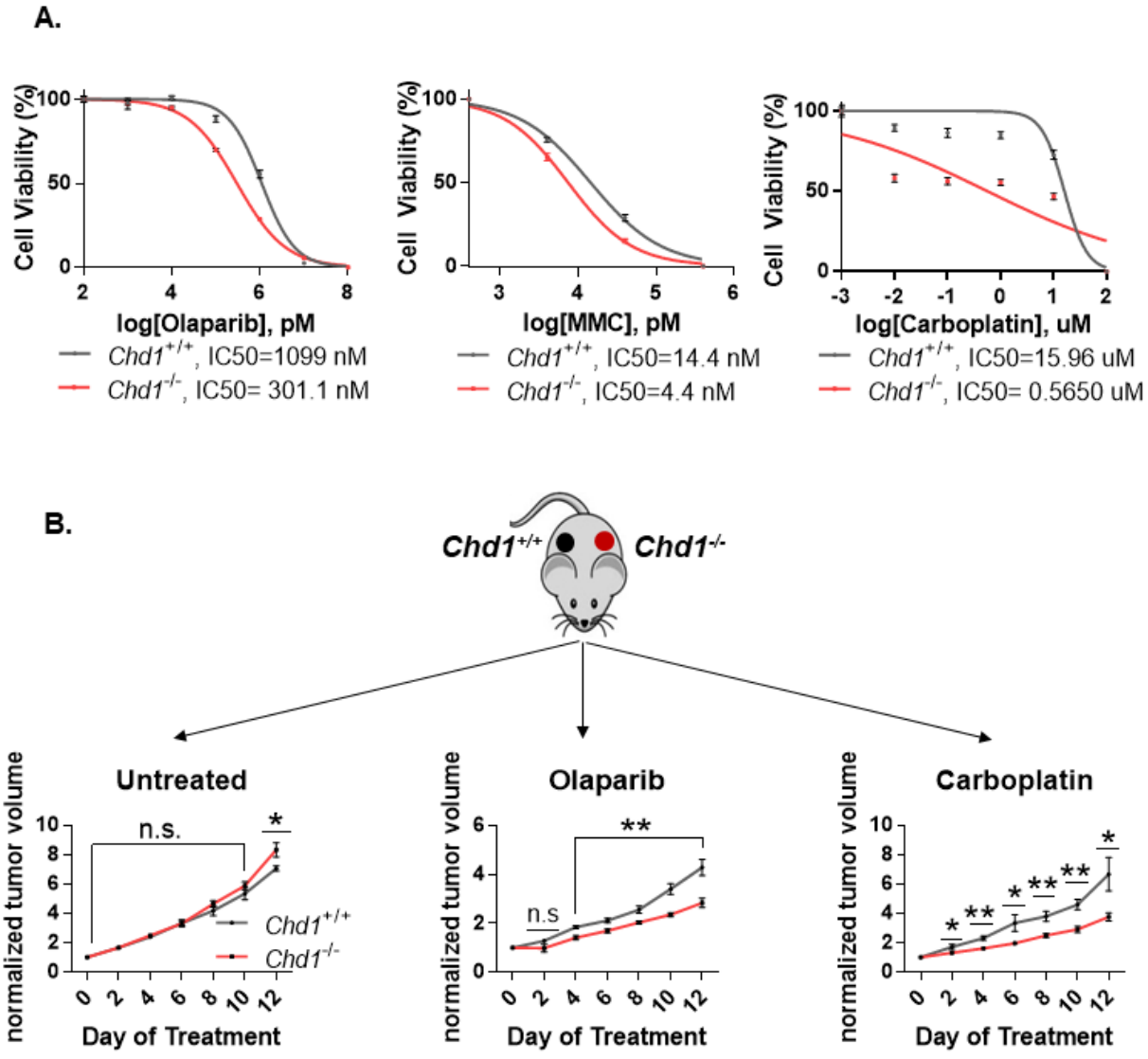

Figure 6: CHD1 loss leads to hypersensitivity to PARP inhibition and DNA damaging agents.

A) CHD1 loss leads to hypersensitivity to DNA damage agents *in vitro*. Cell viability, as determined by MTT assay, of *Chd1*$^{+/+}$ and *Chd1*$^{-/-}$mESCs after 48 hours of continuous treatment of olaparib

(left) , mitomycin C (MMC) (middle) , and carboplatin (right). IC50 was determined from the non-linear fit of normalized response curves (variable slope) (n=3). (See also Figure S6)

B) CHD1 loss leads to hypersensitivity to olaparib and carboplatin *in vivo*. Equal numbers of *Chd1*$^{+/+}$ and *Chd1*$^{-/-}$ mESCs were implanted onto the bilateral flanks of nude mice. When tumors became palpable, mice were left untreated (Left) or treated with 100mg/kg olaparib (middle) or 50mg/kg carboplatin (right) twice daily for 6 days. Relative tumor volumes are presented with growth kinetics of untreated controls shown on the left (n=5; *p<0.05, **p<0.01).

Figure 7

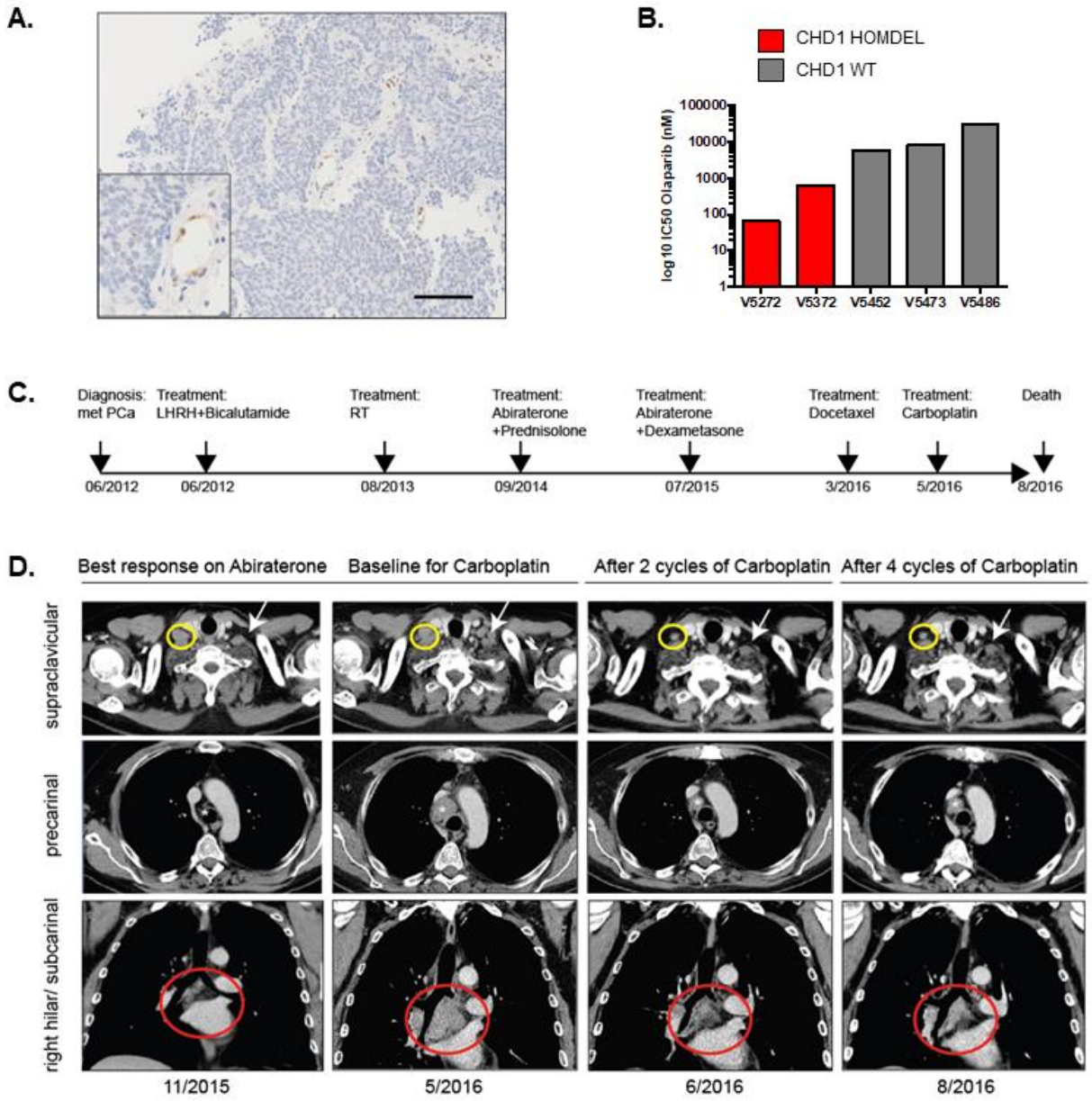

Figure 7: Metastatic CRPCs with homozygous loss of CHD1 are sensitive to carboplatin and olaparib in vivo and ex vivo

A) IHC analysis shows no CHD1 expression in tumors except blood vessels (boxed area) and stromal cells (see also Figure S7A and S7B).

B) mCRPC patient-derived organoids are sensitive to olaparib. Organoids from patients with homozygous loss of *CHD1* (V5272 and V5372) show increased sensitivity to PARP inhibition. Copy number status was determined by digital droplet PCR. HOMDEL = homozygous deletion of *CHD1*, WT = wildtype. IC50 = half maximal inhibitory concentration.

C) Clinical history of the patient represented as timeline. Arrows indicate clinical events.

D) Axial and coronal contrast enhanced CT images during disease progression (first and second columns) and after 2 and 4 cycles of carboplatin (third and fourth columns) showing significant reduction (37%) in the extent of the supraclavicular (yellow circles and white arrows), precarinal (*) and subcarinal (red circles) lymphadenopathy.

Supplementary Figure 1

	Prostates with hyperplasia -PIN	
Age	*Pb-Cre*$^{+}$*;Chd1*$^{L/L}$	WT
0-4 weeks	1/3	0/1
5-6 weeks	9/9	0/1
8-12 weeks	8/8	0/9
19-30 weeks	9/9	0/10
40 weeks +	5/5	0/6

Figure S1, related to Figure 1. Loss of CHD1 leads to prostatic intraepithelial neoplasia in mice.

Development of prostate hyperplasia and PIN in *Pb-Cre*$^{+}$*;Chd1*$^{L/L}$ mice compared to age-matched *Pb-Cre*$^{-}$*;Chd1*$^{L/L}$ littermates at different ages.

Supplementary Figure 2

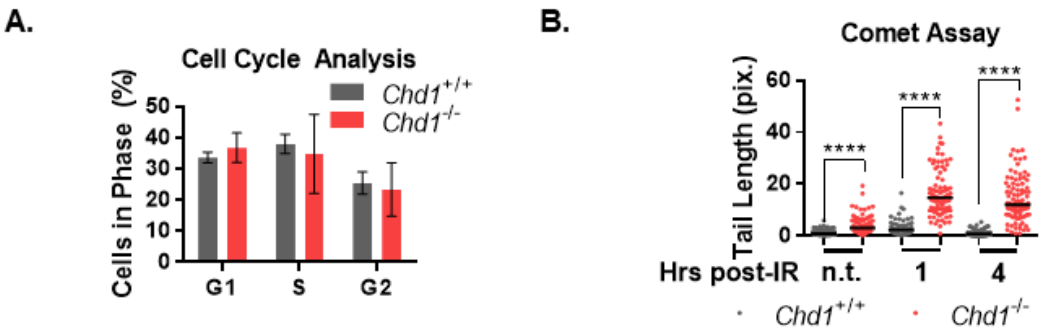

Figure S2, related to Figure 2. Loss of CHD1 leads to increased sensitivity to ionizing radiation

A) Cell cycle profile of *Chd1*$^{+/+}$ and *Chd1*$^{-/-}$ mESCs. Mean +/- s.e.m. (n=5).

B) Neutral comet assay of *Chd1*$^{+/+}$ and *Chd1*$^{-/-}$ mESCs treated with 5Gy of IR and analyzed at the indicated time points. More than 100 cells were measured per time point.

Supplementary Figure 3

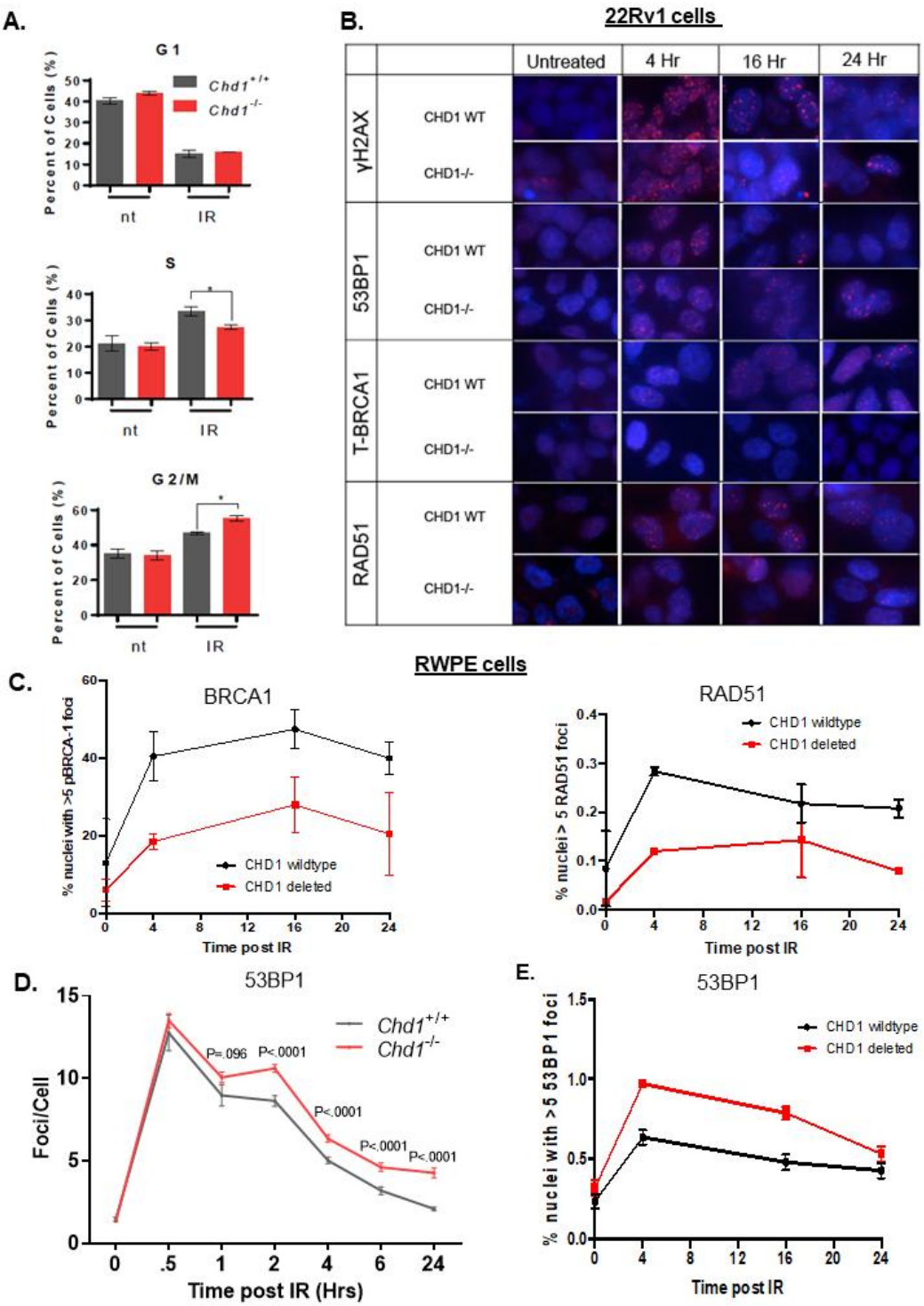

Figure S3, related to Figure 3. CHD1 regulates DSB repair pathway choice

A) Cell cycle kinetics of *Chd1*$^{+/+}$ and *Chd1*$^{-/-}$ mESCs before and 6 hours after irradiation (5Gy). DNA content in mESCs was measured with DAPI using fluorescence-activated cell sorting. Percentage of cells in each cell cycle phase was quantified and presented. P-values were calculated using the paired t-test (2 tailed). *P<0.05

B) Representative images of γH2AX foci (Top), 53BP1 Foci (second row), total BRCA1 foci (third row), and RAD51 foci (bottom), quantified in Figure 3C and 3E in WT and *CHD1*$^{-/-}$ 22Rv1 cells treated with 5Gy ionizing radiation and collected at the indicated times.

C) BRCA1 (left) and RAD51 (right) foci formation and resolution after irradiation-mediate DNA-double strand break induction (5Gy) in isogenic RWPE cells with or without *CHD1.* Mean +/- s.e.m (n=3).

D) Quantification of P-53BP1 foci per nucleus in *Chd1*$^{+/+}$ and *Chd1*$^{-/-}$ mESCs treated with 5Gy ionizing radiation and collected at the indicated times. More than 75 cells were analyzed per time point for each of three independent experiments. Mean +/- s.e.m (n=3)

E) 53BP1 foci formation and resolution after irradiation-mediate DNA-double strand break induction (5Gy) in isogenic RWPE cells with or without *CHD1.* Mean +/- s.e.m (n=3).

Supplementary Figure 4

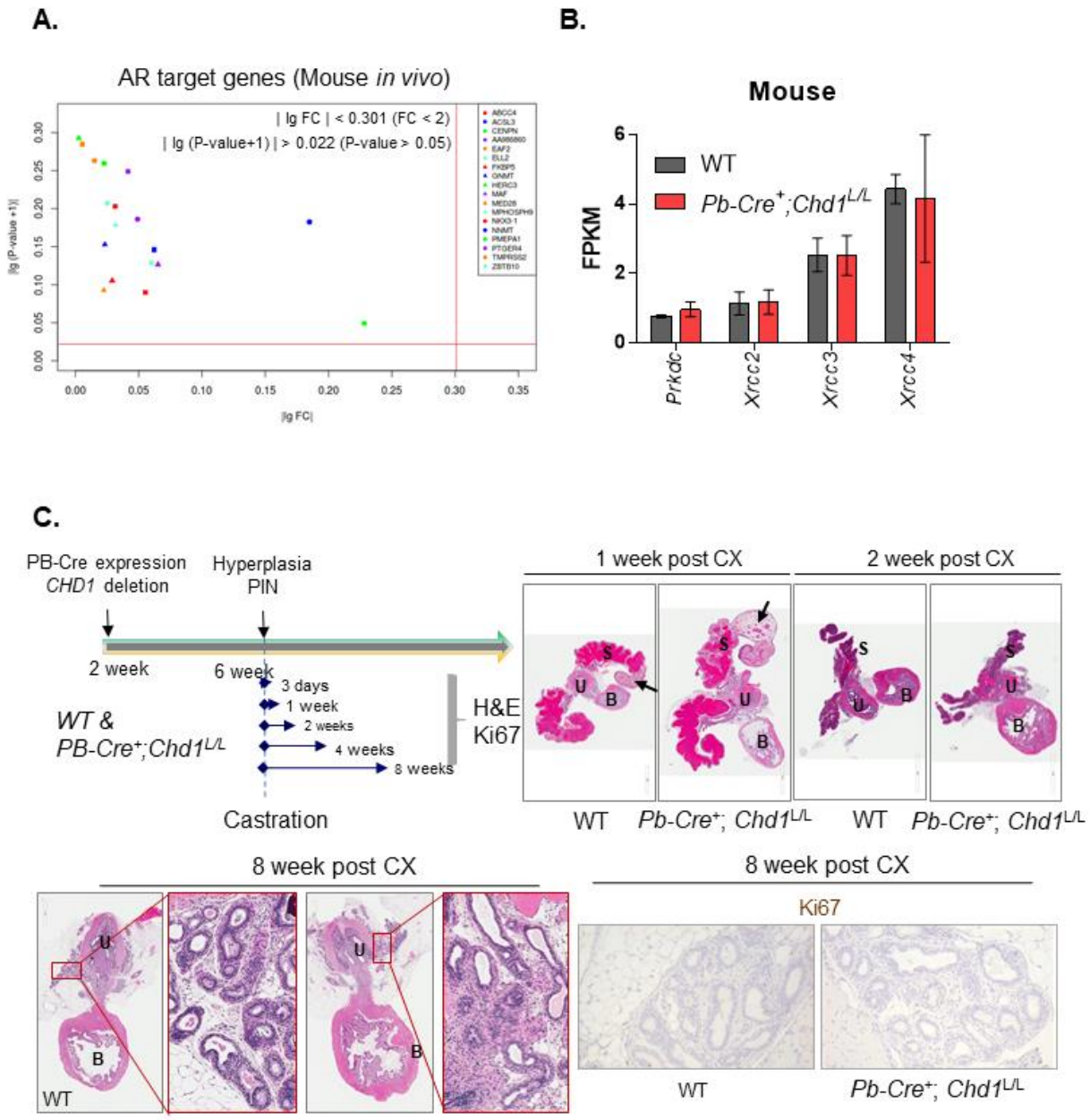

Figure S4, related to Figure 4. CHD1 regulates DDR independent of AR signaling pathway.

A) No significant difference in the expression of 20 AR target genes in WT versus *Chd1*-null mouse prostates. 2-dimensional analysis of absolute fold change (lgFC;X-axis) versus P-value (y-axis). Upper left quadrant of the graph represents FC<2 and P>0.05.

B) RNA expression levels of AR-regulated DNA damage repair (DDR) genes, in prostates of 10-week old WT (n=6) or *Pb-Cre*$^{+}$;*Chd1*$^{L/L}$ (n=5) mice. Mean +/- s.e.m.

C) (Top Left) Schematic illustration of castration kinetic experiments (Top right) H&E images in WT and *Chd1*-null prostates 1 week (two left panels) and 2 weeks (two right panels) after castration (CX). (Bottom Left) H&E images in WT and *Chd1*-null prostates 8 weeks after castration (CX). (Bottom Right) ki67 IHC images of WT and *Chd1*-null prostates 8 weeks after castration (CX).

Supplementary Figure 5

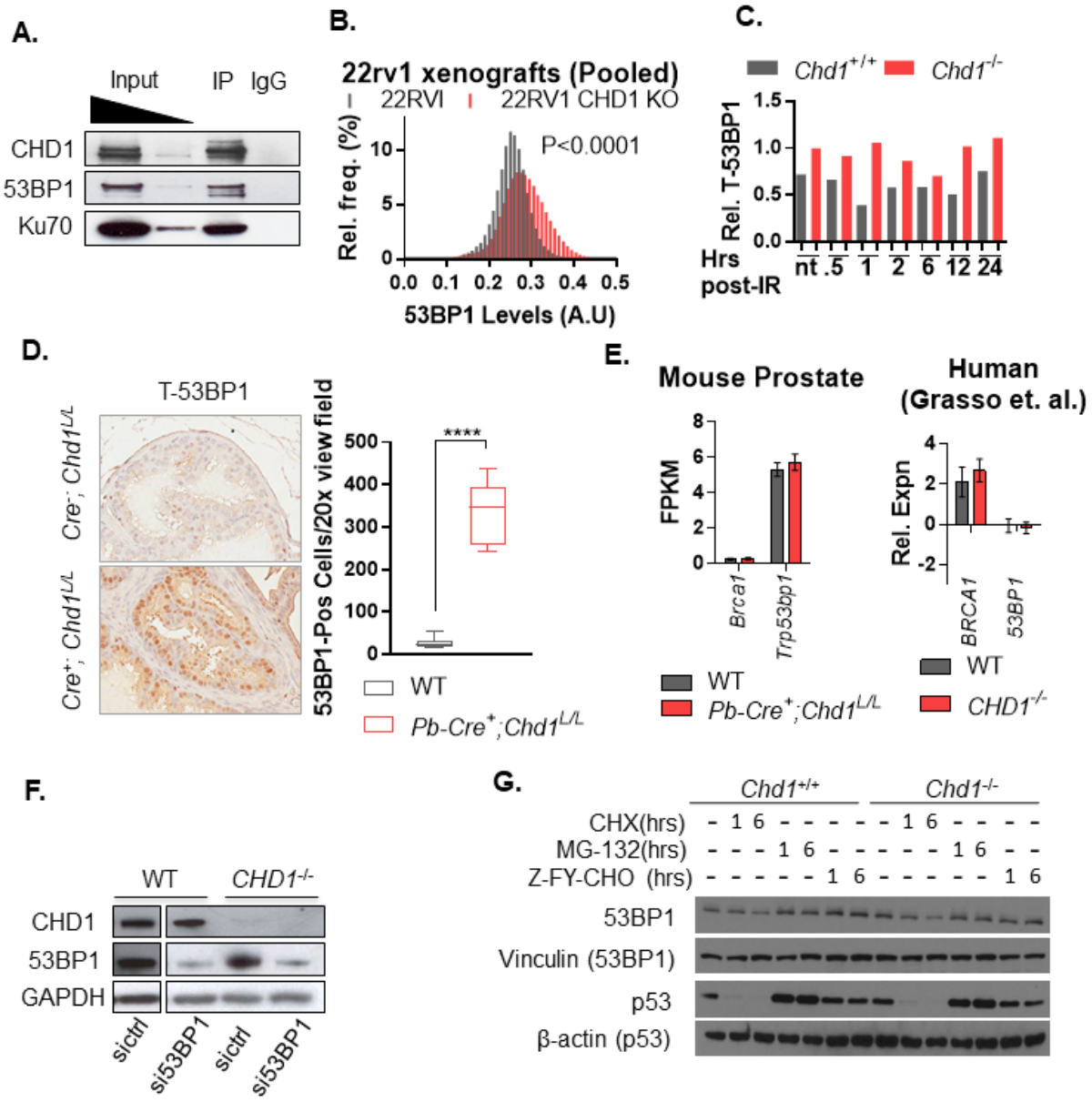

Figure S5, Related to Figure 5. CHD1 interacts with components of NHEJ and stabilizes 53BP1.

A) Co-immunoprecipitation of endogenous CHD1 and the NHEJ proteins 53BP1 and

Ku70 in 22RV1 cells. Two different amounts of precipitate analyzed in first two lanes. IgG functions as negative control.

B) Absolute chromogen values of total 53BP1 in WT or CHD1 KO 22Rv1 xenograft tumors were quantified by Definiens Analysis Software (n=3). P-values of the frequency distributions of the two pooled datasets were determined using the Kolmogorov-Smirnov test.

C) Quantified T-53BP1 levels normalized to actin, from western blot in Figure 5D.

D) (Left) Representative IHC images of total 53BP1 in the anterior lobe of 6 week old *Pb-Cre*$^{+}$;*Chd1*$^{L/L}$ and WT mice. (Right) Quantification of IHC-stained total 53BP1-positive cells in the anterior lobe of 6 week old *Pb-Cre*$^{+}$;*Chd1*$^{L/L}$ and WT mice. ****P<.0001

E) (Left) RNA expression levels of *Brca1* and *Trp53BP1* (encodes 53BP1) in WT (n=6) and *Chd1*-null (n=5) prostates derived from 10-week old mice. (Right) RNA expression levels of *BRCA1* and *53BP1* from publicly available prostate tumor expression data[1].

F) Representative western blot of CHD1 and 53BP1 levels in WT and *CHD1*$^{-/-}$ 22Rv1 cells with or without siRNA of 53BP1.

G) Total 53BP1 and P53 levels in WT and *Chd1*-null mESCs treated with 50µg/mL cycloheximide (CHX), 10 µM ZY-F-CHO, or 10 µM MG-132 and analyzed 1 hour and 6 hours after continuous treatment.

Supplementary Figure 6

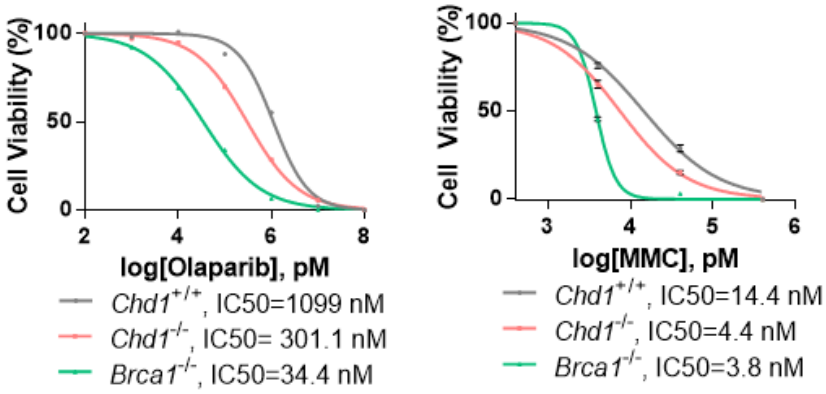

Figure S6, related to Figure 6. CHD1 loss leads to hypersensitivity to PARP inhibition and DNA damaging agents

A) *Chd1* loss leads to hypersensitivity to DNA damaging agents *in vitro*. Cell viability, as determined by MTT assay, of *Chd1*$^{+/+}$, *Chd1*$^{-/-}$, and *Brca1*$^{-/-}$ mESCs 48 hours after continuous treatment of olaparib (left) or mitomycin C (right). IC50 was determined from the non-linear fit of normalized response curves (variable slope) (n=3).

Supplementary Figure 7

A.

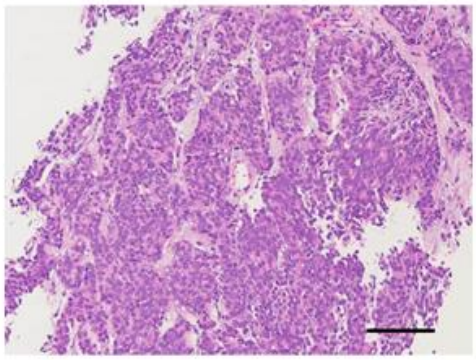

B.

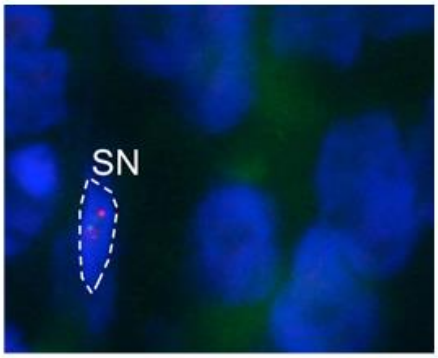

V5272: FISH Ch 5; CHD1; DAPI

C.

	Hb g/L	LDH U/L	AlkP U/L	AST U/L	ALT U/L	PSA ug/L	CTC
11/19/15 (abiraterone)	136	143	38	15	18	12	4
11/05/16 (Pre - carboplatin)	112	780	485	179	165	1300	1157
06/24/16 (Post-carboplatin	105	360	248	22	42	806	30

D.

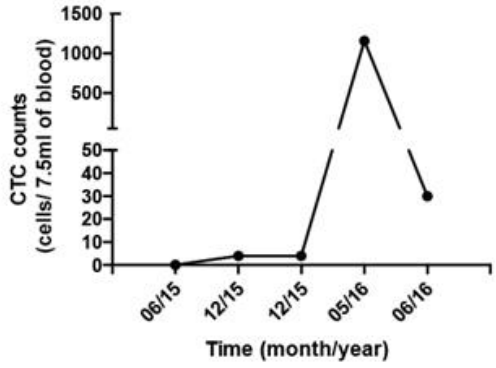

E.

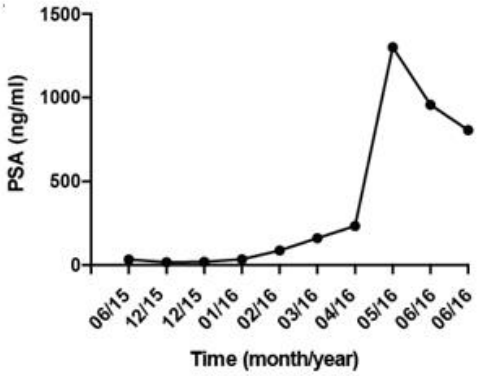

Figure S7, related to Figure 7. Metastatic CRPCs with homozygous loss of CHD1 are sensitive to carboplatin and olaparib in vivo and ex vivo

A) H&E staining of a consecutive section of the lymph node biopsy used for CHD1 IHC as shown in Figure 7A.

B) Representative image of FISH staining for CHD1 in lymph node biopsy from the mCRPC who responded to carboplatin and whose organoids were sensitive to olaparib. Green: CHD1 probe. Red: control probe (chromosome 5p). SN – nucleus of a stromal cell with 2 red and 2 green signals, functioning as positive internal control.

C) Blood test results before and after carboplatin treatment.

D) Circulating tumor cell (CTC) counts during disease progression and response to carboplatin.

E) Prostate-specific antigen (PSA) level during disease progression and response to carboplatin.

Methods

Statistical Analysis

The results are represented as means of at least three independent experiments (standard error of the mean (s.e.m.) are indicated by errors bars). Details on statistical analysis are provided in Supplemental Experimental Procedures.

Mouse Strains

All studies were performed under the regulation of the division of Laboratory Animal Medicine at the University of California at Los Angeles (UCLA). Male *Pb-Cre*$^{+/-}$*;Pten*$^{L/+}$*;Chd1*$^{L/+}$ mice were then back-crossed to female *Chd1*$^{L/L}$ mice. Mice were maintained on a mixed background. *Pb-Cre*$^{+/-}$*;Chd1*$^{L/L}$ were generated by crossing mixed-background *Pb-Cre*$^{+/-}$*;Pten*$^{L/L}$ male mice with C57/Bl female *Chd1*$^{L/L}$ mice (Guzman-Ayala et al., 2015; Koh et al., 2015b)

Mouse xenograft tumor formation assays

All mouse work was carried out in accordance with the Institute of Cancer Research (ICR) guidelines and with the UK Animals (Scientific Procedures) Act 1986 and approved by the ICR Animal Welfare and Ethical Review Body. 2.5x10^6 22Rv1 WT or isogenic CHD1 deleted cells were mixed 1:1 in LDEV-free matrigel (Corning, SLS 354234) and injected subcutaneously into the left flank of male CD1 Nude (CD1-Foxn1^{nu}) mice. The tumors were measured twice per week and tumor volume was calculated using the following calculation: volume (mm^3) = (length x width x width)/ 2.

For PARPi treatment, equal number of *Chd1*$^{+/+}$ and *Chd1*$^{-/-}$ mES cells (2x10^6) were mixed 1:1 in matrigel and implanted onto bilateral flank of nude or NSG mice. The xenograft growth was

monitored daily. When becoming palpable, mice were treated with 100 mg/kg PARP inhibitor olaparib (Selleck; Catalog No.S1060) twice daily IP for 6 days. Olaparib was fresh prepared in 10% DMSO plus 10% 2-hydroxyl-propyl-B cyclodextrin in PBS. Xenograph tumors were measured every 2 days with a caliper and tumor volumes were as above.

Ionizing radiation of mice and cell lines

Pb-Cre^{+}*;Chd1*$^{L/L}$ and *Pb-Cre*$^{-}$*;Chd1*$^{L/L}$ between 12-16 weeks of age were treated with whole body irradiation using an RS320 Irradiation system (Gulmay Medical). Prostates were collected 24 hours after treatment and processed for immunohistochemical analysis. 22Rv1 isogenic cell lines were irradiated at indicated doses. Cells were subsequently processed for immunofluorescence and comet assay.

Chd1$^{+/+}$ and *Chd1*$^{-/-}$ mouse embryonic stem cells were routinely passaged in 0.2% gelatin-coated 100mm dishes every other day in 2i/LIF medium. 2i/LIF medium consists of 1x penicillin/streptomycin, 1x L-Glutamine, 1x N2 supplement (Thermo Scientific, 17502048), 1x B27 supplement (Thermo Scientific, 17504-044), 50µg/ml BSA Fraction V, 1000 U/ml LIF (Millipore, ESG1107), 1µM PD0325901 (LC Laboratories, P-9688), 3µM CHIR99021 (LC Laboratories, C6556), and 150µM monothioglycerol (Sigma M1753) in a basal medium consisting of a 1:1 mixture of DMEM-F12 (Thermo Scientific, 10565-018) and Neurobasal TM (Thermo Scientific 21103049).

Immediately after electroporation, HPRT-DRGFP mESC clones were incubated for 18-24 hours in 15% mESC medium, which consists of 1x penicillin/streptomycin, 1x L-Glutamine, 1000 U/mL LIF (Millipore, ESG1107), 1x MEM nonessential amino acids (Thermo Scientific 11140050),

0.1mM β-mercaptoethanol (Sigma, M6250), and 15% ES cell-qualified fetal bovine serum (Thermo Scientific, 16141079) in knockout DMEM (Thermo Scientific, 10829018).

HEK-293 cells were cultured in freestyle medium (Thermo Scientific 17420999/8116235) containing 1% Fetal Calf Serum (Gibco 42G5550K), and 1% L-Glutamine with shaking at 130 r.p.m.

CRISPR/Cas9 design, generation and screening of CHD1-modified clones

CRISPR/Cas9 design: The online CRISPR Design Tool (http://tools.genome-engineering.org) was used to design single guided RNAs (sgRNA) targeting exon 11 of CHD1 (based on reference sequence: NM_001270). Single guided RNAs were cloned into pSpCas9n (BB)-2A-GFP (Addgene, PX461) as described (Ran et al., 2013).

Cell culture and transfections: The prostate epithelium carcinoma cell line 22Rv1 (ATCC, CRL-2505) was grown in RPMI 1640 supplemented with 2mM Glutamine and 10% fetal Bovine serum (FBS) (Gibco). The prostate epithelium-derived cell line RWPE-1 (ATCC, CRL-11609) was maintained in Keratinocyte-SFM with L-Glutamine (Gibco) supplemented with 0.05mg/ml bovine pituitary extract (BPE) and 5ng/ml human EGF (Miltenyi Biotec, 130-093-825). Cells were transfected with CRISPR/Cas9 plasmids as described using lipofectamine 2000 (Life Technologies) (Ran et al., 2013).

Screening of CHD1-modified clones: Single GFP positive, CAS9 expressing cells were sorted into 96-well plates using FACSAria cell sorter (BD Bioscience) 48 hours post-transfection. Visual monitoring of single-cell-derived clones was performed daily. Only those clones, which were clearly derived from single cells, were expanded and screened for CRISPR/Cas9-mediated genome editing using SURVEYOR mutation assay (IDT, 706020) (Qiu et al., 2004). Briefly, cells

were lysed using the 'hotshot' technique (Truett et al., 2000) and PCR-based amplification of a part of CHD1 exon 11 was carried out in 25µl reactions using Herculase II Fusion DNA polymerase (Agilent Technologies, 600677) using primers which flank the sgRNA biniding sites. Cleavage fragments were analysed using gel electrophoresis and GelRed stain (Biotium, 41003). Single-cell derived clones with presence of insertions/ deletion (Indels) in exon 11 were further validated by Sanger sequencing using the TOPO cloning strategy (Life Technologies). Oligonucleotide sequences can be found in the Supplementary Table.

Immunoblotting

mESCs were harvested in NETN buffer (100 mM NaCl, 20 mM Tris-Cl pH 8.0, 0.5 mM EDTA, 0.5% v/v Igepal CA-430) containing protease (Roche, 11697498001) and phosphatase (Biotool.com, B15001) inhibitors and lysed using freeze-thaw lysis. The soluble fraction was isolated using centrifugation and quantified by bicinchonininc acid assay (BCA) (Pierce, QG219588). Cell lysates were mixed with SDS sample loading buffer (10% SDS (w/v), 30% glycerol (v/v), 0.35M Tris-HCl, pH 6.8, .012% (w/v) Bromophenol Blue, and 0.5 M β-mercaptoethanol (Sigma, M6250). 20-50 µg of total protein were loaded onto hand-cast 8% or 10% SDS acrylamide gels. Transfer to nitrocellulose membrane was performed at 100V for 60 minutes at 4˚C. Protein bands were detected using HRP substrate (GE, RPN2232). Primary and secondary antibodies for immunoblotting are listed below.

22Rv1 isogenic clones were harvested in RIPA buffer (Pierce, 89900) containing protease and phosphatase inhibitors (complete mini protease inhibitor cocktail tablets, Roche, 11374600). The soluble fraction was isolated using centrifugation and quantified by bicinchonininc acid assay (BCA) (Pierce, QG219588). Cell lysates were mixed with LDS sample buffer (Life Technologies, 1621149) and 30-50µg of total protein were loaded onto a 4-12% gradient SDS acrylamide gel

(Life Technologies, NP0322). Transfer to PDVF membrane (Millipore, IPV400010) was performed at 90V for 90min at room temperature. Protein bands were detected using HRP-substrate (Millipore, WBLUC0500). Primary and secondary antibodies for immunoblotting are listed below.

Immunofluorescence

Mouse embryonic stem cells were grown on Matrigel (Corning, 354234)-coated 12mm glass coverslips (Electron Microscopy Sciences, 72196-2), exposed to 5Gy of X-ray irradiation using an RS320 Irradiation system (Gulmay Medical), and incubated for the indicated time intervals. The cells were then pre-extracted by incubating coverslips in ice-cold CSK buffer (10mM PIPES pH 7, 300mM sucrose, 50mM NaCl, 3mM EDTA, 0.5% (v/v) TX-100, protease inhibitor (Roche, 11697498001), Phosphatase inhibitors (Biotools.com, B15001)) for 5 minutes on ice. Cells were washed in cold PBS and fixed with 4% (v/v) paraformaldehyde for 15 minutes at room temperature followed by 2 washes in cold PBS. Cells were subsequently blocked in 5% (w/v) donkey serum (Jackson ImmunoResearch, 17000121) in Dulbecco's PBS (D-PBS) for 30 minutes at room temperature. Primary antibodies diluted in blocking buffer were incubated overnight at 4˚C. Cells were then washed in D-PBS 3x before incubation with alexa fluor-conjugated secondary antibodies (Thermofisher Scientific) diluted in blocking buffer. Cells were washed three times in PBS and coverslips were then mounded on slides in Gold Antifade mounting medium containing DAPI (Thermo Fisher, P36931). Cells were imaged with a Nikon 90i microscope using a Nikon DS-Fi1 camera and a 40x objective. Foci were quantitated using ImageJ software (NIH). Primary and secondary antibodies used for immunofluorescence are listed below.

22Rv1 human isogenic prostate cancer cells were grown on chamber slides (Sigma-Aldrich, C7182) irradiated (5Gy) and fixed in 4% PFA at the indicated time points. Cells were subsequently permeabilized in PBS (0.5% Triton-X) and blocked in 1% BSA in 1x PBS for 30min. Cells were

then incubated in anti-phospho (Ser 139) H2AX (Novus Biologicals, NBP1-61896, 1:500), anti-53BP1 (Novus Biologicals, NB 100-904, 1:500), anti-RAD51 (Calbiochem, PC130, 1:500), anti-BRCA1 (abcam, ab131360) or anti-phospho- (S1524) BRCA1 (Cell signaling, 9009) primary antibodies followed by Alexa-Fluor 555 anti-rabbit secondary antibody (Life Technologies, A21428). Images were taken on the Bioview Duet automated imaging system (Bioview) using a Olympus U-CMAD3 camera and a 40x objective (Olympus, LUCPlan FLN).

RT-PCR analysis

Total RNA was extracted from *Chd1*$^{+/+}$ and *Chd1*$^{-/-}$ cells using the RNeasy Mini Kit (Qiagen, 74104). RNA was reverse-transcribed into cDNA with HiScript II Q RT SuperMix system (Vazyme, R223). Quantitative RT-PCR was performed using SYBR Green master mix (without ROX) system (Vazyme, Q121). Primer sequences are described in Supplementary Table 1.

Cell Cycle Analysis

Approximately 5x10^6 cells were harvested and permeabilized with 1% (v/v) triton X-100 in D-PBS for 5 minutes. Cells were then resuspended in 1µg/mL DAPI and incubated for 30 minutes on ice. Cells were analyzed by FACS on the LSR II (BD Biosciences). For Propidium Iodide staining, 22Rv1 cells were harvested and resuspended in 200µl of PBS. A volume of 2ml ice-cold 70% ethanol and 30% PBS was added vigorously using vortex. Cells were incubated 30min in cold then centrifuged and resuspended in 800µl of PBS. Cells were assessed microscopically for the presence of clumps. If clumps were present cell suspension was passed through a 25-gauge syringe needle. A volume of 100µl of RNase (1mg/ml) (Sigma) and 200µl of PI (250 µg /ml) (Invitrogen) was added and incubated at 37°C for 30min. Analysis of DNA content was performed in the BD LSRII FACS analyzer.

Drug Toxicity Assay

To investigate cytotoxicity, 3-[4,5-dimethylthiazol-2-yl]-2,5-diphenyltetrazolium (MTT) colorimetric assay was used (Thermo Fisher, M6494). $2.5x10^4$ cells were plated into each well of a 24-well plate and incubated overnight. Cells were continuously treated with various concentrations of Olaparib (LC Laboratories, O-9201), nu7441 (SelleckChem, S2638), and Mitomycin C (R&D Systems, 3258) for 48 hours. After incubation, 50 µL of 12 mM MTT (Thermo Fisher, V6494) was added to each well for 4 hours at 37˚C. Formazan crystals were dissolved by addition of 10% (w/v) SDS dissolved in 0.01 M HCl. The absorbance was read at 570 nm on a microplate reader (Bio-Rad).

Patient-derived organoids were harvested in PBS and trypsinized as described previously (Drost et al., 2016). Single cells were mixed in a 1:2 ratio with growth factor depleted matrigel. The matrigel-cell suspension was plated as 5µl drops into wells of a 96 well plate. Sensitivity to Olaparib (Selleckchem, S1060) was determined in a 6-point dilution curve (0µM-100µM) of Olaparib in organoid medium using 0.2% DMSO as control. Cell viability was measured after 7 days by using the CellTiter-Glo 3D cell viability assay (Promega, G9681). Luminescence intensity was quantified using plate reader (Biotek Synergy HT). The IC50 was calculated using Graph Pad Prism 6 (Graph Pad Software Inc).

Clonogenic assay

Mouse embryonic stem cells growing exponentially were harvested into a single-cell suspension at $2x10^4$ cells/mL in 2i/lif medium and treated with various doses of ionizing radiation (Rad Source, RS2000 X –ray system). $2x10^4$ cells were then seeded into each well of a 24-well plate on

irradiated MEF feeders and incubated for 4 days in 2i/lif medium. Cell numbers from each well were then counted using Trypan Blue exclusion (Thermo Fisher, 15250061).

Neutral Comet Assay

The neutral comet assay was performed using Trevigen Comet Assay™ kit (Trevigen, Inc). Slides were imaged using an Olympus Ix73 fluorescence microscope with a 10x objective lens. Casp Lab software v1.2.2 (University of Wroclaw, Wroclaw, Poland) was used to quantify the comet tail length of each cell. At least 100 cells were analyzed at each indicated time-point.

Co-immunoprecipitation

Prostate cancer cell line 22Rv1 cells were harvest and nuclear extracts (NE) were isolated using NE-PER Nuclear and cytoplasmic extraction kit (Thermo Scientific).

200µg of NE were used for immunoprecipitation (IP) with 10µl CHD1 antibody (NB100-60411, Novus). Protein-antibody complexes were pulled down using magnetic beads (Millipore). A quarter of CHD1 IP was boiled in SDS sample buffer and loaded on a 4-12% PAGE for immunoblotting.

HEK-293 cells were harvested, washed twice with PBS and lysed in Sucrose-Lysis buffer (25mM Tris-HCl pH 7.5, 150mM NaCl, 5mM $MgCl_2$, 0.5% NP-40, 0.25M Sucrose, 10mM NaF, 1mM $NaVO_3$, 1mM DTT, 1mM PSMF and protease and phosphatase inhibitors (Roche, 04906837001 and 04693132001)) for 30min on ice. Cell lysates were spun at 90000 rpm for 15min at 4˚C and the supernatant was transferred to another tube containing CHD1 antibody (Bethyl, A310-411A or Proteintech, 20576-1-AP) and pre-washed with protein A-beads (GE 17-5280-02. The mixture was rotated in the cold room on a rotator for 3-4h. The immunoprecipitate was collected by centrifugation (1000 rpm, 1min), washed four times with wash buffer (25mM Tris-HCl pH 7.5,

150mM NaCl, 5mM $MgCl_2$, NP-40 0.1%, Glycerol 10%,1mM DTT, 1mM PSMF), eluted with glycine (100mM pH2.5) then neutralized by 1/10 volume of Tris-HCl (1M, pH 8.0) before analyzed by SDS-PAGE and immunoblotting as described.

Gel Filtration

Cells were lysed in Sucrose-Lysis buffer as described previously. After lysis on ice for 30min and centrifugation, samples were applied to a Sephacryl S-300 column (Amersham Biosciences) and eluted with PBS in 2-ml fraction volumes with a 0.5 ml/min flow rate followed by immunoblot analysis as described previously.

Generation of HPRT-DRGFP mESC Clones

Seventy microgram of linearized pHPRT-DRGFP (Addgene, 26475) plasmids were electroporated at 0.8kV, 3 µF into approximately $4x10^6$ *Chd1*$^{-/-}$ and *Chd1*$^{+/+}$ mESCs that were resuspended in pre-warmed D-PBS. Successful HPRT-specific integrants were selected by culturing electroporated cells with 2 µg/mL Puromycin and 10µg/mL 6-thioguanine. Drug-resistant clones were picked 2 weeks after electroporated and cultured under non-selective conditions. Clones with a single copy of DR-GFP integrated into the HPRT locus were identified by PCR using the following primers: HPRTIntegration-F: 5'-AGT GCT TCA GCC GCT ACC, HPRTIntegration-R: 5'-GCT GGG ACT GCA CAG AGA GT, GFPInternal-F: 5'-CCT GAA GTT CAT CTG CAC CA, GFPInternal-R: 5'-GGT CTT GTA GTT GCC GTC GT. These clones were then used for measuring HR Recombination proficiency.

HPRT DR-GFP Assays

Briefly, approximately $4x10^7$ *Chd1*$^{+/+}$-DRGFP, *Chd1*$^{-/-}$-DRGFP, or *Brca1*$^{-/-}$-DRGFP (kindly provided by Maria Jasin) cells were trypsinized and resuspended in pre-warmed D-PBS. Either

50µg of pCBASceI (Addgene, 26477) and 50µg of pCAGGs-mCherry (Addgene, 41583) together or 50µg of pCAGGs-mCherry only as an empty vector control, were electroporated in a 0.4cm cuvette at 250V, 1000µF (Biorad). Electroporated cells were immediately transferred to 0.2% gelatin-coated 100mm plates with pre-warmed 15% ES media for 18-24 hours. The next day, cells were rinsed 2x with pre-warmed D-PBS and incubated in pre-warmed 2i/lif media. 96 hours after electroporation, approximately $1x10^6$ cells were harvested and analyzed on a LSRII (BD) using FlowJo Software. At least 200,000 events were scored per sample, and the proportion of GFP-positive events provided the measure of DSB repair.

To determine the percentage of I-SceI site loss for each electroporation, genomic DNA was isolated 7 days after transfection. Genomic DNA (0.4µg) was used as the template for PCR with primers in a reaction volume of 50µL. The sequences of primers were as follows: F-DRGFP: 5'-AGGGCGGGGTTCGGCTTCTGG, R-DRGFP: 5'-CCTTCGGGCATGGCGGACTTGA. PCRs were performed using the GC-RICH PCR System (Roche, 12140306001). PCR was performed for 27 cycles with a 1 minute amplification time. After amplification, PCR products were digested overnight with 10 units of I-SceI (New England BioLabs, R0694S). After I-SceI digestion, products were purified using the PureLink Gel Extraction Kit (Invitrogen, K210012). Half the volume of products was digested with 10 units of BcgI overnight (New England BioLabs, R0545S). The products digested with I-SceI and both I-SceI and BcgI were separated on a 1.2% agarose gel. The gel was stained with ethidium bromide, the image was acquired and the ethidium signals for the enzyme-resistant and enzyme-cleaved bands quantified using the ChemiDoc imager and ImageLab software (Bio-Rad).

Protein Stability Assays

For protein stability with irradiation, $4x10^7$ cells were plated overnight in 100mm plates and then pre-treated with 50µg/mL of cycloheximide (Sigma, C7698) , 10µM MG-132 (Millipore, 47490), for 15 minutes before being treated with 5 Gy of ionizing radiation. Cells were continuously treated with cycloheximide or MG-132 for the indicated times until collection and processing for immunoblotting. For protein stability assays without irradiation, cells $4x10^7$ cells were plated overnight in 100mm plates and then treated continuously for the indicated times with 50ug/mL cycloheximide, 10µM MG-132, or 10µM Z-FY-CHO (Santa Cruz Biotech, sc-3132).

siRNA transfection

siRNAs targeting 53BP1 and non-targeting controls were purchased from Dharmacon (siGenome smartpool 53BP1:M-003548-01, siGenome smartpool non-targeting control: D-001206-13-05). siRNA oligonucleotides were transfected with lipofectamine 3000 (Life Technologies) at a final concentration of 100pmol and incubated for 48hrs.

Human prostate cancer metastasis biopsies

Biopsies from metastases within bone, lymph node and liver were obtained under imaging guidance from patients with metastatic-castration resistant prostate cancer. All patients gave their written informed consent and were enrolled in institutional protocols approved by the Royal Marsden NHS Foundation Trust Hospital (London, UK) ethics review committee (reference no. 04/Q0801/60).

Patient-derived organoid culture

Biopsies from patients suffering from metastatic castration-resistant prostate cancer were processed for organoid culture as described previously (Drost et al., 2016). Briefly, biopsy tissue was washed in PBS (0.5%BSA, 10µM Y-27632 (Abmole Bioscience, M1817) and subsequently

minced into small pieces by using a scalpel followed by digestion using collagenase II (Life Technologies, 17101-015, 1:250 dilution v/v) for 30-45min at 37°C. Digested biopsies were then washed in PBS (%BSA, 10µM Y-27632), centrifuged at 800xg for 5min and resuspended in fresh PBS (%BSA, 10µM Y-27632). The crude cell suspension was further separated into single cells by using a 20µM cell strainer (BD Biosciences, 352340). The resulting single cells were collected by centrifugation (800xg) and resuspended in 50µl of organoid medium (Drost et al., 2016). Two to five microliter of the single cell suspension were used for a cytosmear using Menzel glass tissue slides (Thermo Scientific, BS 7011/2). The remaining cell suspension was mixed on ice in a 1:2 ratio with cold growth factor depleted matrigel (BD Biosciences, 356231) and the cell-matrigel mixture was plated in 20µl drops into wells of 24-well tissue culture plates. Organoid medium was added approximately 30 minutes after plating when the matrigel solidified. For replating, prostate cancer organoids were harvested with ice cold PBS (0.5%BSA, 10µM Y-27632), centrifuged at 800xg and resuspended in the appropriate amount of cold growth factor depleted matrigel.

Clinical data on reported case

Response to treatment was evaluated according to the Response Evaluation Criteria in Solid Tumors (RECIST) version 1.1 criteria (Eisenhauer et al., 2009; Scher et al., 2016), reduction in the prostate-specific antigen (PSA) and reduction in the number of circulating tumor cell (CTC) count. CTC counts were quantified by using the CellSearch system (Veridex) as published previously(de Bono et al., 2008; Mateo et al., 2015a).

Digital droplet PCR analysis

CHD1 copy number aberration (CNA) in patient-derived organoids were assessed using droplet digital PCR (ddPCR). Organoid DNA was purified using QIAamp Mini Kit (Qiagen, 51304).

Purified genomic DNA (5-10ng) was added directly to ddPCR supermix for probes (Bio-Rad) together with primers for CHD1-intron 1 (Hs06044820_cn) or CHD-intron 34 (Hs06041478_cn), labelled with FAM (Applied Biosystems) and EIF2C1 (dHs CP2500349) reference assay, labelled with HEX (Bio-Rad). Droplets were generated using Bio-Rad droplet generator. Thermal cycling conditions were 95 °C × 10 min (1 cycle), 94 °C × 30 s and 60 °C × 60 s (40 cycles), 98 °C × 10 min (1 cycle), and 12 °C hold on Eppendorf NexusGSX1 cycler. Droplets were analyzed immediately on the Bio-Rad reader and quantified using Quanta Soft (Bio-Rad).

Histology and immunohistochemistry

For mouse tissue, immunohistochemistry was performed on FFPE tissues. Slides were dewaxed using xylene. Antigen retrieval was performed by boiling 4µm tissue sections in 10mM citrate buffer (10mM citric acid in deionized water) (pH 6) for 30 minutes followed by 1 hour cooling at room temperature. Primary and secondary antibodies for immunohistochemistry are listed below. Immunohistochemistry on 22Rv1 xenograft tumors was performed on FFPE tissue. Slides were dewaxed using xylene. Antigen retrieval was performed by boiling 3µM tissue sections in citrate buffer (TCS Biosciences Ltd., HDS05, 1:100 dilution, pH 6) for 18min using a microwave. Sections were subsequently washed in running tap water for 5min and rinsed in distilled water before soaking in TBST (0.2% Tween) for 25min. CHD1 immunostaining was done on the i6000 IHC autostainer using a 1:50 dilution of primary antibody (Cell Signaling, 4351 for 1hr) followed by the Novolink polymer detection method (Leica, RE7200-CE). Tumor content, morphology and intensity of CHD1 expression was evaluated by a pathologist (D.N.R.)

RNA-seq library and analysis

The right anterior lobes of *Pb-Cre*$^{+}$*;Chd1*$^{L/L}$ and *Pb-Cre*$^{-}$ mice from 9-12 weeks of age were dissected and stored in RNA-later (Thermo Fisher, AM7020). RNA extraction, RNA quality control, library preparation, and sequencing were performed by the UCLA Clinical Microarray Core (http://pathology.ucla.edu/cmc). High throughput sequencing with 100bp paired-end reads was performed using an Illumina HiSeq 2500 system. The RNA-seq raw sequences were mapped to mouse genome mm9 using TopHat (v2.0.13)(Trapnell et al., 2009) utilizing bowtie (v1.1.1)(Langmead et al., 2009) with default parameters. The Fragments Per Kilobase of transcript per million mapped reads (FPKMs) were calculated and normalized by cufflinks (v2.2.1)(Trapnell et al., 2012). The differentially transcribed genes analysis was carried out by cuffdiff.

For the 22Rv1 isogenic cell clones RNA-seq raw data were aligned to the human genome GRCh37.61 using TopHat (v2.0.7) with default parameters and transcripts were assembled based on Homo_sapiens.GRCh37.61.gtf file. Relative expression level, represented as FPKM, were estimated by cufflinks (v2.2.1) and normalized against total mapped reads per sample.

Fluorescence In Situ Hybridization (FISH)

FISH for assessing CHD1 copy number status in formalin-fixed and paraffin-embedded tumor tissue was performed as described previously (Ferraldeschi et al., 2015). The probes were a kind gift of Prof Mark Rubin (WCMC, NYC): CHD1 (RP11-58M12, chr. 5q21) and reference (RP11-429D13, chr. 5p13.1). Probes were amplified using the GenomiPhi v3 DNA amplification kit (Illustra, 25-6601-24) and directly labeled with CY3 (CHD1) and CY5 using the Bioprime DNA labeling system (Thermo Fisher Scientific, 18094011). Fluorescence images were taken using the Bioview Duet imaging system and copy number status of at least 50 tumor cell nuclei was determined by a pathologist (D.N.R).

Antibodies

Primary antibodies used for immunohistochemistry include phospho- (Ser 139) H2AX (Cell Signaling; 9718), 53BP1 (Novus Biologicals, NB100-304), Androgen Receptor (Santa Cruz Biotechnologies, Sc-816), ki67 (Vector Labs, VPRM04), Cleaved Caspase 3 (Cell Signaling 9664), Smooth Muscle Actin (Sigma, A2547). Secondary antibodies used were Biotin-conjugated Donkey Anti-Rabbit and Anti-Mouse IgG H&L (Abcam, ab6801 and ab97028). Primary antibodies used for immunoblotting include phospho-(Ser 139) H2AX (Cell signaling, 9718), phoshpho-53BP1 (Cell Signaling, 3428), 53BP1 (Novus Biologicals, NB100-304), β-actin (Sigma), phospho-P53 (Cell Signaling, 12571 XP), P53 (Cell Signaling, 2524), cleaved PARP (Cell signaling, 9544), phospho-histone H3 (Cell Signaling, 3377), RAD51 (Calbiochem, PC130), KU70 (Abcam, ab3114), 53BP1 (Millipore, MAB3804), SSRP1 (Biolegend, 609701) and CHD1 (Cell Signaling, 4351). Secondary antibodies were anti-Rabbit and anti-Mouse horseradish peroxidase-conjugated whole antibody from sheep (GE, NA934V and NXA93). Primary antibodies used for immunofluorescence include phosphor- (Ser 139) H2AX (Cell Signaling; 9718), 53BP1 (Novus Biologicals, NB100-304), RAD51 (Calbiochem, PC130), and. Secondary antibodies were Donkey anti-Rabbit IgG (H+L) Alexa Fluor 488 conjugate (Thermo Fisher, A-21206). Antibodies for Immunoprecipitation and Gel filtration experiments: CHD1(Bethyl A310-411A), 53BP1 (Abcam,ab175933), Ku70(proteintech 10723-1-AP), Ku80(proteintech 16389-1-AP), Rad51(proteintech 14961-1-AP), Rif1(Sigma SAB2502070)

Statistical Analysis

The results are represented as means of at least three independent experiments (standard error of the mean (s.e.m.) are indicated by errors bars). Fisher's exact test (two sided) was used to

assess the statistical significance of differences in the foci experiments. Student’s t-test was used to calculate the statistical significance of differences in cell cycle distribution.

Comparisons between two groups were assessed with a two-tailed Student's t-test for paired and unpaired data if data were normally distributed. Mann-Whitney unpaired tests were used when the populations were not normally distributed. Multiple groups were analyzed by one-way ANOVA with corresponding Tukey's multiple comparison test if normally distributed, or by the Kruskal-Wallis test with Dunn's multiple comparison test if not normally distributed. All statistical analyses were performed with GraphPad Prism 6. A p value of less than 0.05 was considered statistically significant.

22Rv1 xenograft growth: Differences in tumor growth of 22Rv1 isogenic cell line xenografts were analyzed by Kaplan-Meier analysis.

IC50 was determined from the non-linear fit of normalized response curves (variable slope) in the ex vivo mCRPC-derived organoid olaparib sensitivity assays and the mESC drug sensitivity assays. .

Acknowledgments:

We thank Dr. Maria Jasin for providing BRCA1 null mESC line, HDRGFP construct and helpful discussions; Wenkai Yi and Bohan Chen for technical assistance; members of the Wu and De Bono laboratories for comments and suggestions. MYW is supported by the Presidential Fellowship of Peking University; GB is supported by Marie Sklodowska-Curie Individual Fellowship and WLG is supported by a General Financial Grant from the China Postdoctoral Science Foundation (2015M570010).

This work was supported in part by awards from the Peking-Tsinghua Center for Life sciences (to HW); grants from the NIH (P50 CA092131 and U01 CA164188 to HW and R01GM113014 to MR-S); a PCa UK project grant (PG13-036 to JDB), a Movember/PCUK Programme grant to the London PCa Centre of Excellence, a Cancer Research UK Centre grant, an ECMC grant and a Royal Marsden Biomedical Research Centre flagship grant (A34 to JDB).

References

Abeshouse, A., Ahn, J., Akbani, R., Ally, A., Amin, S., Andry, C.D., Annala, M., Aprikian, A., Armenia, J., Arora, A.*, et al.* (2015). The Molecular Taxonomy of Primary Prostate Cancer. Cell *163*, 1011-1025.

Al-Ubaidi, F.L., Schultz, N., Loseva, O., Egevad, L., Granfors, T., and Helleday, T. (2013). Castration therapy results in decreased Ku70 levels in prostate cancer. Clin Cancer Res *19*, 1547-1556.

Baca, S.C., Prandi, D., Lawrence, M.S., Mosquera, J.M., Romanel, A., Drier, Y., Park, K., Kitabayashi, N., MacDonald, T.Y., Ghandi, M.*, et al.* (2013a). Punctuated Evolution of Prostate Cancer Genomes. Cell *153*, 666-677.

Baca, S.C., Prandi, D., Lawrence, M.S., Mosquera, J.M., Romanel, A., Drier, Y., Park, K., Kitabayashi, N., MacDonald, T.Y., Ghandi, M.*, et al.* (2013b). Punctuated evolution of prostate cancer genomes. Cell *153*, 666-677.

Bhatia-Gaur, R., Donjacour, A.A., Sciavolino, P.J., Kim, M., Desai, N., Young, P., Norton, C.R., Gridley, T., Cardiff, R.D., Cunha, G.R.*, et al.* (1999). Roles for Nkx3.1 in prostate development and cancer. Genes Dev *13*, 966-977.

Boysen, G., Barbieri, C.E., Prandi, D., Blattner, M., Chae, S.S., Dahija, A., Nataraj, S., Huang, D., Marotz, C., Xu, L.*, et al.* (2015). SPOP mutation leads to genomic instability in prostate cancer. Elife *4*.

Brown, C.E., and Warren, S. (1978). Carcinoma of the prostate in irradiated parabiotic rats. Cancer Res *38*, 159-162.

Bryant, H.E., Schultz, N., Thomas, H.D., Parker, K.M., Flower, D., Lopez, E., Kyle, S., Meuth, M., Curtin, N.J., and Helleday, T. (2005). Specific killing of BRCA2-deficient tumours with inhibitors of poly(ADP-ribose) polymerase. Nature *434*, 913-917.

Bunting, S.F., Callen, E., Wong, N., Chen, H.T., Polato, F., Gunn, A., Bothmer, A., Feldhahn, N., Fernandez-Capetillo, O., Cao, L.*, et al.* (2010). 53BP1 inhibits homologous recombination in Brca1-deficient cells by blocking resection of DNA breaks. Cell *141*, 243-254.

Bunting, S.F., and Nussenzweig, A. (2013). End-joining, translocations and cancer. Nature Reviews Cancer *13*, 443-454.

Burkhardt, L., Fuchs, S., Krohn, A., Masser, S., Mader, M., Kluth, M., Bachmann, F., Huland, H., Steuber, T., Graefen, M.*, et al.* (2013). CHD1 Is a 5q21 Tumor Suppressor Required for ERG Rearrangement in Prostate Cancer. Cancer research *73*, 2795-2805.

Chapman, J.R., Taylor, M.R., and Boulton, S.J. (2012). Playing the end game: DNA double-strand break repair pathway choice. Molecular cell *47*, 497-510.

Chen, Z., Trotman, L.C., Shaffer, D., Lin, H.K., Dotan, Z.A., Niki, M., Koutcher, J.A., Scher, H.I., Ludwig, T., Gerald, W.*, et al.* (2005). Crucial role of p53-dependent cellular senescence in suppression of Pten-deficient tumorigenesis. Nature *436*, 725-730.

Cunha, G.R. (1973). The role of androgens in the epithelio-mesenchymal interactions involved in prostatic morphogenesis in embryonic mice. Anat Rec *175*, 87-96.

de Bono, J.S., Scher, H.I., Montgomery, R.B., Parker, C., Miller, M.C., Tissing, H., Doyle, G.V., Terstappen, L.W., Pienta, K.J., and Raghavan, D. (2008). Circulating tumor cells predict survival benefit from treatment in metastatic castration-resistant prostate cancer. Clin Cancer Res *14*, 6302-6309.

Drost, J., Karthaus, W.R., Gao, D., Driehuis, E., Sawyers, C.L., Chen, Y., and Clevers, H. (2016). Organoid culture systems for prostate epithelial and cancer tissue. Nat Protoc *11*, 347-358.

Eisenhauer, E.A., Therasse, P., Bogaerts, J., Schwartz, L.H., Sargent, D., Ford, R., Dancey, J., Arbuck, S., Gwyther, S., Mooney, M.*, et al.* (2009). New response evaluation criteria in solid tumours: revised RECIST guideline (version 1.1). Eur J Cancer *45*, 228-247.

Ferraldeschi, R., Nava Rodrigues, D., Riisnaes, R., Miranda, S., Figueiredo, I., Rescigno, P., Ravi, P., Pezaro, C., Omlin, A., Lorente, D.*, et al.* (2015). PTEN protein loss and clinical outcome from castration-resistant prostate cancer treated with abiraterone acetate. Eur Urol *67*, 795-802.

Francis, J.C., McCarthy, A., Thomsen, M.K., Ashworth, A., and Swain, A. (2010). Brca2 and Trp53 deficiency cooperate in the progression of mouse prostate tumourigenesis. PLoS Genet *6*, e1000995.

Gao, D., Vela, I., Sboner, A., Iaquinta, P.J., Karthaus, W.R., Gopalan, A., Dowling, C., Wanjala, J.N., Undvall, E.A., Arora, V.K.*, et al.* (2014). Organoid cultures derived from patients with advanced prostate cancer. Cell *159*, 176-187.

Gaspar-Maia, A., Alajem, A., Polesso, F., Sridharan, R., Mason, M.J., Heidersbach, A., Ramalho-Santos, J., McManus, M.T., Plath, K., Meshorer, E.*, et al.* (2009). Chd1 regulates open chromatin and pluripotency of embryonic stem cells. Nature *460*, 863-868.

Gonzalez-Suarez, I., Redwood, A.B., Grotsky, D.A., Neumann, M.A., Cheng, E.H., Stewart, C.L., Dusso, A., and Gonzalo, S. (2011). A new pathway that regulates 53BP1 stability implicates cathepsin L and vitamin D in DNA repair. Embo J *30*, 3383-3396.

Goodwin, J.F., Schiewer, M.J., Dean, J.L., Schrecengost, R.S., de Leeuw, R., Han, S.M., Ma, T., Den, R.B., Dicker, A.P., Feng, F.Y.*, et al.* (2013). A Hormone-DNA Repair Circuit Governs the Response to Genotoxic Insult. Cancer discovery *3*, 1254-1271.

Grasso, C.S., Wu, Y.M., Robinson, D.R., Cao, X.H., Dhanasekaran, S.M., Khan, A.P., Quist, M.J., Jing, X., Lonigro, R.J., Brenner, J.C.*, et al.* (2012). The mutational landscape of lethal castration-resistant prostate cancer. Nature *487*, 239-243.

Guzman-Ayala, M., Sachs, M., Koh, F.M., Onodera, C., Bulut-Karslioglu, A., Lin, C.J., Wong, P., Nitta, R., Song, J.S., and Ramalho-Santos, M. (2015). Chd1 is essential for the high transcriptional output and rapid growth of the mouse epiblast. Development *142*, 118-127.

Han, X., Zhang, L., Chung, J., Mayca Pozo, F., Tran, A., Seachrist, D.D., Jacobberger, J.W., Keri, R.A., Gilmore, H., and Zhang, Y. (2014). UbcH7 regulates 53BP1 stability and DSB repair. Proceedings of the National Academy of Sciences of the United States of America *111*, 17456-17461.

Hieronymus, H., Lamb, J., Ross, K.N., Peng, X.P., Clement, C., Rodina, A., Nieto, M., Du, J., Stegmaier, K., Raj, S.M.*, et al.* (2006). Gene expression signature-based chemical genomic prediction identifies a novel class of HSP90 pathway modulators. Cancer Cell *10*, 321-330.

Hu, Y., Wang, C., Huang, K., Xia, F., Parvin, J.D., and Mondal, N. (2014). Regulation of 53BP1 protein stability by RNF8 and RNF168 is important for efficient DNA double-strand break repair. PLoS One *9*, e110522.

Huang, S., Gulzar, Z.G., Salari, K., Lapointe, J., Brooks, J.D., and Pollack, J.R. (2012). Recurrent deletion of CHD1 in prostate cancer with relevance to cell invasiveness. Oncogene *31*, 4164-4170.

Johnson, N., Johnson, S.F., Yao, W., Li, Y.C., Choi, Y.E., Bernhardy, A.J., Wang, Y., Capelletti, M., Sarosiek, K.A., Moreau, L.A.*, et al.* (2013). Stabilization of mutant BRCA1 protein confers PARP inhibitor and platinum resistance. Proceedings of the National Academy of Sciences of the United States of America *110*, 17041-17046.

Kari, V., Mansour, W.Y., Raul, S.K., Baumgart, S.J., Mund, A., Grade, M., Sirma, H., Simon, R., Will, H., Dobbelstein, M.*, et al.* (2016). Loss of CHD1 causes DNA repair defects and enhances prostate cancer therapeutic responsiveness. EMBO Rep *17*, 1609-1623.

Koh, F.M., Lizama, C.O., Wong, P., Hawkins, J.S., Zovein, A.C., and Ramalho-Santos, M. (2015a). Emergence of hematopoietic stem and progenitor cells involves a Chd1-dependent increase in total nascent transcription. Proceedings of the National Academy of Sciences of the United States of America *112*, E1734-E1743.

Koh, F.M., Lizama, C.O., Wong, P., Hawkins, J.S., Zovein, A.C., and Ramalho-Santos, M. (2015b). Emergence of hematopoietic stem and progenitor cells involves a Chd1-dependent increase in total nascent transcription. Proc Natl Acad Sci U S A *112*, E1734-1743.

Konev, A.Y., Tribus, M., Park, S.Y., Podhraski, V., Lim, C.Y., Emelyanov, A.V., Vershilova, E., Pirrotta, V., Kadonaga, J.T., Lusser, A.*, et al.* (2007). CHD1 motor protein is required for deposition of histone variant h3.3 into chromatin in vivo. Science *317*, 1087-1090.

Kumar, A., Coleman, I., Morrissey, C., Zhang, X., True, L.D., Gulati, R., Etzioni, R., Bolouri, H., Montgomery, B., White, T.*, et al.* (2016). Substantial interindividual and limited intraindividual genomic diversity among tumors from men with metastatic prostate cancer. Nat Med *22*, 369-378.

Kyprianou, N., and Isaacs, J.T. (1988). Activation of programmed cell death in the rat ventral prostate after castration. Endocrinology *122*, 552-562.

Langmead, B., Trapnell, C., Pop, M., and Salzberg, S.L. (2009). Ultrafast and memory-efficient alignment of short DNA sequences to the human genome. Genome Biol *10*.

Lin, J.J., Lehmann, L.W., Bonora, G., Sridharan, R., Vashisht, A.A., Tran, N., Plath, K., Wohlschlegel, J.A., and Carey, M. (2011). Mediator coordinates PIC assembly with recruitment of CHD1. Genes & development *25*, 2198-2209.

Liu, W., Lindberg, J., Sui, G., Luo, J., Egevad, L., Li, T., Xie, C., Wan, M., Kim, S.T., Wang, Z.*, et al.* (2012). Identification of novel CHD1-associated collaborative alterations of genomic structure and functional assessment of CHD1 in prostate cancer. Oncogene *31*, 3939-3948.

Lusser, A., Urwin, D.L., and Kadonaga, J.T. (2005). Distinct activities of CHD1 and ACF in ATP-dependent chromatin assembly. Nature structural & molecular biology *12*, 160-166.

Maddison, L.A., Sutherland, B.W., Barrios, R.J., and Greenberg, N.M. (2004). Conditional deletion of Rb causes early stage prostate cancer. Cancer Res *64*, 6018-6025.

Mallette, F.A., and Richard, S. (2012). K48-linked ubiquitination and protein degradation regulate 53BP1 recruitment at DNA damage sites. Cell Res *22*, 1221-1223.

Mateo, J., Carreira, S., Sandhu, S., Miranda, S., Mossop, H., Perez-Lopez, R., Nava Rodrigues, D., Robinson, D., Omlin, A., Tunariu, N.*, et al.* (2015a). DNA-Repair Defects and Olaparib in Metastatic Prostate Cancer. N Engl J Med *373*, 1697-1708.

Mateo, J., Carreira, S., Sandhu, S., Miranda, S., Mossop, H., Perez-Lopez, R., Rodrigues, D.N., Robinson, D., Omlin, A., Tunariu, N.*, et al.* (2015b). DNA-Repair Defects and Olaparib in Metastatic Prostate Cancer. New Engl J Med *373*, 1697-1708.

Metzger, E., Willmann, D., McMillan, J., Forne, I., Metzger, P., Gerhardt, S., Petroll, K., von Maessenhausen, A., Urban, S., Schott, A.K.*, et al.* (2016a). Assembly of methylated KDM1A and CHD1 drives androgen receptor-dependent transcription and translocation. Nature structural & molecular biology *23*, 132-+.

Metzger, E., Willmann, D., McMillan, J., Forne, I., Metzger, P., Gerhardt, S., Petroll, K., von Maessenhausen, A., Urban, S., Schott, A.K.*, et al.* (2016b). Assembly of methylated KDM1A and CHD1 drives androgen receptor-dependent transcription and translocation. Nat Struct Mol Biol *23*, 132-139.

Mulholland, D.J., Tran, L.M., Li, Y., Cai, H., Morim, A., Wang, S., Plaisier, S., Garraway, I.P., Huang, J., Graeber, T.G.*, et al.* (2011). Cell autonomous role of PTEN in regulating castration-resistant prostate cancer growth. Cancer cell *19*, 792-804.

Nelson, P.S., Clegg, N., Arnold, H., Ferguson, C., Bonham, M., White, J., Hood, L., and Lin, B. (2002). The program of androgen-responsive genes in neoplastic prostate epithelium. Proc Natl Acad Sci U S A *99*, 11890-11895.

Pearl, L.H., Schierz, A.C., Ward, S.E., Al-Lazikani, B., and Pearl, F.M. (2015). Therapeutic opportunities within the DNA damage response. Nat Rev Cancer *15*, 166-180.

Pierce, A.J., Johnson, R.D., Thompson, L.H., and Jasin, M. (1999). XRCC3 promotes homology-directed repair of DNA damage in mammalian cells. Genes & development *13*, 2633-2638.

Polkinghorn, W.R., Parker, J.S., Lee, M.X., Kass, E.M., Spratt, D.E., Iaquinta, P.J., Arora, V.K., Yen, W.F., Cai, L., Zheng, D.*, et al.* (2013). Androgen receptor signaling regulates DNA repair in prostate cancers. Cancer discovery *3*, 1245-1253.

Qiu, P., Shandilya, H., D'Alessio, J.M., O'Connor, K., Durocher, J., and Gerard, G.F. (2004). Mutation detection using Surveyor nuclease. Biotechniques *36*, 702-707.

Ran, F.A., Hsu, P.D., Wright, J., Agarwala, V., Scott, D.A., and Zhang, F. (2013). Genome engineering using the CRISPR-Cas9 system. Nat Protoc *8*, 2281-2308.

Robinson, D., Van Allen, E.M., Wu, Y.M., Schultz, N., Lonigro, R.J., Mosquera, J.M., Montgomery, B., Taplin, M.E., Pritchard, C.C., Attard, G.*, et al.* (2015). Integrative clinical genomics of advanced prostate cancer. Cell *161*, 1215-1228.

Scher, H.I., Morris, M.J., Stadler, W.M., Higano, C., Basch, E., Fizazi, K., Antonarakis, E.S., Beer, T.M., Carducci, M.A., Chi, K.N.*, et al.* (2016). Trial Design and Objectives for Castration-Resistant Prostate Cancer: Updated Recommendations From the Prostate Cancer Clinical Trials Working Group 3. J Clin Oncol *34*, 1402-1418.

Simic, R., Lindstrom, D.L., Tran, H.G., Roinick, K.L., Costa, P.J., Johnson, A.D., Hartzog, G.A., and Arndt, K.M. (2003). Chromatin remodeling protein Chd1 interacts with transcription elongation factors and localizes to transcribed genes. Embo Journal *22*, 1846-1856.

Sims, R.J., Millhouse, S., Chen, C.F., Lewis, B.A., Erdjument-Bromage, H., Tempst, P., Manley, J.L., and Reinberg, D. (2007). Recognition of trimethylated histone h3 lysine 4 facilitates the recruitment of transcription postinitiation factors and pre-mRNA splicing. Molecular cell *28*, 665-676.

Tarish, F.L., Schultz, N., Tanoglidi, A., Hamberg, H., Letocha, H., Karaszi, K., Hamdy, F.C., Granfors, T., and Helleday, T. (2015). Castration radiosensitizes prostate cancer tissue by impairing DNA double-strand break repair. Sci Transl Med *7*, 312re311.

Taylor, B.S., Schultz, N., Hieronymus, H., Gopalan, A., Xiao, Y.H., Carver, B.S., Arora, V.K., Kaushik, P., Cerami, E., Reva, B.*, et al.* (2010). Integrative Genomic Profiling of Human Prostate Cancer. Cancer cell *18*, 11-22.

Trapnell, C., Pachter, L., and Salzberg, S.L. (2009). TopHat: discovering splice junctions with RNA-Seq. Bioinformatics *25*, 1105-1111.

Trapnell, C., Roberts, A., Goff, L., Pertea, G., Kim, D., Kelley, D.R., Pimentel, H., Salzberg, S.L., Rinn, J.L., and Pachter, L. (2012). Differential gene and transcript expression analysis of RNA-seq experiments with TopHat and Cufflinks. Nat Protoc *7*, 562-578.

Truett, G.E., Heeger, P., Mynatt, R.L., Truett, A.A., Walker, J.A., and Warman, M.L. (2000). Preparation of PCR-quality mouse genomic DNA with hot sodium hydroxide and tris (HotSHOT). Biotechniques *29*, 52, 54.

Wang, S., Gao, J., Lei, Q., Rozengurt, N., Pritchard, C., Jiao, J., Thomas, G.V., Li, G., Roy-Burman, P., Nelson, P.S.*, et al.* (2003). Prostate-specific deletion of the murine Pten tumor suppressor gene leads to metastatic prostate cancer. Cancer cell *4*, 209-221.

Weinstock, D.M., Nakanishi, K., Helgadottir, H.R., and Jasin, M. (2006). Assaying double-strand break repair pathway choice in mammalian cells using a targeted endonuclease or the RAG recombinase. Methods in enzymology *409*, 524-540.

Wu, X., Wu, J., Huang, J., Powell, W.C., Zhang, J., Matusik, R.J., Sangiorgi, F.O., Maxson, R.E., Sucov, H.M., and Roy-Burman, P. (2001). Generation of a prostate epithelial cell-specific Cre transgenic mouse model for tissue-specific gene ablation. Mechanisms of development *101*, 61-69.

Zhao, D., Lu, X., Wang, G., Lan, Z., Liao, W., Li, J., Liang, X., Chen, J.R., Shah, S., Shang, X.*, et al.* (2017). Synthetic essentiality of chromatin remodelling factor CHD1 in PTEN-deficient cancer. Nature *542*, 484-488.

Zhou, Z., Flesken-Nikitin, A., Corney, D.C., Wang, W., Goodrich, D.W., Roy-Burman, P., and Nikitin, A.Y. (2006). Synergy of p53 and Rb deficiency in a conditional mouse model for metastatic prostate cancer. Cancer Res *66*, 7889-7898.

Appendix A: Co-Targeting the Cell Intrinsic and Microenvironment Pathways of Prostate Cancer by PI3Kα/β/δ Inhibitor BAY1082439

Co-Targeting the Cell Intrinsic and Microenvironment Pathways of Prostate Cancer by PI3Kα/β/δ Inhibitor BAY1082439

Yongkong Zou1^, Zhi Qi1^, Weilong Guo1, Liuzhen Zhang1, Marcus Ruscetti2, Tanu Shenoy2, Ningshu Liu3 and Hong Wu1,2*

1The MOE Key Laboratory of Cell Proliferation and Differentiation, School of Life Sciences, Peking-Tsinghua Center for Life Sciences and Beijing Advanced Innovation Center for Genomics, Peking University, Beijing 100871, China; 2Department of Molecular and Medical Pharmacology, University of California, Los Angeles, CA 90095, USA

3Bayer AG, Drug Discovery TRG Oncology, Muellerstrasse 178, 13353 Berlin, Germany

^These authors contributed equally to this work

Abstract

Targeting the PI3K pathway is a promising strategy for treating prostate cancers (PCas) with PTEN loss. However, current anti-PI3K therapies fail to show long-lasting in vivo effects. We find that not only the PI3Kα and PI3kβ, but also PI3Kδ isoforms are involved in the epithelial-mesenchymal transition (EMT), a critical process distinguishing indolent from aggressive PCas. This suggests that co-targeting PI3Kα/β/δ could pre-empt the rebound activation of the parallel pathways induced by an α- or β- isoform-selective inhibitor and could prevent EMT. Indeed, BAY 1082439, a new selective PI3Kα/β/δ inhibitor, is highly effective in inhibiting Pten-null PCa growth in vivo, preventing EMT and tumor progression in the mutant Pten/Kras metastatic model. The anti-PI3Kδ property of BAY 1082439 further blocks B cell infiltration and lymphotoxin release, which are tumor microenvironment factors that promote castration-resistant growth. Together, our

data suggest a new approach for the treatment of PCa by targeting both tumor cells and tumor microenvironment with PI3Kα/β/δ inhibitor.

Significance

We show that PI3Kα/β/δ inhibition targets the major nodes of Pten-null PCa initiation, progression and castration-resistant growth. Our study demonstrates that inhibiting PI3Kα/β/δ isoforms by drugs such as BAY1082439 could be an effective strategy for co-targeting both intrinsic and microenvironment pathways that orchestrate PCa development and response to therapies.

Introduction

Prostate cancer (PCa) is among the most common malignancy in males, and the third leading cause of male cancer-related death in the Western world (Siegel et al., 2017). Activation of the PI3K pathway, either through loss-of-function mutations in the PTEN tumor suppressor gene or by gain-of-function alterations in components of the PI3K pathway, is associated with adverse outcomes of PCa (Taylor et al., 2010a). Ablation of PI3Kβ, but not PI3Kα, has been shown to hinder prostate intraepithelial neoplasia (PIN) development in the genetically engineered Pten conditional knockout mouse model (*Pb-Cre*$^{+}$*;Pten*$^{L/L}$, CP model) (Jia et al., 2008; Wang et al., 2003). This suggests that among the various PI3K isoforms, the PI3Kβ subunit is predominantly responsible for PTEN-loss-induced PCa. However, selective inhibition of PI3Kβ showed no significant anti-tumor efficacy in PTEN-null PCa cell lines due to compensatory activation of the PI3Kα isoform. Similarly, selective inhibition of the PI3Kα isoform resulted in rebound activation of PI3Kβ in breast tumors with a PIK3CA activating mutation (Cescon et al., 2015). Therefore, simultaneously inhibiting both PI3Kα and PI3Kβ activities may be a promising strategy for the treatment of cancers with PTEN loss or PI3K activation.

The epithelial-to-mesenchymal transition (EMT) is a potential mechanism by which PCa cells acquire lethal metastatic features and mediate therapeutic resistance (Nauseef and Henry, 2011). We have previously demonstrated that combined Pten loss and Kras/Mapk activation in the mouse prostate (*Pb-Cre*$^{+}$*;Pten*$^{L/L}$*;Kras*$^{R12D/L}$, CPK model) mimics late-stage metastatic PCa with EMT features (Mulholland et al., 2012). While prostate epithelial cells derived from the CPK model are highly sensitive to PI3K and MAPK inhibitors, CPK prostate cells with EMT and mesenchymal (M-like) features are resistant to these treatments (Ruscetti et al., 2016) through an unknown mechanism.

Androgen deprivation therapy (ADT) is the mainstream treatment for PCa. However, many patients progress to highly aggressive castration-resistant prostate cancer (CRPC) within 2 years (Watson et al., 2015). Various hypotheses for CRPC growth have been investigated, such as amplification, mutation and splice variants of the androgen receptor (AR) gene (Watson et al., 2015); crosstalk between the PI3K and AR signaling pathways (Carver et al., 2011; Mulholland et al., 2011); EMT (Li et al., 2014); and neuroendocrine differentiation due to lineage plasticity (Ku et al., 2017). Recently, the role of tumor infiltrating leukocytes (TIL) in PCa and CRPC progression has been revealed (Ammirante et al., 2010; Garcia et al., 2014), suggesting that simultaneously targeting both cancer cell-intrinsic and tumor microenvironment pathways is crucial for the treatment of PCa and preventing CRPC development.

In this study, we tested the in vitro and in vivo efficacy of BAY 1082439 (Hung et al., 2015), a new, selective PI3K inhibitor with equal potency against PI3Kα/β/δ isoforms, in treating PCa with PTEN loss.

Results

The PI3Kα/β/δ inhibitor BAY 1082439 is more effective than PI3Kα and/or PI3Kβ-selective inhibitors in blocking PTEN-null prostate cancer cells growing in vitro.

To test whether BAY 1082439 (Hung et al., 2015) (Fig. S1A) could achieve better efficacy by preventing rebound activation of the PI3K pathway, we treated PC3 and LNCaP cells, both PTEN-null human PCa lines, with various concentrations of BAY 1082439 for 72 hours. BAY 1082439 effectively inhibited cell growth in these lines (Fig. 1A) by blocking the G1/S cell cycle transition and by inducing apoptosis (Fig. S1B-C and data not shown). The PI3Kβ-specific inhibitor TGX-221 and the PI3Ka-specific inhibitor BYL-719 were significantly less effective and inhibiting cell growth and blocking the G1 to S transition (Fig. 1A; Fig. S1C). When we compared isogenic PC3 PTEN-WT and PTEN-null cells, PTEN-null cells were three orders of magnitude more sensitive to BAY 1082439 than WT cells (Fig. 1B), indicating a wide, PTEN status-dependent therapeutic window. In both human PCa cell lines and the CaP8 and CaP2 cell lines derived from *Pb-Cre*$^{+}$*;Pt*$^{L/L}$ mice (Jiao et al., 2007), BAY 1082439 prevented the feedback activation of the PI3K pathway and the rebound AKT phosphorylation seen with TGX-221 treatment (Fig. 1C and Fig 1E), and demonstrated equal potency to inhibit cell growth as the combination of the PI3Kα and PI3Kβ inhibitors TGX-221 and BYL-719 (Fig. 1D; Fig. S1C).

BAY 1082439 is effective in preventing Pten null prostate cancer progression in vivo.

Based on the superior activity of BAY 1082439 to inhibit AKT phosphorylation and the cell proliferation of human and mouse PTEN-null PCa lines compared to selective PI3Kβ or PI3Kα inhibitors (Fig. 1E and data not shown), we tested the ability of BAY 1082439 to prevent PCa progression in vivo. CP mice were treated with 75 mg/kg of BAY 1082439, starting at 6 weeks when PINs form, and ending at 10 weeks when untreated tumors progress to localized adenocarcinoma (Fig. 1F). BAY 1082439 was well tolerated over the course of the study (Fig.

S1D). In comparison to the vehicle controls, the BAY 1082439 treatment group showed a significantly decreased tumor size and P-AKT staining, nearly normal luminal architecture (Fig. 1G; Fig. S1E), and a significant reduction of Ki67-positive cells (Fig. 1H). Smooth muscle actin (SMA) staining indicated no local invasion in the BAY 1082439 treatment group compared to vehicle controls (Fig. S1F). Together, these results showed that BAY 1082439 effectively prevented prostate cancer initiation and progression in the clinically relevant CP model.

The PI3Kδ isoform is upregulated during the EMT process and can be effectively inhibited by BAY 1082439.

We have previously demonstrated that PI3K pathway activation can collaborate with Ras/MAPK pathway activation to induce EMT and PCa metastasis in the CPK mouse model (Mulholland et al., 2012; Ruscetti et al., 2016). Interestingly EMT and M-like prostate cancer cells isolated from the CPK model (PKV cells) are more resistant to the PI3K/mTOR inhibitor PKI-587 and the MEK inhibitor PD0325901 than epithelial tumor cells isolated from the same in vivo model (Ruscetti et al., 2016), suggesting that the response to targeted therapies is not solely dependent on their primary genetic alterations.

By analyzing RNA sequencing data derived from epithelial, EMT and M-like cancer cells of the CPK prostate tissue, we found that compared to epithelial cells, *Pik3ca* and *Pik3cb* were slightly up and down-regulated in M-like cancer cells, respectively. The expression of *Pik3cd* (PI3Kδ) was increased in EMT cells and further enhanced in M-like cancer cells, suggesting that PI3Kδ might play an important role in the transition process from EMT to M-like stage (Fig. 2A). The differential expression of *Pik3cd* is likely controlled by an epigenetic mechanism— reduced representation bisulfite sequencing (RRBS) analysis demonstrated that the *Pik3cd* promoter is hypermethylated in epithelial and EMT subpopulations compared to the M-like subpopulation (Fig. 2B). We also

explored the relationship between *Pik3cd* promoter methylation and mRNA expression levels in 494 PCa clinical samples from the Cancer Genome Atlas (TCGA) (Cancer Genome Atlas Research, 2015), and found a negative correlation between DNA methylation of the *Pik3cd* promoter and its mRNA level (Fig. 2C). Corresponding to their higher expression of *Pik3cd*, both the EMT and M-like subpopulations were more sensitive to the PI3Kδ inhibitor CAL-101 than the epithelial subpopulation (Fig. 2D, left). Since BAY 1082439 can potently inhibit PI3Kδ at an IC50 approximately half that of CAL-101 (Fig. S1A), we tested whether BAY 1082439 could target epithelial, EMT and M-like states. As shown in Fig. 2D, BAY 1082439 effectively inhibited tumor cell growth in all three cell subpopulations with comparable activity to the combination of the PI3Kα/β and δ inhibitors BYL-719, TGX-221, and CAL-101. These data suggest that BAY 1082439 inhibits epithelial cancer cells preferentially with its PI3Kα/β activity and suppresses M-like cancer cells with additional activity against PI3Kδ.

The ability of BAY 1082439 to inhibit epithelial as well as EMT and M-like cancer cells prompted us to test whether it could prevent EMT in vivo. Six-week-old CPK mice (n=6 per group) were treated with 75 mg/kg BAY 1082439 once daily for 4 weeks (Fig. S2A). Significant reduction in tumor size and weight was observed upon BAY 1082439 treatment as compared to the vehicle group (Fig. S2B-C). While the vehicle-treated mice developed poorly differentiated invasive carcinoma, the BAY 1082439-treated mice had PIN lesions as evidenced by intact SMA staining and a reduction in Ki67 index (Fig. 2E). Although EMT regions, defined by positive epithelial (E-cadherin) and mesenchymal (vimentin) markers, clearly appeared in vehicle-treated mice (Fig. 2F, circled areas in the left panels), no obvious EMT regions in BAY 1082439-treated mice could be observed (Fig. 2F, right panels), indicating that BAY 1082439 was able to effectively suppress EMT-mediated cancer progression. Collectively, these data reveal that BAY 1082439 inhibits the

growth and survival of both epithelial and M-like cancer cells and therefore can effectively prevent and/or delay the development of invasive and metastatic carcinoma in CPK mice.

BAY 1082439 can inhibit castration resistance tumor growth.

We and others have shown that EMT (Li et al., 2014; Mulholland et al., 2012) as well as the reciprocal crosstalk between the PI3K and AR pathways (Carver et al., 2011; Mulholland et al., 2011) can mediate castration resistant tumor growth. Given the strong inhibitory effects of BAY 1082439 on the PI3K pathway and EMT, we tested its effect on CRPC growth.

We castrated CP mice at 10 weeks of age when the animals develop invasive adenocarcinoma and compared castration resistant growth with or without BAY 1082439 treatment 4 weeks later (Fig. 3A). As a control, we also performed similar treatment with rapamycin, an inhibitor targeting the PI3K downstream effector mTOR. After 4 weeks of castration, CP mice developed CRPC with increased Ki67-positive cells and diffuse AR staining (Fig. 3C). In contrast, the prostates from the mice treated with BAY 1082439 showed significant inhibition of the PI3K pathway and tumor cell proliferation, as assessed by P-AKT level and Ki67 IHC, respectively, which led to significant reduction in tumor weight (Fig. 3B, Fig. 3C; Fig. S3). Although rapamycin could also reduce tumor weight (Fig. 3B), there were more Ki67 positive tumor cells compared to the BAY 1082439-treated group (Fig. 3C).

BAY 1082439 can block B cell infiltration and lymphotoxin-mediated survival signaling from tumor microenvironment.

Recent studies revealed that tumor microenvironment factors, such as lymphotoxin produced by B cells, can promote CRPC growth (Ammirante et al., 2010); other studies have also indicated that PI3Kδ is important for B-cell receptor signaling (Vanhaesebroeck and Khwaja, 2014). Given its potent anti-PI3Kα/β/δ activities, we hypothesized that BAY 1082439 may be more effective in

suppressing PI3Kδ-driven B cell-dependent tumor-promoting signaling than the PI3Kα or β isoform-specific inhibitors or than rapamycin. Indeed, BAY 1082439 was more effective at inhibiting the growth of freshly isolated splenocytes in vitro when compared to the PI3Kδ-specific inhibitor CAL-101, while the PI3Kα-specific inhibitor BYL-719 or rapamycin had no obvious effect (Fig. S4A). Quantitative FACS and IHC analyses showed that compared to castrated mice, BAY 1082439 but not rapamycin treatment led to significantly decreased tumor infiltrating B cells (Fig. 4A) while the number of CD8-positive T cells was not changed (Fig. S4B), suggesting that T cell-mediated anti-tumor functions were not influenced by BAY 1082439 treatment. Cxcl13 expression, a B cell chemotactic chemokine, was decreased upon BAY 1082439 treatment (Fig. 4B), consistent with the reduction of tumor-infiltrating B cells in the treatment group (Fig. 4A). Furthermore, the mRNA levels of B cell-released lymphotoxin-α and β (Lta and Ltb) were significantly reduced in BAY 1082439-treated tumor remnants (Fig. 4C).

Histologically B220-positive B cells were surrounded by Ki67-positive tumor cells in the castrated and rapamycin-treated prostates (Fig. 4D, upper and lower panels), These ki67-positive cells are almost absent in the BAY 1082439-treated tumor remnants (Fig. 4D, middle panels), suggesting that infiltrating B cells may promote tumor growth.The LTA and LTB heterotrimer promotes androgen-independent growth via LTBR-mediated activation of IKKα and STAT3 phosphorylation (P-STAT3) (Ammirante et al., 2010). In line with reduced B cell infiltration and *Lta* and *Ltb* expression, we also observed that the P-STAT3 level was significantly reduced in castrated BAY 1082439-treated prostates (Fig. 4E). In the rapamycin treatment group, however, the number of tumor infiltrating B cells, the Cxcl13 and Ltb expression levels as well as the P-STAT3 level were not changed (Fig. 4A-E), indicating that the CXCL13/lymphotoxin/P-STAT3 pathway may support CRPC growth in the rapamycin treatment group. Together, these results support the notion that BAY 1082439 not only targets cancer cell-intrinsic proliferation and survival pathways by inhibiting

PI3Kα and PI3Kβ, but also suppresses castration-induced EMT and inhibits B cell-driven tumor-promoting signaling pathways through its inhibitory effect on PI3Kδ.

Discussion

The activation of the PI3K pathway is associated with the pathogenesis of PCa as well as treatment resistance. Attempts at developing effective anti-PI3K inhibitors for the treatment of PCa and other human cancers have been hindered by insufficient efficacy and/or therapeutic window (Armstrong et al., 2017; Massard et al., 2017; Mateo et al., 2017) as well as the development of resistance mechanisms involving feedback and parallel pathways (Cescon et al., 2015). We demonstrate in this study that BAY 1082439, a new PI3Kα/β/δ inhibitor has much higher efficacy to inhibit PTEN-null prostate cancer cell growth than the α or β-isoform specific inhibitors BYL-719 and TGX-221 by blocking the mutual feedback activation between PI3Kα and PIK3β. BAY 1082439 also inhibits PCa progression in our in vivo preclinical Pten-null PCa model. Importantly, BAY 1082439 can prevent EMT and PCa progression by blocking PI3Kδ, an isoform found in this study to be upregulated during the EMT process. Furthermore, the anti-PI3Kδ activity of BAY 1082439 is critical for inhibiting B-cell infiltration after surgical castration and preventing B-cell released lymphotoxin-mediated castration resistant growth. Therefore BAY 1082439 can target multiple stages of PCa such as Pten-null PCa initiation, progression and castration resistant growth, and preempt both cancer cell-intrinsic and microenvironment-derived therapeutic resistance mechanisms.

Although different PI3K isoforms share similar structures and enzyme activities, each isoform has a unique upstream regulatory pathway and tissue-specific expression pattern. PI3Kα and PIK3β are predominantly expressed in solid tumors, whereas PI3Kγ and PI3Kδ are mainly but not exclusively expressed in hematopoietic cells (Okkenhaug et al., 2016). While the PIK3β isoform is required for Pten-null PCa development (Jia et al., 2008), we show in this study the previously unrecognized essential role that PI3Kδ plays in EMT during PCa progression and castration resistant growth. The PI3Kδ isoform is differentially expressed in epithelial, EMT and M-like cells

by an epigenetic regulatory mechanism. Upregulated PI3Kδ is responsible for resistance to anti-PI3Kα and β treatment, which is observed in EMT and M-like cells (Ruscetti et al., 2016). Therefore, the anti-PI3Kα/β/δ activity of BAY 1082439, is critical for inhibiting this newly discovered resistant mechanism during cancer progression.

The most common treatment for advanced PCa is androgen deprivation therapy (ADT) because of the central role AR signaling plays in prostate tumor growth. Although most men initially respond to ADT, its therapeutic benefits are short-lived, and some patients succumb to CRPC within 18–24 months (Watson et al., 2015). Previous studies have identified EMT and PI3K-AR reciprocal cross-talk as the key mechanisms for CRPC growth (Carver et al., 2011; Li et al., 2014; Mulholland et al., 2012; Mulholland et al., 2011) and have suggested the benefit of co-targeting PI3K and AR signaling pathways and inhibiting EMT to prevent CRPC development. Here we show in our Pten-null mouse model that co-inhibiting EMT and the PI3K pathway by BAY 1082439 and shutting down AR signaling by castration leads to significant inhibition of CRPC growth.

Tumor infiltrating immune cells are known to play essential roles in tumor development and therapeutic resistance (Quail and Joyce, 2013). Immune therapies, aimed at alleviating T cell check-point inhibitions, such as anti-CTLA-4/PD-1/PD-L1 antibodies, have been approved by the FDA for melanoma and lung cancers (Pico de Coana et al., 2015). However, understanding the contribution of B-cells in tumor development and targeting B-cell mediated resistance mechanisms in solid tumors have been a much less studied field. Recent studies on the role of tumor-infiltrating B cells in pancreatic ductal adenocarcinoma development and progression (Pylayeva-Gupta et al., 2016) and the presence of B cells in clinical CRPC specimens have highlighted the potential role of B cells in CRPC development (Ammirante et al., 2010). Similar to subcutaneous Myc-CaP and spontaneous TRAMP mouse models (Ammirante et al., 2010), we

also observed significant increases in B cell tumor infiltration, lymphotoxin release and upregulated STAT3 signaling in our castrated Pten-null PCa model. Importantly, BAY 1082439, with its anti-PI3Kδ activity, can effectively reduce the number of infiltrating B cells and suppress lymphotoxin α/β release, STAT3 activation, and androgen-independent growth in castrated tumor tissue.

In summary, our results highlight the unique role of BAY 1082439 in targeting multiple PI3K isoforms that are critical for PCa progression and therapeutic resistance. As a single drug with anti-PI3Kα/β/δ activity, BAY 1082439 may also have considerable clinical benefit by avoiding the potential side effects caused when combining multiple isoform-specific inhibitors. Our results also suggest that co-targeting the cell-intrinsic and microenvironment pathways are essential for late stage PCas and should be further explored.

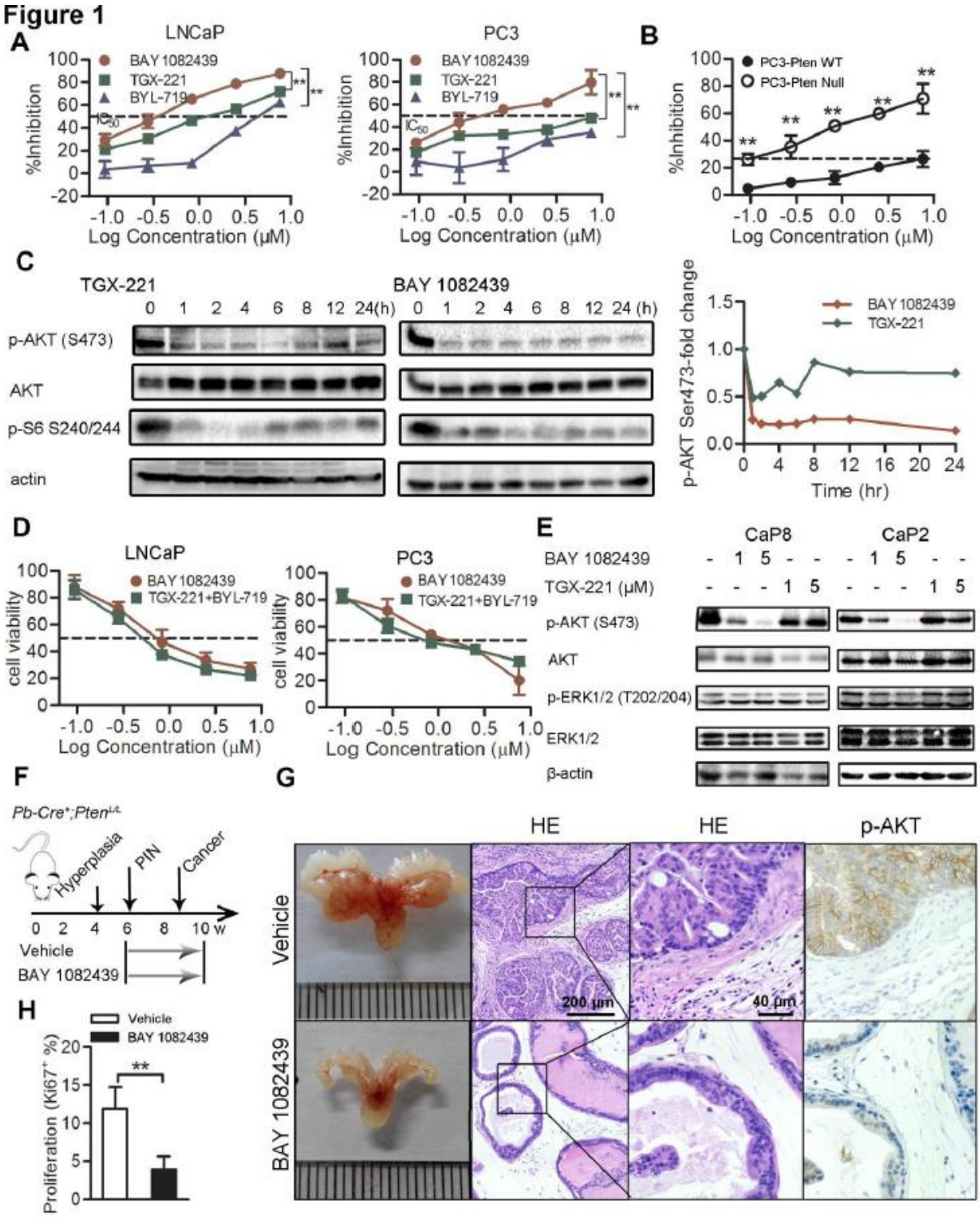

Figure 1. PI3Kα/β dual-balanced inhibitor BAY 1082439 inhibits proliferation of PTEN-null prostate cells in vitro and in vivo.

(A) LNCaP and PC3 cells were treated with BAY 1082439, TGX-221 or BYL-719 in different concentrations and the inhibition effects on cell growth were analyzed.

(B) PC3-WT and PC3-PTEN null cells were treated with BAY 1082439 at different concentrations and the effects on cell growth were analyzed.

(C) PC3 cells were treated with 1 μmol TGX-221 or BAY 1082439 and the effects on P-AKT (S473) and P-S6 (Ser 240/244) levels were analyzed by Western blot analysis; the fold change in P-AKT (S473) was determined by densitometry analysis using total AKT as loading control.

(D) LNCaP and PC3 cells were treated with BAY 1082439 or TGX-221+BYL-719 in different concentrations and cell viability was analyzed.

(E) LNCaP and PC3 cells were treated with BAY 1082439 or TGX-221 and P-AKT (S473) and P-ERK1/2 (Thr 202/204) levels were analyzed.

(F) Experimental setup of the CP mice used to evaluate in vivo anti-tumor efficacy of BAY 1082439, each cohort has 6 mice.

(G) HE and immunohistochemistry (IHC) staining of prostate tumors from mice treated with BAY 1082439 or vehicle.

(H) Cell proliferation index in prostate tumors treated with BAY 1082439 or vehicle. For in vitro studies, each data point had 3 replicates and each experiment was repeated at least 3 times. Student's t-test was used for data evaluation where*, $P < 0.01$. BYL-719: PI3Kα inhibitor, TGX-221: PI3Kβ inhibitor.

Figure 2

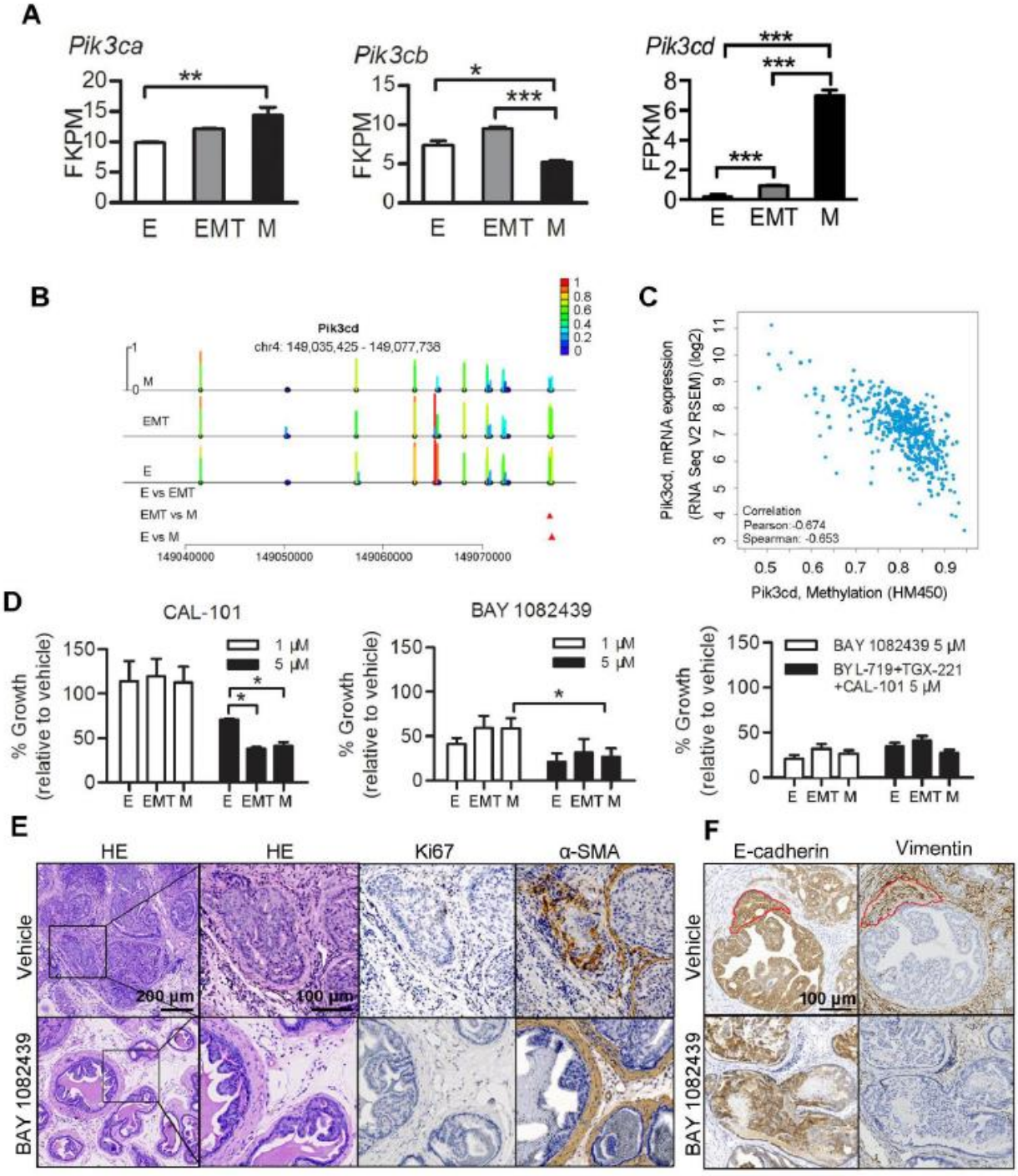

Figure 2. PI3Kδ upregulation is a novel resistance mechanism for EMT and mesenchymal-like cells and BAY 1082439 can target all three tumor cell states.

(A) RT-PCR analysis for Pik3cd, Pik3ca and Pik3cb expression levels in FACS-sorted epithelial, EMT and M-like cells from the PKV cell line; 3 replicates in each cell type.

(B) DNA methylation status of Pik3cd promoter assessed by RRBS in epithelial, EMT and M-like cells.

(C) Negative correlation between PIK3CD promoter DNA methylation and mRNA expression in prostate cancer database of TCGA.

(D) PKV cells were treated with CAL-101 (left), BAY 1082439 (middle and right) or BYL-719+TGX-221+CAL-101 (right). Cell growth rate in epithelial, EMT and M-like cells was analyzed, 3 replicates in each study.

(E) HE and IHC staining of CPK prostate tumors treated with BAY 1082439 (n=3) or vehicle (n=3).

(F) IHC staining of epithelial marker (E-cadherin) and M-like marker (vimentin) of CPK prostate tumors treated with BAY 1082439 or vehicle. Data represent mean ± SD. Student's t-test was used. *, $P < 0.05$, **, $P < 0.01$. ***, $P < 0.001$.

Figure 3

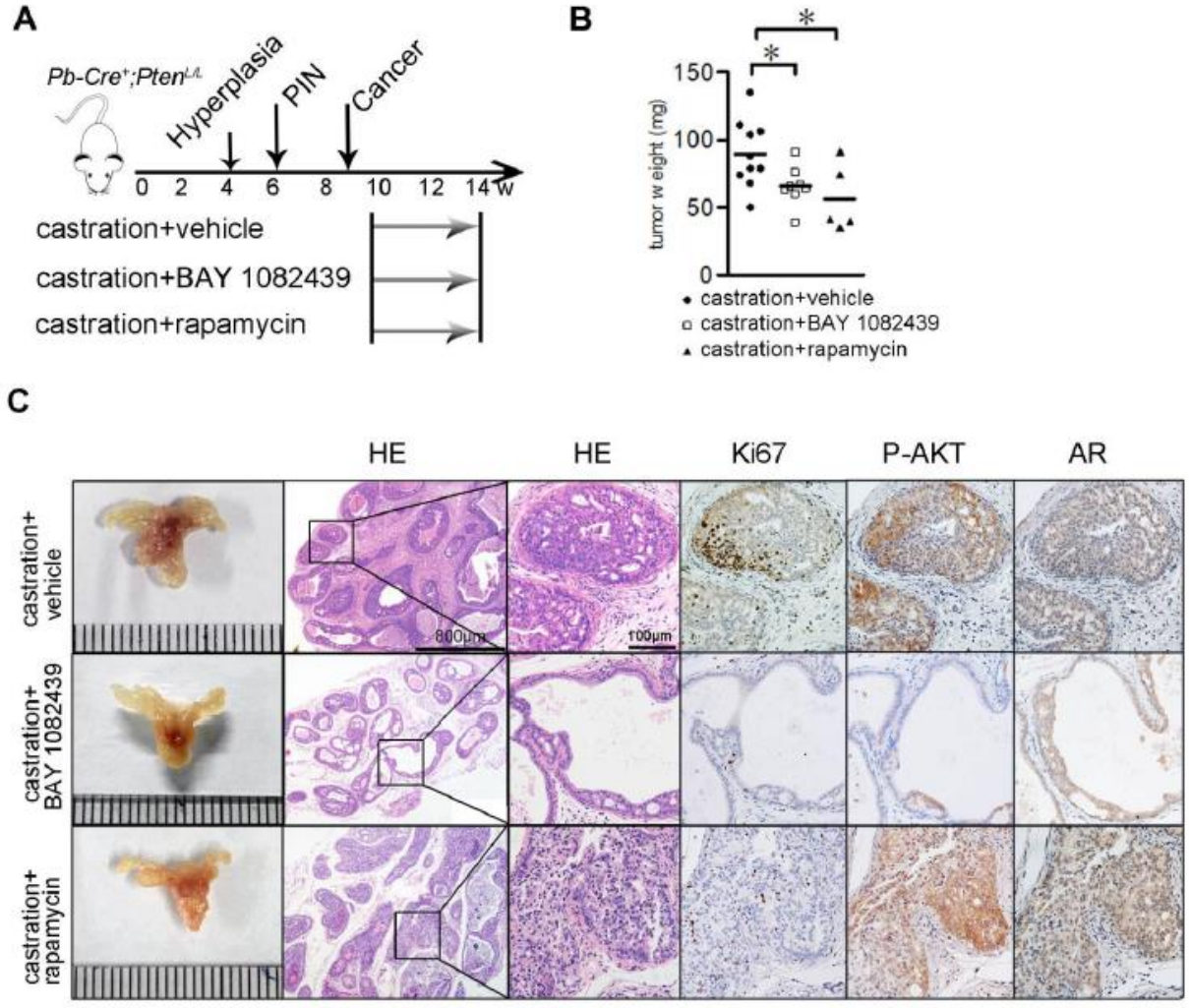

Figure 3. BAY 1082439 inhibits CRPC growth.

(A) Ten-week-old CP mice were castrated then treated with vehicle (n=10), BAY 1082439 (n=8) or rapamycin (n=5);

(B) Prostate tumor weight was analyzed;

(C) HE and IHC staining of castrated prostate tumors under different treatments. Student's t-test was used. *, $P < 0.05$.

Figure 4

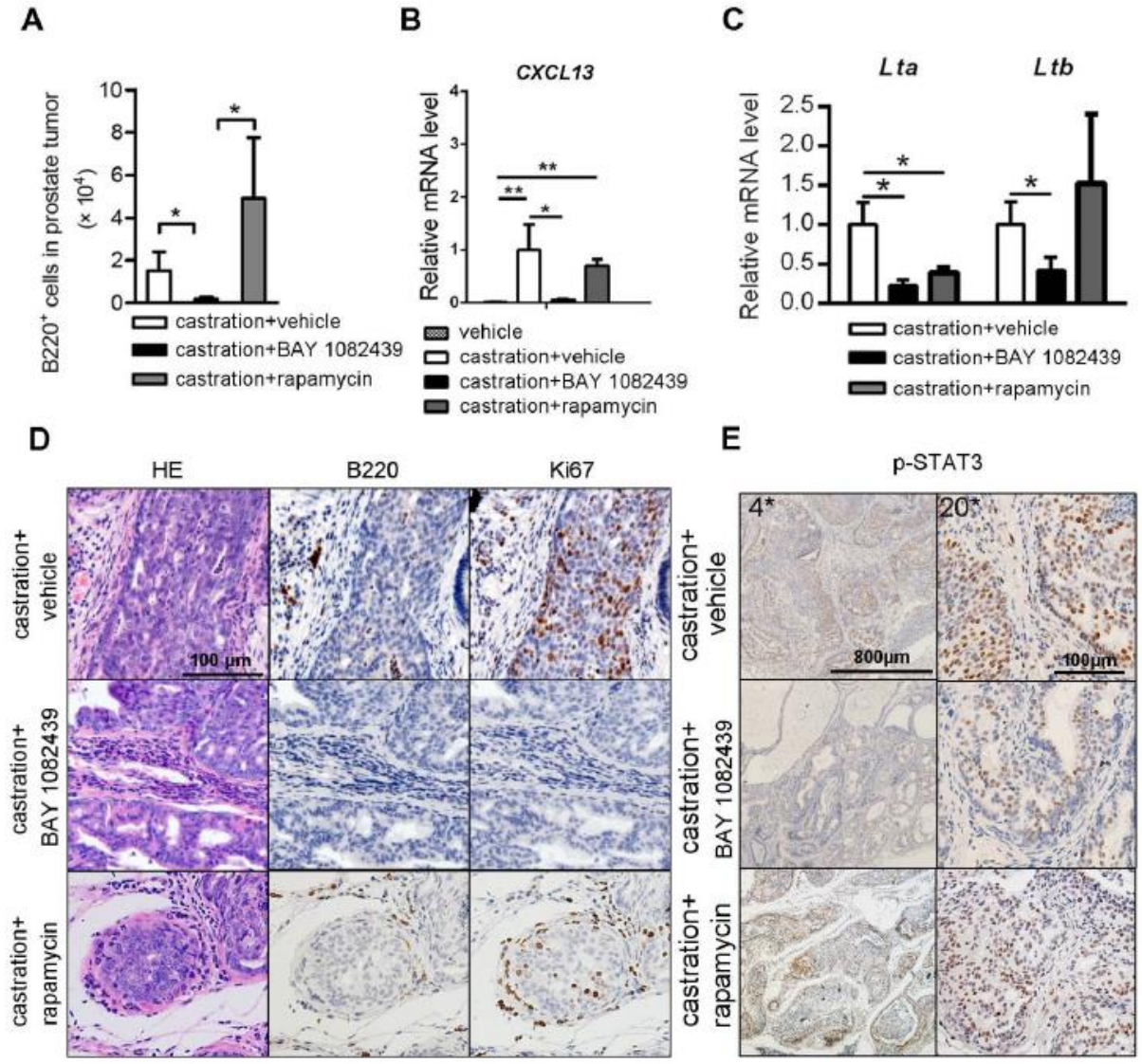

Figure 4. BAY 1082439 inhibits CRPC growth by blocking B cell infiltration and lymphotoxin release.

(A) Quantitative analysis of prostate tumor infiltrating B cells in animals shown in Fig. 3A; (B) and (C) RT-PCR analysis of CXCL13, LTA and LTB expression levels in prostate tumor tissues from intact (n=6) and castrated CP mice treated with vehicle(n=10), BAY 1082439 (n=8) and rapamycin (n=5);

(D) HE, Ki67 and B220 IHC staining of prostate tumor tissues from castrated CP mice treated with vehicle, BAY 1082439 or rapamycin.

(E) IHC analysis for phosphorylated STAT3 in prostate tumors from castrated CP mice treated with vehicle, BAY 1082439 or rapamycin. Data in A-D and E are represented as mean ± SD. Two-way ANOVA was used in A. Student's t-test was used in D and E. 3 replicates were analyzed in A-C. *, $P < 0.05$, **, $P < 0.01$.

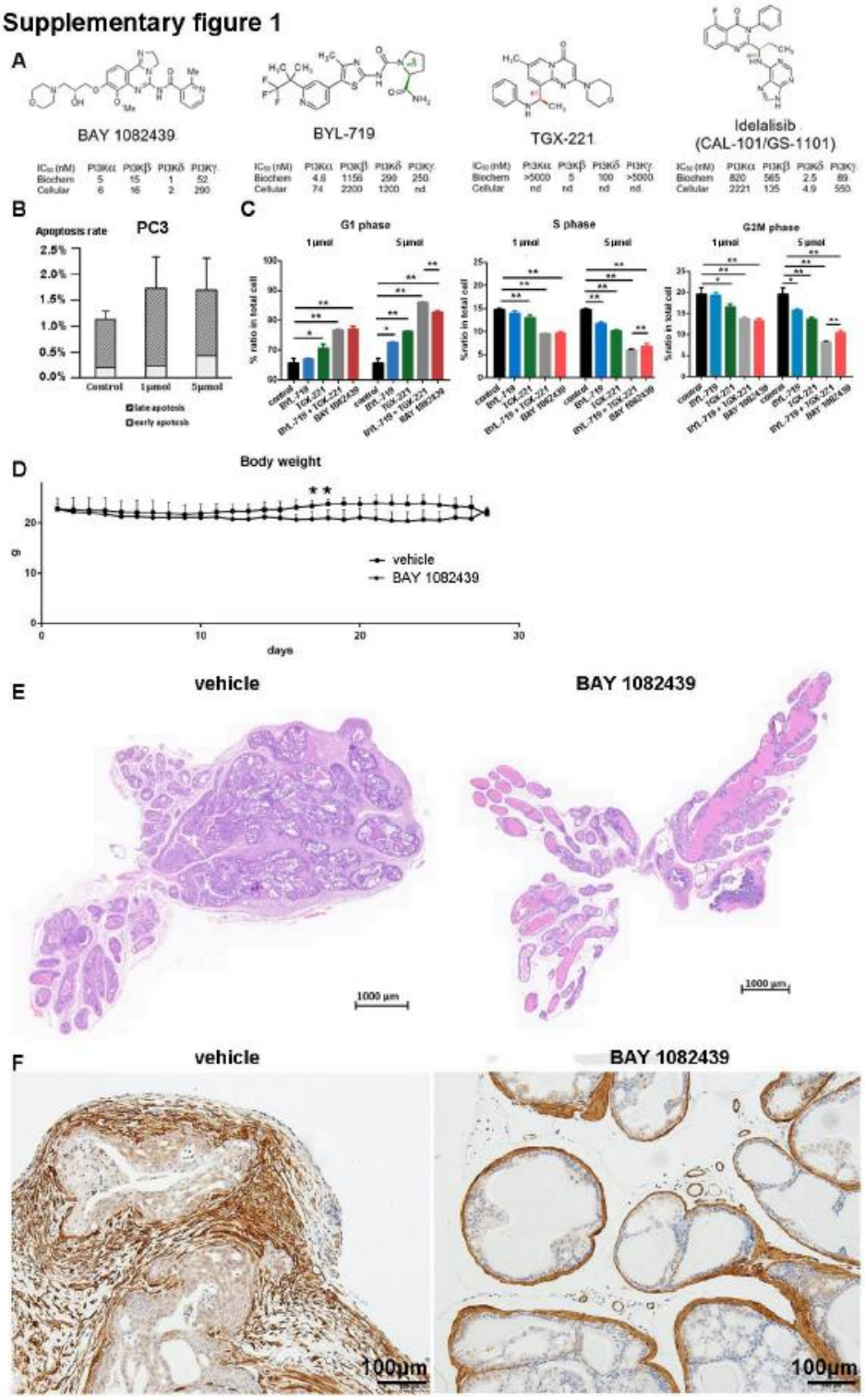

Figure S1. (Related to Figure 1)

(A) Structure and therapeutic properties of BAY 1082439, BYL-719, TGX-221 and CAL-101.

(B) PC3 cells were treated with solvent, 1 μmol and 5 μmol BAY 1082439 for 3 days, and cell apoptosis rate was determined by annexin V combined with 7-AAD staining.

(C) PC3 cells were treated with solvent, 1 μmol and 5 μmol BAY 1082439, BYL-719, TGX-221 or BYL-719+TGX-221 for 3 days, cell cycle phase was determined by PI staining;

(D) Average CP mice body weight in BAY 1082439 or vehicle treatment group.

(E) Overview of CP mice prostate tumors treated with vehicle or BAY 1082439.

(F) α-SMA staining in prostate tumors from CP mice treated with vehicle or BAY 1082439. In in vitro study, each treatment had 3 replicates. Student's t-test was used. *, $P < 0.05$, **, $P < 0.01$.

Supplementary figure 2

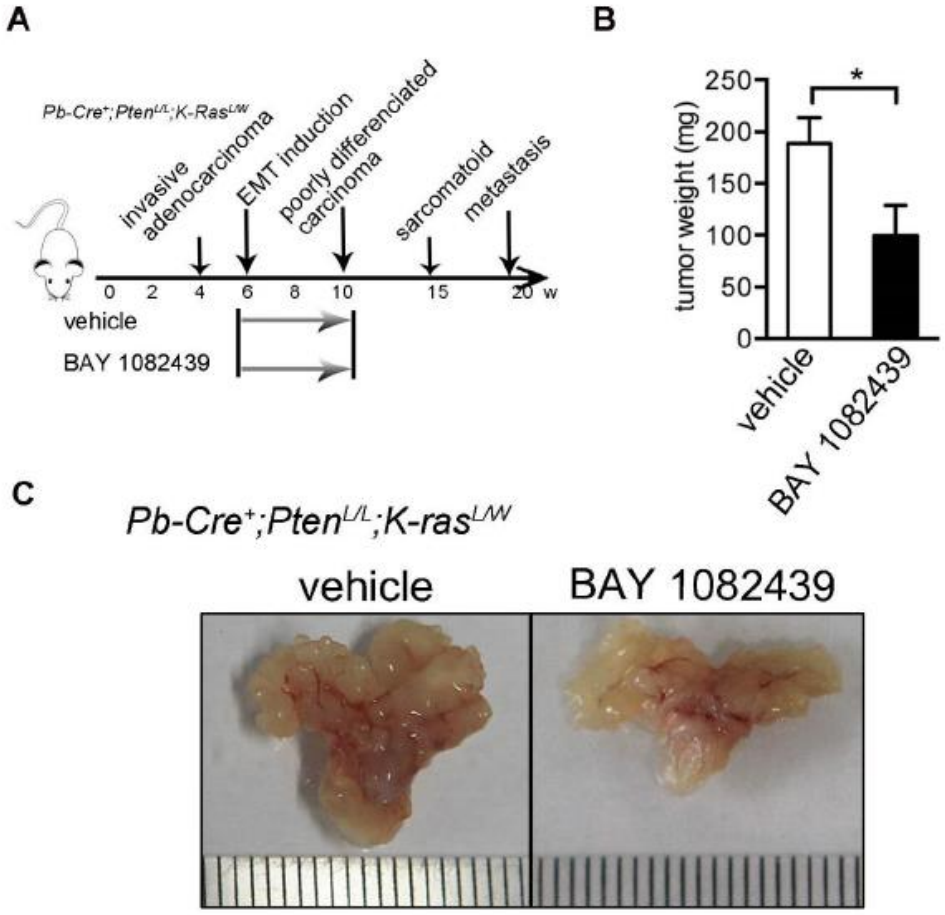

Figure S2. (Related to Figure 2).

(A) Six-week-old CPK mice were treated with vehicle or BAY 1082439.

(B) Prostate tumor weight was analyzed.

(C) Photos of prostate tumors from CPK mice treated with vehicle or BAY 1082439. *, $P < 0.05$.

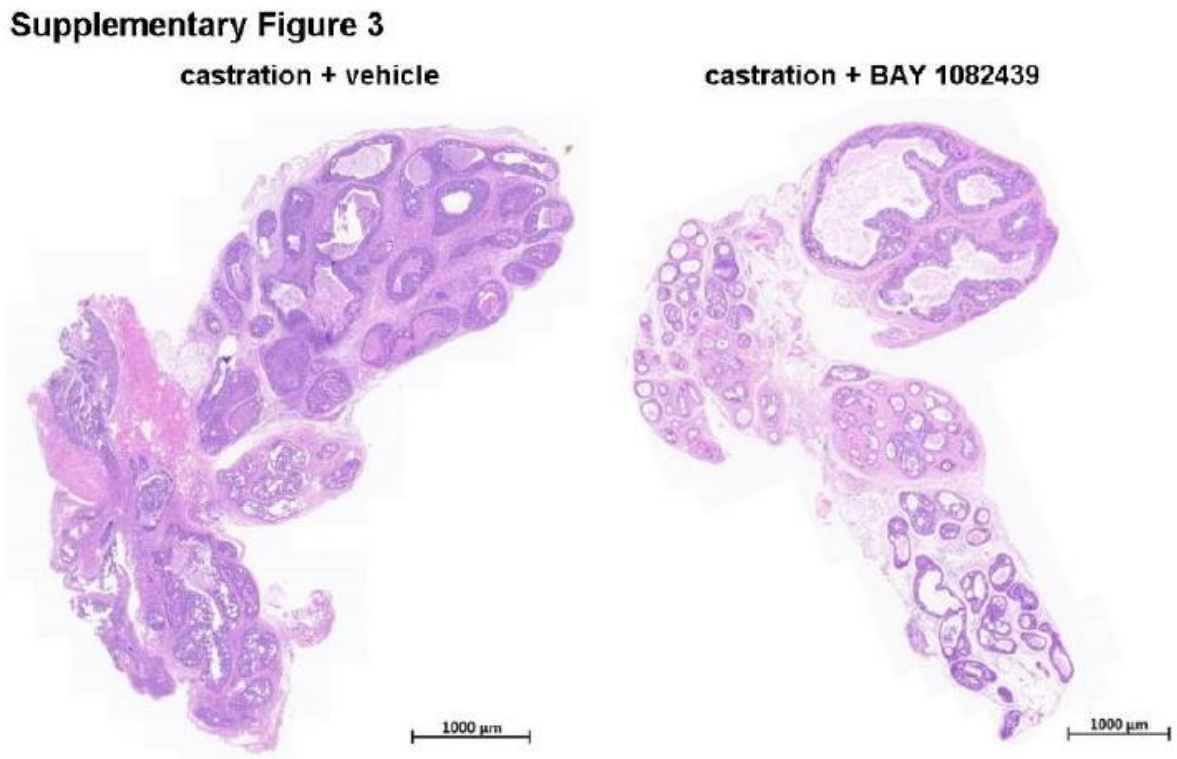

Figure S3. (Related to Figure 3.)

Overview of prostate tumors of castrated CP mice treated with vehicle or BAY 1082439.

Supplementary Figure 4

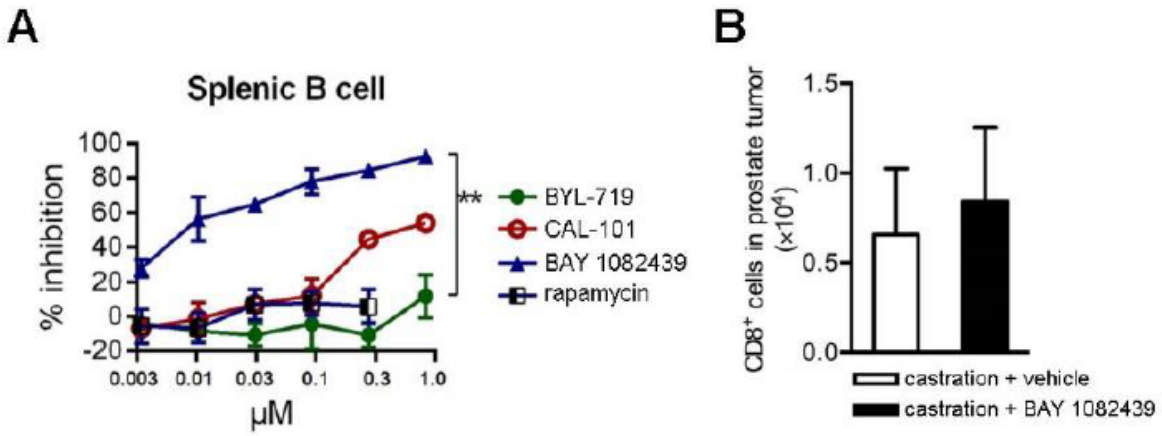

Figure S4. (Related to Figure 4)

(A) Growth inhibition rates by BYL-719, CAL-101, BAY 1082439 and rapamycin in splenic B cells, each treatment had 3 replicates.

(B) Tumor infiltrating CD3+CD8+ cytotoxic T cell number in castrated CP mice after treatment with vehicle (n=6) or BAY 1082439 (n=6). **, $P < 0.01$.

Methods

Animals

Mice with a conditional deletion of *Pten* (*Pb-Cre*$^{+}$*;Pten*$^{L/L}$) (Wang et al., 2003) and a conditional deletion of *Pten* and an activation of *Kras* (*Pb-Cre*$^{+}$*;Pten*$^{L/L}$*;K-ras*$^{G12D/W}$) (Mulholland et al., 2012) in the murine prostate were generated as previously described. All animal housing, breeding, and surgical procedures were conducted under the regulation of the Division of Laboratory Animal Medicine at the Peking University (PKU; Beijing, China) and was approved by the Ethics Committee of the Peking University with ID LSC-WuH-1.

Inhibitors

BAY 1082439 was provided by Bayer AG. TGX-221, BYL-719, CAL-101 and rapamycin were purchased from Selleckchem.com.

Cell Culture and inhibitor treatment

The LNCaP and PC3 cell lines were purchased from ATCC. The CaP2, CaP8, and CPKV cell lines were established and cultured as previously described (Jiao et al., 2007; Ruscetti et al., 2016). Freshly isolated splenic cells were cultured in RPMI-1640 medium with 10% heat-inactivated fetal calf serum (FCS), penicillin (100 U/mL), streptomycin (100 µg/mL), 2 mM L-glutamine, 10 mM HEPES, 0.1 mM non-essential amino acids, and 1 mM sodium pyruvate (all from Sigma, Oakville, ON, Canada). The B cells were stimulated with 10 µg/mL LPS and 1 µg/mL anti-CD40 (BioLegend 102809). Inhibitors were used in vitro at the concentrations indicated in the figures due to the different purposes of the experiments.

Protein and RNA Analysis

Protein was extracted with 1% SDS-lysis buffer and separated by 10% SDS-PAGE. The following antibodies were used: Actin (sc-1616; Santa Cruz), P-AKT (S473) (4060; Cell Signaling Technology), total AKT (4691; Cell Signaling Technology), P-S6 (S240/244) (5364; Cell Signaling Technology), S6 (2317; Cell Signaling Technology). P-ERK1/2 (Thr202/Tyr204) (4370; Cell Signaling Technology), ERK (4695; Cell Signaling Technology). RNA was extracted with the Eastep Super Total RNA extraction Kit (Promega) then reverse transcribed into cDNA, and analyzed by quantitative real-time PCR using the Invitrogen mix. The following primer pairs were used: Lta forward, 5'- GCTTGGCACCCCTCCTGTC-3', reverse, 5'- GATGCCATGGGTCAAGTGCT-3'; Ltb forward, 5'- CCAGCTGCGGATTCTACACCA-3', reverse, 5'- AGCCCTTGCCCACTCATCC-3'; Cxcl13 forward, 5'-GCACAGCAACGCTGCTTCT-3', reverse, 5'- TCTTTGAACCATTTGGCAGC-3'; Actin forward, 5'- CCAGCCTTCCTTCTTGGGTAT-3', reverse, 5'- TGCTGGAAGGTGGACAGTGAG-3'.

Cell Growth Assays

The cell apoptosis rate was determined using a PE Annexin V apoptosis detection kit (cat number: 559783) from BD Pharmingen. For cell cycle phase analysis, PC3 cells were seeded in 6-well plates and cultured under different concentrations of inhibitors for 72 hours, harvested and fixed by 70% alcohol for 2 hours, incubated with 100 μg/mL propidium iodide in PBS for 30 minutes, after which the cell cycle phase ratio was analyzed by FACS.

CaP2, CaP8, PC3 and LNCaP cell growth was measured using the Cell Counting Kit-8. Briefly, cells were seeded in 96-well plates and cultured under different concentrations of inhibitors for 72 hours. The medium was aspirated and medium containing 10% CCK-8 solution was added. Absorbance was measured at 450 nm using a plate reader. The total number of PKV cells were counted manually by trypan blue exclusion. The PKV cells from each treatment condition were

sorted into epithelial, EMT and M-like using FACS as previously described (Ruscetti et al., 2016). Cell numbers for each population were calculated by multiplying the total number of cells by the percentage of each population as assessed by FACS. The ratio of cell growth was calculated by dividing the total number of cells in each drug treated population by the total number of cells in each vehicle treated population.

Histology and IHC Analysis

Prostate tumor tissues from various models were fixed in 10% buffered formalin for 24 hours. Paraffin-embedded tissues were sectioned into 4 μm thick slices, placed on charged glass slides, and stained with H&E or the appropriate antibodies as previously described (Wang et al., 2003). The slides were stained with the following antibodies: AR (N-20): sc-816 from Santa Cruz; Vimentin (5741), E-Cadherin (3195), P-AKT (S473) (4060), P-STAT3 (Tyr705) (9145), P-ERK (Thr202/Tyr204) (4370) from Cell Signaling Technology; Anti-ki67 (Abcam15580), Anti-αSMA (ab5694), CD45R/B220 (553084), from Abcam.

Tissue Dissociation, Single-cell Suspension and FACS analysis/sorting

Prostate tumors, spleen, and bone marrow (BM) were separated from age and genetic background-matched models at the indicated time points, weighed and photographed. Single-cell suspensions were prepared from these tissues as previously described (Garcia et al., 2014). The separation of epithelial, EMT and M-like cells from CPKV prostate tumor tissue was done as previously described (Ruscetti et al., 2016). Spleens were subjected to a red blood cell lysis step using RBC lysis buffer (BioLegend) followed by passage through a 70-μm filter. Single-cell suspensions were stained with directly conjugated antibodies against CD45, CD4, CD8, B220 (BioLegend) according to the manufacturers' instructions. Flow cytometric analysis was

performed on a FACSFortesa instrument (BD Biosciences), and data were analyzed by using BDFACS Diva software (BD Biosciences). All immune cell populations were gated as CD45-positive.

Promoter methylation profile analysis

Bisulfite sequencing libraries were prepared from separated epithelial, EMT and M-like cancer cells of CPK prostate tissues. The relationship between PI3Kα/β/δ expression and DNA methylation profile was obtained by analysis of 494 prostate adenocarcinoma sample data (from TCGA, provisional datasets) from cbioportal.org.com.

Data Analysis

Graphpad Prism software was used to calculate means and standard deviations (SD). The Student's t-test or two-way ANOVA were used to determine statistical significance, and $P < 0.05$ was considered statistically significant. Data are presented as means ±SD.

References

Abeshouse, A., Ahn, J., Akbani, R., Ally, A., Amin, S., Andry, C.D., Annala, M., Aprikian, A., Armenia, J., Arora, A.*, et al.* (2015). The Molecular Taxonomy of Primary Prostate Cancer. Cell *163*, 1011-1025.

Akamatsu, Y., and Jasin, M. (2010). Role for the Mammalian Swi5-Sfr1 Complex in DNA Strand Break Repair through Homologous Recombination. Plos Genet *6*.

Al-Ubaidi, F.L., Schultz, N., Loseva, O., Egevad, L., Granfors, T., and Helleday, T. (2013). Castration therapy results in decreased Ku70 levels in prostate cancer. Clin Cancer Res *19*, 1547-1556.

Ammirante, M., Luo, J.L., Grivennikov, S., Nedospasov, S., and Karin, M. (2010). B-cell-derived lymphotoxin promotes castration-resistant prostate cancer. Nature *464*, 302-305.

An, J., Ren, S., Murphy, S.J., Dalangood, S., Chang, C., Pang, X., Cui, Y., Wang, L., Pan, Y., Zhang, X.*, et al.* (2015). Truncated ERG Oncoproteins from TMPRSS2-ERG Fusions Are Resistant to SPOP-Mediated Proteasome Degradation. Mol Cell *59*, 904-916.

An, J., Wang, C., Deng, Y., Yu, L., and Huang, H. (2014). Destruction of full-length androgen receptor by wild-type SPOP, but not prostate-cancer-associated mutants. Cell Rep *6*, 657-669.

Armstrong, A.J., Halabi, S., Healy, P., Alumkal, J.J., Winters, C., Kephart, J., Bitting, R.L., Hobbs, C., Soleau, C.F., Beer, T.M.*, et al.* (2017). Phase II trial of the PI3 kinase inhibitor buparlisib (BKM-120) with or without enzalutamide in men with metastatic castration resistant prostate cancer. Eur J Cancer *81*, 228-236.

Attard, G., Clark, J., Ambroisine, L., Fisher, G., Kovacs, G., Flohr, P., Berney, D., Foster, C.S., Fletcher, A., Gerald, W.L.*, et al.* (2008). Duplication of the fusion of TMPRSS2 to ERG sequences identifies fatal human prostate cancer. Oncogene *27*, 253-263.

Baca, S.C., Prandi, D., Lawrence, M.S., Mosquera, J.M., Romanel, A., Drier, Y., Park, K., Kitabayashi, N., MacDonald, T.Y., Ghandi, M.*, et al.* (2013a). Punctuated evolution of prostate cancer genomes. Cell *153*, 666-677.

Baca, S.C., Prandi, D., Lawrence, M.S., Mosquera, J.M., Romanel, A., Drier, Y., Park, K., Kitabayashi, N., MacDonald, T.Y., Ghandi, M.*, et al.* (2013b). Punctuated Evolution of Prostate Cancer Genomes. Cell *153*, 666-677.

Bagchi, A., Papazoglu, C., Wu, Y., Capurso, D., Brodt, M., Francis, D., Bredel, M., Vogel, H., and Mills, A.A. (2007). CHD5 is a tumor suppressor at human 1p36. Cell *128*, 459-475.

Barbieri, C.E., Baca, S.C., Lawrence, M.S., Demichelis, F., Blattner, M., Theurillat, J.P., White, T.A., Stojanov, P., Van Allen, E., Stransky, N.*, et al.* (2012). Exome sequencing identifies recurrent SPOP, FOXA1 and MED12 mutations in prostate cancer. Nat Genet *44*, 685-689.

Barbieri, C.E., Bangma, C.H., Bjartell, A., Catto, J.W., Culig, Z., Gronberg, H., Luo, J., Visakorpi, T., and Rubin, M.A. (2013). The mutational landscape of prostate cancer. Eur Urol *64*, 567-576.

Bell, D., Berchuck, A., Birrer, M., Chien, J., Cramer, D.W., Dao, F., Dhir, R., DiSaia, P., Gabra, H., Glenn, P.*, et al.* (2011). Integrated genomic analyses of ovarian carcinoma. Nature *474*, 609-615.

Beltran, H., Yelensky, R., Frampton, G.M., Park, K., Downing, S.R., MacDonald, T.Y., Jarosz, M., Lipson, D., Tagawa, S.T., Nanus, D.M.*, et al.* (2013). Targeted next-generation sequencing of advanced prostate cancer identifies potential therapeutic targets and disease heterogeneity. Eur Urol *63*, 920-926.

Berger, M.F., Lawrence, M.S., Demichelis, F., Drier, Y., Cibulskis, K., Sivachenko, A.Y., Sboner, A., Esgueva, R., Pflueger, D., Sougnez, C.*, et al.* (2011). The genomic complexity of primary human prostate cancer. Nature *470*, 214-220.

Bhagavan, N.V., and Ha, C.-E. (2011). Essentials of medical biochemistry : with clinical cases, 1st edn (Amsterdam ; Boston: Elsevier/Academic Press).

Bhatia-Gaur, R., Donjacour, A.A., Sciavolino, P.J., Kim, M., Desai, N., Young, P., Norton, C.R., Gridley, T., Cardiff, R.D., Cunha, G.R.*, et al.* (1999). Roles for Nkx3.1 in prostate development and cancer. Genes Dev *13*, 966-977.

Biswas, D., Takahata, S., Xin, H., Dutta-Biswas, R., Yu, Y., Formosa, T., and Stillman, D.J. (2008). A role for Chd1 and Set2 in negatively regulating DNA replication in Saccharomyces cerevisiae. Genetics *178*, 649-659.

Blattner, M., Lee, D.J., O'Reilly, C., Park, K., MacDonald, T.Y., Khani, F., Turner, K.R., Chiu, Y.L., Wild, P.J., Dolgalev, I.*, et al.* (2014). SPOP mutations in prostate cancer across demographically diverse patient cohorts. Neoplasia *16*, 14-20.

Blattner, M., Liu, D., Robinson, B.D., Huang, D., Poliakov, A., Gao, D., Nataraj, S., Deonarine, L.D., Augello, M.A., Sailer, V.*, et al.* (2017). SPOP Mutation Drives Prostate Tumorigenesis In Vivo through Coordinate Regulation of PI3K/mTOR and AR Signaling. Cancer Cell *31*, 436-451.

Boland, C.R., and Goel, A. (2010). Microsatellite instability in colorectal cancer. Gastroenterology *138*, 2073-2087 e2073.

Boysen, G., Barbieri, C.E., Prandi, D., Blattner, M., Chae, S.S., Dahija, A., Nataraj, S., Huang, D., Marotz, C., Xu, L.*, et al.* (2015). SPOP mutation leads to genomic instability in prostate cancer. Elife *4*.

Brown, C.E., and Warren, S. (1978). Carcinoma of the prostate in irradiated parabiotic rats. Cancer Res *38*, 159-162.

Bryant, H.E., Schultz, N., Thomas, H.D., Parker, K.M., Flower, D., Lopez, E., Kyle, S., Meuth, M., Curtin, N.J., and Helleday, T. (2005). Specific killing of BRCA2-deficient tumours with inhibitors of poly(ADP-ribose) polymerase. Nature *434*, 913-917.

Bunting, S.F., Callen, E., Wong, N., Chen, H.T., Polato, F., Gunn, A., Bothmer, A., Feldhahn, N., Fernandez-Capetillo, O., Cao, L.*, et al.* (2010). 53BP1 inhibits homologous recombination in Brca1-deficient cells by blocking resection of DNA breaks. Cell *141*, 243-254.

Bunting, S.F., and Nussenzweig, A. (2013). End-joining, translocations and cancer. Nature Reviews Cancer *13*, 443-454.

Burkhardt, L., Fuchs, S., Krohn, A., Masser, S., Mader, M., Kluth, M., Bachmann, F., Huland, H., Steuber, T., Graefen, M.*, et al.* (2013a). CHD1 is a 5q21 tumor suppressor required for ERG rearrangement in prostate cancer. Cancer Res *73*, 2795-2805.

Burkhardt, L., Fuchs, S., Krohn, A., Masser, S., Mader, M., Kluth, M., Bachmann, F., Huland, H., Steuber, T., Graefen, M.*, et al.* (2013b). CHD1 Is a 5q21 Tumor Suppressor Required for ERG Rearrangement in Prostate Cancer. Cancer research *73*, 2795-2805.

Bzymek, K.P., and Colman, R.F. (2007). Role of alpha-Asp181, beta-Asp192, and gamma-Asp190 in the distinctive subunits of human NAD-specific isocitrate dehydrogenase. Biochemistry *46*, 5391-5397.

Cancer Genome Atlas Research, N. (2015). The Molecular Taxonomy of Primary Prostate Cancer. Cell *163*, 1011-1025.

Canitrot, Y., Cazaux, C., Frechet, M., Bouayadi, K., Lesca, C., Salles, B., and Hoffmann, J.S. (1998). Overexpression of DNA polymerase beta in cell results in a mutator phenotype and a decreased sensitivity to anticancer drugs. Proc Natl Acad Sci U S A *95*, 12586-12590.

Carnevale, J., and Ashworth, A. (2015). Assessing the Significance of BRCA1 and BRCA2 Mutations in Pancreatic Cancer. J Clin Oncol *33*, 3080-+.

Carter, R.J., and Parsons, J.L. (2016). Base Excision Repair, a Pathway Regulated by Posttranslational Modifications. Mol Cell Biol *36*, 1426-1437.

Carver, B.S., Chapinski, C., Wongvipat, J., Hieronymus, H., Chen, Y., Chandarlapaty, S., Arora, V.K., Le, C., Koutcher, J., Scher, H.*, et al.* (2011). Reciprocal feedback regulation of PI3K and androgen receptor signaling in PTEN-deficient prostate cancer. Cancer Cell *19*, 575-586.

Cerbinskaite, A., Mukhopadhyay, A., Plummer, E.R., Curtin, N.J., and Edmondson, R.J. (2012). Defective homologous recombination in human cancers. Cancer Treat Rev *38*, 89-100.

Cerveira, N., Ribeiro, F.R., Peixoto, A., Costa, V., Henrique, R., Jeronimo, C., and Teixeira, M.R. (2006). TMPRSS2-ERG gene fusion causing ERG overexpression precedes chromosome copy number changes in prostate carcinomas and paired HGPIN lesions. Neoplasia *8*, 826-832.

Cescon, D.W., Gorrini, C., and Mak, T.W. (2015). Breaking up is hard to do: PI3K isoforms on the rebound. Cancer Cell *27*, 5-7.

Chapman, J.R., Taylor, M.R., and Boulton, S.J. (2012). Playing the end game: DNA double-strand break repair pathway choice. Molecular cell *47*, 497-510.

Chen, Z., Trotman, L.C., Shaffer, D., Lin, H.K., Dotan, Z.A., Niki, M., Koutcher, J.A., Scher, H.I., Ludwig, T., Gerald, W.*, et al.* (2005). Crucial role of p53-dependent cellular senescence in suppression of Pten-deficient tumorigenesis. Nature *436*, 725-730.

Choo, R., Klotz, L., Danjoux, C., Morton, G.C., DeBoer, G., Szumacher, E., Fleshner, N., Bunting, P., and Hruby, G. (2002). Feasibility study: watchful waiting for localized low to intermediate grade prostate carcinoma with selective delayed intervention based on prostate specific antigen, histological and/or clinical progression. J Urol *167*, 1664-1669.

Ciccia, A., and Elledge, S.J. (2010). The DNA damage response: making it safe to play with knives. Mol Cell *40*, 179-204.

Clark, J.P., and Cooper, C.S. (2009). ETS gene fusions in prostate cancer. Nat Rev Urol *6*, 429-439.

Cooperberg, M.R., Broering, J.M., and Carroll, P.R. (2009). Risk assessment for prostate cancer metastasis and mortality at the time of diagnosis. J Natl Cancer Inst *101*, 878-887.

Cunha, G.R. (1973). The role of androgens in the epithelio-mesenchymal interactions involved in prostatic morphogenesis in embryonic mice. Anat Rec *175*, 87-96.

D'Amico, A.V., Whittington, R., Malkowicz, S.B., Schultz, D., Blank, K., Broderick, G.A., Tomaszewski, J.E., Renshaw, A.A., Kaplan, I., Beard, C.J.*, et al.* (1998). Biochemical outcome after radical prostatectomy, external beam radiation therapy, or interstitial radiation therapy for clinically localized prostate cancer. JAMA *280*, 969-974.

Davis, A.J., and Chen, D.J. (2013). DNA double strand break repair via non-homologous end-joining. Transl Cancer Res *2*, 130-143.

de Boer, J., and Hoeijmakers, J.H. (2000). Nucleotide excision repair and human syndromes. Carcinogenesis *21*, 453-460.

de Bono, J.S., Scher, H.I., Montgomery, R.B., Parker, C., Miller, M.C., Tissing, H., Doyle, G.V., Terstappen, L.W., Pienta, K.J., and Raghavan, D. (2008). Circulating tumor cells predict survival benefit from treatment in metastatic castration-resistant prostate cancer. Clin Cancer Res *14*, 6302-6309.

de Dieuleveult, M., Yen, K., Hmitou, I., Depaux, A., Boussouar, F., Bou Dargham, D., Jounier, S., Humbertclaude, H., Ribierre, F., Baulard, C.*, et al.* (2016). Genome-wide nucleosome specificity and function of chromatin remodellers in ES cells. Nature *530*, 113-116.

De Lorenzo, S.B., Patel, A.G., Hurley, R.M., and Kaufmann, S.H. (2013). The Elephant and the Blind Men: Making Sense of PARP Inhibitors in Homologous Recombination Deficient Tumor Cells. Front Oncol *3*, 228.

Demichelis, F., Fall, K., Perner, S., Andren, O., Schmidt, F., Setlur, S.R., Hoshida, Y., Mosquera, J.M., Pawitan, Y., Lee, C.*, et al.* (2007). TMPRSS2:ERG gene fusion associated with lethal prostate cancer in a watchful waiting cohort. Oncogene *26*, 4596-4599.

Dietlein, F., Thelen, L., and Reinhardt, H.C. (2014). Cancer-specific defects in DNA repair pathways as targets for personalized therapeutic approaches. Trends Genet *30*, 326-339.

Difilippantonio, M.J., Zhu, J., Chen, H.T., Meffre, E., Nussenzweig, M.C., Max, E.E., Ried, T., and Nussenzweig, A. (2000). DNA repair protein Ku80 suppresses chromosomal aberrations and malignant transformation. Nature *404*, 510-514.

Dimitrov, L., Hong, C.S., Yang, C., Zhuang, Z., and Heiss, J.D. (2015). New developments in the pathogenesis and therapeutic targeting of the IDH1 mutation in glioma. Int J Med Sci *12*, 201-213.

Dominguez-Valentin, M., Joost, P., Therkildsen, C., Jonsson, M., Rambech, E., and Nilbert, M. (2016). Frequent mismatch-repair defects link prostate cancer to Lynch syndrome. Bmc Urol *16*.

Drost, J., Karthaus, W.R., Gao, D., Driehuis, E., Sawyers, C.L., Chen, Y., and Clevers, H. (2016). Organoid culture systems for prostate epithelial and cancer tissue. Nat Protoc *11*, 347-358.

Duan, S., and Pagano, M. (2015). SPOP Mutations or ERG Rearrangements Result in Enhanced Levels of ERG to Promote Cell Invasion in Prostate Cancer. Mol Cell *59*, 883-884.

Eisenhauer, E.A., Therasse, P., Bogaerts, J., Schwartz, L.H., Sargent, D., Ford, R., Dancey, J., Arbuck, S., Gwyther, S., Mooney, M.*, et al.* (2009). New response evaluation criteria in solid tumours: revised RECIST guideline (version 1.1). Eur J Cancer *45*, 228-247.

Emmert, S., Kobayashi, N., Khan, S.G., and Kraemer, K.H. (2000). The xeroderma pigmentosum group C gene leads to selective repair of cyclobutane pyrimidine dimers rather than 6-4 photoproducts. Proc Natl Acad Sci U S A *97*, 2151-2156.

Emmert, S., Leibeling, D., and Runger, T.M. (2006). Syndromes with genetic instability: model diseases for (skin) cancerogenesis. J Dtsch Dermatol Ges *4*, 721-731.

Emmert, S., Schneider, T.D., Khan, S.G., and Kraemer, K.H. (2001). The human XPG gene: gene architecture, alternative splicing and single nucleotide polymorphisms. Nucleic Acids Res *29*, 1443-1452.

Emmert, S., Slor, H., Busch, D.B., Batko, S., Albert, R.B., Coleman, D., Khan, S.G., Abu-Libdeh, B., DiGiovanna, J.J., Cunningham, B.B.*, et al.* (2002). Relationship of neurologic degeneration to genotype in three xeroderma pigmentosum group G patients. J Invest Dermatol *118*, 972-982.

Farmer, H., McCabe, N., Lord, C.J., Tutt, A.N.J., Johnson, D.A., Richardson, T.B., Santarosa, M., Dillon, K.J., Hickson, I., Knights, C.*, et al.* (2005). Targeting the DNA repair defect in BRCA mutant cells as a therapeutic strategy. Nature *434*, 917-921.

Ferraldeschi, R., Nava Rodrigues, D., Riisnaes, R., Miranda, S., Figueiredo, I., Rescigno, P., Ravi, P., Pezaro, C., Omlin, A., Lorente, D.*, et al.* (2015). PTEN protein loss and clinical outcome from castration-resistant prostate cancer treated with abiraterone acetate. Eur Urol *67*, 795-802.

Francis, J.C., McCarthy, A., Thomsen, M.K., Ashworth, A., and Swain, A. (2010). Brca2 and Trp53 deficiency cooperate in the progression of mouse prostate tumourigenesis. PLoS Genet *6*, e1000995.

Frank, K.M., Sharpless, N.E., Gao, Y.J., Sekiguchi, J.M., Ferguson, D.O., Zhu, C.M., Manis, J.P., Horner, J., DePinho, R.A., and Alt, F.W. (2000). DNA ligase IV deficiency in mice leads to defective neurogenesis and embryonic lethality via the p53 pathway. Molecular Cell *5*, 993-1002.

Fujii, T., Khawaja, M.R., DiNardo, C.D., Atkins, J.T., and Janku, F. (2016). Targeting isocitrate dehydrogenase (IDH) in cancer. Discov Med *21*, 373-380.

Fukui, K. (2010). DNA mismatch repair in eukaryotes and bacteria. J Nucleic Acids *2010*.

Futreal, P.A., Liu, Q.Y., Shattuckeidens, D., Cochran, C., Harshman, K., Tavtigian, S., Bennett, L.M., Haugenstrano, A., Swensen, J., Miki, Y.*, et al.* (1994). Brca1 Mutations in Primary Breast and Ovarian Carcinomas. Science *266*, 120-122.

Gan, W., Dai, X., Lunardi, A., Li, Z., Inuzuka, H., Liu, P., Varmeh, S., Zhang, J., Cheng, L., Sun, Y.*, et al.* (2015). SPOP Promotes Ubiquitination and Degradation of the ERG Oncoprotein to Suppress Prostate Cancer Progression. Mol Cell *59*, 917-930.

Gao, D., Vela, I., Sboner, A., Iaquinta, P.J., Karthaus, W.R., Gopalan, A., Dowling, C., Wanjala, J.N., Undvall, E.A., Arora, V.K.*, et al.* (2014). Organoid cultures derived from patients with advanced prostate cancer. Cell *159*, 176-187.

Gao, N., Ishii, K., Mirosevich, J., Kuwajima, S., Oppenheimer, S.R., Roberts, R.L., Jiang, M., Yu, X., Shappell, S.B., Caprioli, R.M.*, et al.* (2005). Forkhead box A1 regulates prostate ductal morphogenesis and promotes epithelial cell maturation. Development *132*, 3431-3443.

Gao, N., Zhang, J., Rao, M.A., Case, T.C., Mirosevich, J., Wang, Y., Jin, R., Gupta, A., Rennie, P.S., and Matusik, R.J. (2003). The role of hepatocyte nuclear factor-3 alpha (Forkhead Box A1) and androgen receptor in transcriptional regulation of prostatic genes. Mol Endocrinol *17*, 1484-1507.

Garcia, A.J., Ruscetti, M., Arenzana, T.L., Tran, L.M., Bianci-Frias, D., Sybert, E., Priceman, S.J., Wu, L., Nelson, P.S., Smale, S.T.*, et al.* (2014). Pten null prostate epithelium promotes localized myeloid-derived suppressor cell expansion and immune suppression during tumor initiation and progression. Mol Cell Biol *34*, 2017-2028.

Gaspar-Maia, A., Alajem, A., Polesso, F., Sridharan, R., Mason, M.J., Heidersbach, A., Ramalho-Santos, J., McManus, M.T., Plath, K., Meshorer, E.*, et al.* (2009). Chd1 regulates open chromatin and pluripotency of embryonic stem cells. Nature *460*, 863-868.

Gonzalez-Suarez, I., Redwood, A.B., Grotsky, D.A., Neumann, M.A., Cheng, E.H., Stewart, C.L., Dusso, A., and Gonzalo, S. (2011). A new pathway that regulates 53BP1 stability implicates cathepsin L and vitamin D in DNA repair. Embo J *30*, 3383-3396.

Goodwin, J.F., Schiewer, M.J., Dean, J.L., Schrecengost, R.S., de Leeuw, R., Han, S.M., Ma, T., Den, R.B., Dicker, A.P., Feng, F.Y.*, et al.* (2013). A Hormone-DNA Repair Circuit Governs the Response to Genotoxic Insult. Cancer discovery *3*, 1254-1271.

Grasso, C.S., Wu, Y.M., Robinson, D.R., Cao, X., Dhanasekaran, S.M., Khan, A.P., Quist, M.J., Jing, X., Lonigro, R.J., Brenner, J.C.*, et al.* (2012a). The mutational landscape of lethal castration-resistant prostate cancer. Nature *487*, 239-243.

Grasso, C.S., Wu, Y.M., Robinson, D.R., Cao, X.H., Dhanasekaran, S.M., Khan, A.P., Quist, M.J., Jing, X., Lonigro, R.J., Brenner, J.C.*, et al.* (2012b). The mutational landscape of lethal castration-resistant prostate cancer. Nature *487*, 239-243.

Guidos, C.J., Williams, C.J., Grandal, I., Knowles, G., Huang, M.T.F., and Danska, J.S. (1996). V(D)J recombination activates a p53-dependent DNA damage checkpoint in scid lymphocyte precursors. Gene Dev *10*, 2038-2054.

Guzman-Ayala, M., Sachs, M., Koh, F.M., Onodera, C., Bulut-Karslioglu, A., Lin, C.J., Wong, P., Nitta, R., Song, J.S., and Ramalho-Santos, M. (2015). Chd1 is essential for the high transcriptional output and rapid growth of the mouse epiblast. Development *142*, 118-127.

Han, X., Zhang, L., Chung, J., Mayca Pozo, F., Tran, A., Seachrist, D.D., Jacobberger, J.W., Keri, R.A., Gilmore, H., and Zhang, Y. (2014). UbcH7 regulates 53BP1 stability and DSB repair. Proceedings of the National Academy of Sciences of the United States of America *111*, 17456-17461.

Hanahan, D., and Weinberg, R.A. (2000). The hallmarks of cancer. Cell *100*, 57-70.

Hanahan, D., and Weinberg, R.A. (2011). Hallmarks of cancer: the next generation. Cell *144*, 646-674.

Heinlein, C.A., and Chang, C. (2004). Androgen receptor in prostate cancer. Endocr Rev *25*, 276-308.

Hieronymus, H., Lamb, J., Ross, K.N., Peng, X.P., Clement, C., Rodina, A., Nieto, M., Du, J., Stegmaier, K., Raj, S.M.*, et al.* (2006). Gene expression signature-based chemical genomic prediction identifies a novel class of HSP90 pathway modulators. Cancer Cell *10*, 321-330.

Hu, Y., Wang, C., Huang, K., Xia, F., Parvin, J.D., and Mondal, N. (2014). Regulation of 53BP1 protein stability by RNF8 and RNF168 is important for efficient DNA double-strand break repair. PLoS One *9*, e110522.

Huang, S., Gulzar, Z.G., Salari, K., Lapointe, J., Brooks, J.D., and Pollack, J.R. (2012). Recurrent deletion of CHD1 in prostate cancer with relevance to cell invasiveness. Oncogene *31*, 4164-4170.

Hung, H.T., Ong, R., Haike, K., Petrova, E., Chong, M.L., Loh, M., Bhattacharya, B., Soong, R., and Liu, N. (2015). Abstract 2674: Activity of BAY1082439, a balanced PI3Kα/β inhibitor, in gastric cancer. Cancer Research *75*, 2674-2674.

Jia, S., Liu, Z., Zhang, S., Liu, P., Zhang, L., Lee, S.H., Zhang, J., Signoretti, S., Loda, M., Roberts, T.M.*, et al.* (2008). Essential roles of PI(3)K-p110beta in cell growth, metabolism and tumorigenesis. Nature *454*, 776-779.

Jiao, J., Wang, S., Qiao, R., Vivanco, I., Watson, P.A., Sawyers, C.L., and Wu, H. (2007). Murine cell lines derived from Pten null prostate cancer show the critical role of PTEN in hormone refractory prostate cancer development. Cancer Res *67*, 6083-6091.

Jiricny, J. (2006). The multifaceted mismatch-repair system. Nat Rev Mol Cell Biol *7*, 335-346.

Johnson, N., Johnson, S.F., Yao, W., Li, Y.C., Choi, Y.E., Bernhardy, A.J., Wang, Y., Capelletti, M., Sarosiek, K.A., Moreau, L.A.*, et al.* (2013). Stabilization of mutant BRCA1 protein confers PARP inhibitor and platinum resistance. Proceedings of the National Academy of Sciences of the United States of America *110*, 17041-17046.

Johnson, N., Li, Y.C., Walton, Z.E., Cheng, K.A., Li, D.A., Rodig, S.J., Moreau, L.A., Unitt, C., Bronson, R.T., Thomas, H.D.*, et al.* (2011). Compromised CDK1 activity sensitizes BRCA-proficient cancers to PARP inhibition. Nat Med *17*, 875-U257.

Kaffenberger, S.D., and Barbieri, C.E. (2016). Molecular subtyping of prostate cancer. Curr Opin Urol *26*, 213-218.

Kari, V., Mansour, W.Y., Raul, S.K., Baumgart, S.J., Mund, A., Grade, M., Sirma, H., Simon, R., Will, H., Dobbelstein, M.*, et al.* (2016). Loss of CHD1 causes DNA repair defects and enhances prostate cancer therapeutic responsiveness. EMBO Rep *17*, 1609-1623.

Kattan, M.W., Eastham, J.A., Stapleton, A.M., Wheeler, T.M., and Scardino, P.T. (1998). A preoperative nomogram for disease recurrence following radical prostatectomy for prostate cancer. J Natl Cancer Inst *90*, 766-771.

Kelley, M.R., Cheng, L., Foster, R., Tritt, R., Jiang, J., Broshears, J., and Koch, M. (2001). Elevated and altered expression of the multifunctional DNA base excision repair and redox enzyme Ape1/ref-1 in prostate cancer. Clin Cancer Res *7*, 824-830.

Khan, S.G., Metter, E.J., Tarone, R.E., Bohr, V.A., Grossman, L., Hedayati, M., Bale, S.J., Emmert, S., and Kraemer, K.H. (2000). A new xeroderma pigmentosum group C poly(AT) insertion/deletion polymorphism. Carcinogenesis *21*, 1821-1825.

Khan, S.G., Oh, K.S., Shahlavi, T., Ueda, T., Busch, D.B., Inui, H., Emmert, S., Imoto, K., Muniz-Medina, V., Baker, C.C.*, et al.* (2006). Reduced XPC DNA repair gene mRNA levels in clinically normal parents of xeroderma pigmentosum patients. Carcinogenesis *27*, 84-94.

Koh, F.M., Lizama, C.O., Wong, P., Hawkins, J.S., Zovein, A.C., and Ramalho-Santos, M. (2015a). Emergence of hematopoietic stem and progenitor cells involves a Chd1-dependent increase in total nascent transcription. Proceedings of the National Academy of Sciences of the United States of America *112*, E1734-E1743.

Koh, F.M., Lizama, C.O., Wong, P., Hawkins, J.S., Zovein, A.C., and Ramalho-Santos, M. (2015b). Emergence of hematopoietic stem and progenitor cells involves a Chd1-dependent increase in total nascent transcription. Proc Natl Acad Sci U S A *112*, E1734-1743.

Konev, A.Y., Tribus, M., Park, S.Y., Podhraski, V., Lim, C.Y., Emelyanov, A.V., Vershilova, E., Pirrotta, V., Kadonaga, J.T., Lusser, A.*, et al.* (2007). CHD1 motor protein is required for deposition of histone variant h3.3 into chromatin in vivo. Science *317*, 1087-1090.

Krajewska, M., Fehrmann, R.S., de Vries, E.G., and van Vugt, M.A. (2015). Regulators of homologous recombination repair as novel targets for cancer treatment. Front Genet *6*, 96.

Ku, S.Y., Rosario, S., Wang, Y., Mu, P., Seshadri, M., Goodrich, Z.W., Goodrich, M.M., Labbe, D.P., Gomez, E.C., Wang, J.*, et al.* (2017). Rb1 and Trp53 cooperate to suppress prostate cancer lineage plasticity, metastasis, and antiandrogen resistance. Science *355*, 78-83.

Kumar, A., Coleman, I., Morrissey, C., Zhang, X., True, L.D., Gulati, R., Etzioni, R., Bolouri, H., Montgomery, B., White, T.*, et al.* (2016). Substantial interindividual and limited intraindividual genomic diversity among tumors from men with metastatic prostate cancer. Nat Med *22*, 369-378.

Kyprianou, N., and Isaacs, J.T. (1988). Activation of programmed cell death in the rat ventral prostate after castration. Endocrinology *122*, 552-562.

Langmead, B., Trapnell, C., Pop, M., and Salzberg, S.L. (2009). Ultrafast and memory-efficient alignment of short DNA sequences to the human genome. Genome Biol *10*.

Lapointe, J., Li, C., Giacomini, C.P., Salari, K., Huang, S., Wang, P., Ferrari, M., Hernandez-Boussard, T., Brooks, J.D., and Pollack, J.R. (2007). Genomic profiling reveals alternative genetic pathways of prostate tumorigenesis. Cancer Res *67*, 8504-8510.

Larsen, D.H., Poinsignon, C., Gudjonsson, T., Dinant, C., Payne, M.R., Hari, F.J., Rendtlew Danielsen, J.M., Menard, P., Sand, J.C., Stucki, M.*, et al.* (2010). The chromatin-remodeling factor CHD4 coordinates signaling and repair after DNA damage. J Cell Biol *190*, 731-740.

Lehmann, A.R., McGibbon, D., and Stefanini, M. (2011). Xeroderma pigmentosum. Orphanet J Rare Dis *6*, 70.

Leibeling, D., Laspe, P., and Emmert, S. (2006). Nucleotide excision repair and cancer. J Mol Histol *37*, 225-238.

Li, M.L., and Greenberg, R.A. (2012). Links between genome integrity and BRCA1 tumor suppression. Trends Biochem Sci *37*, 418-424.

Li, P., Yang, R., and Gao, W.Q. (2014). Contributions of epithelial-mesenchymal transition and cancer stem cells to the development of castration resistance of prostate cancer. Mol Cancer *13*, 55.

Lin, J.J., Lehmann, L.W., Bonora, G., Sridharan, R., Vashisht, A.A., Tran, N., Plath, K., Wohlschlegel, J.A., and Carey, M. (2011). Mediator coordinates PIC assembly with recruitment of CHD1. Genes & development *25*, 2198-2209.

Liu, W., Lindberg, J., Sui, G., Luo, J., Egevad, L., Li, T., Xie, C., Wan, M., Kim, S.T., Wang, Z.*, et al.* (2012). Identification of novel CHD1-associated collaborative alterations of genomic structure and functional assessment of CHD1 in prostate cancer. Oncogene *31*, 3939-3948.

Lord, C.J., and Ashworth, A. (2012). The DNA damage response and cancer therapy. Nature *481*, 287-294.

Luijsterburg, M.S., de Krijger, I., Wiegant, W.W., Shah, R.G., Smeenk, G., de Groot, A.J., Pines, A., Vertegaal, A.C., Jacobs, J.J., Shah, G.M.*, et al.* (2016). PARP1 Links CHD2-Mediated Chromatin Expansion and H3.3 Deposition to DNA Repair by Non-homologous End-Joining. Mol Cell *61*, 547-562.

Lusser, A., Urwin, D.L., and Kadonaga, J.T. (2005). Distinct activities of CHD1 and ACF in ATP-dependent chromatin assembly. Nature structural & molecular biology *12*, 160-166.

Maddison, L.A., Sutherland, B.W., Barrios, R.J., and Greenberg, N.M. (2004). Conditional deletion of Rb causes early stage prostate cancer. Cancer Res *64*, 6018-6025.

Mallette, F.A., and Richard, S. (2012). K48-linked ubiquitination and protein degradation regulate 53BP1 recruitment at DNA damage sites. Cell Res *22*, 1221-1223.

Marfella, C.G., and Imbalzano, A.N. (2007). The Chd family of chromatin remodelers. Mutat Res *618*, 30-40.

Markkanen, E., Fischer, R., Ledentcova, M., Kessler, B.M., and Dianov, G.L. (2015). Cells deficient in base-excision repair reveal cancer hallmarks originating from adjustments to genetic instability. Nucleic Acids Res *43*, 3667-3679.

Massard, C., Chi, K.N., Castellano, D., de Bono, J., Gravis, G., Dirix, L., Machiels, J.P., Mita, A., Gonzalez, B.M., Turri, S.*, et al.* (2017). Phase Ib dose-finding study of abiraterone acetate plus buparlisib (BKM120) or dactolisib (BEZ235) in patients with castration-resistant prostate cancer. Eur J Cancer *76*, 36-44.

Mateo, J., Carreira, S., Sandhu, S., Miranda, S., Mossop, H., Perez-Lopez, R., Nava Rodrigues, D., Robinson, D., Omlin, A., Tunariu, N.*, et al.* (2015a). DNA-Repair Defects and Olaparib in Metastatic Prostate Cancer. N Engl J Med *373*, 1697-1708.

Mateo, J., Carreira, S., Sandhu, S., Miranda, S., Mossop, H., Perez-Lopez, R., Rodrigues, D.N., Robinson, D., Omlin, A., Tunariu, N.*, et al.* (2015b). DNA-Repair Defects and Olaparib in Metastatic Prostate Cancer. New Engl J Med *373*, 1697-1708.

Mateo, J., Ganji, G., Lemech, C., Burris, H.A., Han, S.W., Swales, K., Decordova, S., DeYoung, M.P., Smith, D.A., Kalyana-Sundaram, S.*, et al.* (2017). A First-Time-in-Human Study of GSK2636771, a Phosphoinositide 3 Kinase Beta-Selective Inhibitor, in Patients with Advanced Solid Tumors. Clin Cancer Res.

McCabe, N., Turner, N.C., Lord, C.J., Kluzek, K., Bialkowska, A., Swift, S., Giavara, S., O'Connor, M.J., Tutt, A.N., Zdzienicka, M.Z.*, et al.* (2006). Deficiency in the repair of DNA damage by homologous recombination and sensitivity to poly(ADP-ribose) polymerase inhibition. Cancer Research *66*, 8109-8115.

McNeill, D.R., Lin, P.C., Miller, M.G., Pistell, P.J., de Souza-Pinto, N.C., Fishbein, K.W., Spencer, R.G., Liu, Y., Pettan-Brewer, C., Ladiges, W.C.*, et al.* (2011). XRCC1 haploinsufficiency in mice has little effect on aging, but adversely modifies exposure-dependent susceptibility. Nucleic Acids Res *39*, 7992-8004.

Metzger, E., Willmann, D., McMillan, J., Forne, I., Metzger, P., Gerhardt, S., Petroll, K., von Maessenhausen, A., Urban, S., Schott, A.K.*, et al.* (2016a). Assembly of methylated KDM1A and CHD1 drives androgen receptor-dependent transcription and translocation. Nat Struct Mol Biol *23*, 132-139.

Metzger, E., Willmann, D., McMillan, J., Forne, I., Metzger, P., Gerhardt, S., Petroll, K., von Maessenhausen, A., Urban, S., Schott, A.K.*, et al.* (2016b). Assembly of methylated KDM1A and CHD1 drives androgen receptor-dependent transcription and translocation. Nature structural & molecular biology *23*, 132-+.

Miki, Y., Swensen, J., Shattuckeidens, D., Futreal, P.A., Harshman, K., Tavtigian, S., Liu, Q.Y., Cochran, C., Bennett, L.M., Ding, W.*, et al.* (1994). A Strong Candidate for the Breast and Ovarian-Cancer Susceptibility Gene Brca1. Science *266*, 66-71.

Moskwa, P., Buffa, F.M., Pan, Y.F., Panchakshari, R., Gottipati, P., Muschel, R.J., Beech, J., Kulshrestha, R., Abdelmohsen, K., Weinstock, D.M.*, et al.* (2011). miR-182-Mediated Downregulation of BRCA1 Impacts DNA Repair and Sensitivity to PARP Inhibitors. Molecular Cell *41*, 210-220.

Moynahan, M.E., Cui, T.Y., and Jasin, M. (2001a). Homology-directed DNA repair, mitomycin-C resistance, and chromosome stability is restored with correction of a Brca1 mutation. Cancer Research *61*, 4842-4850.

Moynahan, M.E., Pierce, A.J., and Jasin, M. (2001b). BRCA2 is required for homology-directed repair of chromosomal breaks. Molecular Cell *7*, 263-272.

Mulholland, D.J., Kobayashi, N., Ruscetti, M., Zhi, A., Tran, L.M., Huang, J., Gleave, M., and Wu, H. (2012). Pten loss and RAS/MAPK activation cooperate to promote EMT and metastasis initiated from prostate cancer stem/progenitor cells. Cancer Res *72*, 1878-1889.

Mulholland, D.J., Tran, L.M., Li, Y., Cai, H., Morim, A., Wang, S., Plaisier, S., Garraway, I.P., Huang, J., Graeber, T.G.*, et al.* (2011). Cell autonomous role of PTEN in regulating castration-resistant prostate cancer growth. Cancer Cell *19*, 792-804.

Murai, J., Yang, K.L., Dejsuphong, D., Hirota, K., Takeda, S., and D'Andrea, A.D. (2011). The USP1/UAF1 Complex Promotes Double-Strand Break Repair through Homologous Recombination. Mol Cell Biol *31*, 2462-2469.

Nagarajan, P., Onami, T.M., Rajagopalan, S., Kania, S., Donnell, R., and Venkatachalam, S. (2009). Role of chromodomain helicase DNA-binding protein 2 in DNA damage response signaling and tumorigenesis. Oncogene *28*, 1053-1062.

Nauseef, J.T., and Henry, M.D. (2011). Epithelial-to-mesenchymal transition in prostate cancer: paradigm or puzzle? Nat Rev Urol *8*, 428-439.

Nelson, P.S., Clegg, N., Arnold, H., Ferguson, C., Bonham, M., White, J., Hood, L., and Lin, B. (2002). The program of androgen-responsive genes in neoplastic prostate epithelium. Proc Natl Acad Sci U S A *99*, 11890-11895.

Nghiem, B., Zhang, X.T., Lam, H.M., True, L.D., Coleman, I., Higano, C.S., Nelson, P.S., Pritchard, C.C., and Morrissey, C. (2016). Mismatch repair enzyme expression in primary and castrate resistant prostate cancer. Asian J Urol *3*, 223-228.

Nussenzweig, A., Sokol, K., Burgman, P., Li, L.G., and Li, G.C. (1997). Hypersensitivity of Ku80-deficient cell lines and mice to DNA damage: The effects of ionizing radiation on growth, survival, and development. P Natl Acad Sci USA *94*, 13588-13593.

Okkenhaug, K., Graupera, M., and Vanhaesebroeck, B. (2016). Targeting PI3K in Cancer: Impact on Tumor Cells, Their Protective Stroma, Angiogenesis, and Immunotherapy. Cancer Discov *6*, 1090-1105.

Pan, M.R., Hsieh, H.J., Dai, H., Hung, W.C., Li, K., Peng, G., and Lin, S.Y. (2012). Chromodomain helicase DNA-binding protein 4 (CHD4) regulates homologous recombination DNA repair, and its deficiency sensitizes cells to poly(ADP-ribose) polymerase (PARP) inhibitor treatment. J Biol Chem *287*, 6764-6772.

Pearl, L.H., Schierz, A.C., Ward, S.E., Al-Lazikani, B., and Pearl, F.M. (2015). Therapeutic opportunities within the DNA damage response. Nat Rev Cancer *15*, 166-180.

Peasland, A., Wang, L.Z., Rowling, E., Kyle, S., Chen, T., Hopkins, A., Cliby, W.A., Sarkaria, J., Beale, G., Edmondson, R.J*., et al.* (2011). Identification and evaluation of a potent novel ATR inhibitor, NU6027, in breast and ovarian cancer cell lines. Brit J Cancer *105*, 372-381.

Penney, K.L., Stampfer, M.J., Jahn, J.L., Sinnott, J.A., Flavin, R., Rider, J.R., Finn, S., Giovannucci, E., Sesso, H.D., Loda, M.*, et al.* (2013). Gleason grade progression is uncommon. Cancer Res *73*, 5163-5168.

Perner, S., Demichelis, F., Beroukhim, R., Schmidt, F.H., Mosquera, J.M., Setlur, S., Tchinda, J., Tomlins, S.A., Hofer, M.D., Pienta, K.G.*, et al.* (2006). TMPRSS2:ERG fusion-associated deletions provide insight into the heterogeneity of prostate cancer. Cancer Res *66*, 8337-8341.

Perner, S., Mosquera, J.M., Demichelis, F., Hofer, M.D., Paris, P.L., Simko, J., Collins, C., Bismar, T.A., Chinnaiyan, A.M., De Marzo, A.M.*, et al.* (2007). TMPRSS2-ERG fusion prostate cancer: an early molecular event associated with invasion. Am J Surg Pathol *31*, 882-888.

Pettersson, A., Graff, R.E., Bauer, S.R., Pitt, M.J., Lis, R.T., Stack, E.C., Martin, N.E., Kunz, L., Penney, K.L., Ligon, A.H.*, et al.* (2012). The TMPRSS2:ERG rearrangement, ERG expression, and prostate cancer outcomes: a cohort study and meta-analysis. Cancer Epidemiol Biomarkers Prev *21*, 1497-1509.

Pflueger, D., Terry, S., Sboner, A., Habegger, L., Esgueva, R., Lin, P.C., Svensson, M.A., Kitabayashi, N., Moss, B.J., MacDonald, T.Y.*, et al.* (2011). Discovery of non-ETS gene fusions in human prostate cancer using next-generation RNA sequencing. Genome Res *21*, 56-67.

Pico de Coana, Y., Choudhury, A., and Kiessling, R. (2015). Checkpoint blockade for cancer therapy: revitalizing a suppressed immune system. Trends Mol Med *21*, 482-491.

Pierce, A.J., Johnson, R.D., Thompson, L.H., and Jasin, M. (1999). XRCC3 promotes homology-directed repair of DNA damage in mammalian cells. Genes & development *13*, 2633-2638.

Polkinghorn, W.R., Parker, J.S., Lee, M.X., Kass, E.M., Spratt, D.E., Iaquinta, P.J., Arora, V.K., Yen, W.F., Cai, L., Zheng, D.*, et al.* (2013). Androgen receptor signaling regulates DNA repair in prostate cancers. Cancer discovery *3*, 1245-1253.

Polo, S.E., Kaidi, A., Baskcomb, L., Galanty, Y., and Jackson, S.P. (2010). Regulation of DNA-damage responses and cell-cycle progression by the chromatin remodelling factor CHD4. EMBO J *29*, 3130-3139.

Pritchard, C.C., Mateo, J., Walsh, M.F., De Sarkar, N., Abida, W., Beltran, H., Garofalo, A., Gulati, R., Carreira, S., Eeles, R.*, et al.* (2016). Inherited DNA-Repair Gene Mutations in Men with Metastatic Prostate Cancer. N Engl J Med *375*, 443-453.

Pylayeva-Gupta, Y., Das, S., Handler, J.S., Hajdu, C.H., Coffre, M., Koralov, S.B., and Bar-Sagi, D. (2016). IL35-Producing B Cells Promote the Development of Pancreatic Neoplasia. Cancer Discov *6*, 247-255.

Qiu, P., Shandilya, H., D'Alessio, J.M., O'Connor, K., Durocher, J., and Gerard, G.F. (2004). Mutation detection using Surveyor nuclease. Biotechniques *36*, 702-707.

Quail, D.F., and Joyce, J.A. (2013). Microenvironmental regulation of tumor progression and metastasis. Nat Med *19*, 1423-1437.

Ran, F.A., Hsu, P.D., Wright, J., Agarwala, V., Scott, D.A., and Zhang, F. (2013). Genome engineering using the CRISPR-Cas9 system. Nat Protoc *8*, 2281-2308.

Robinson, D., Van Allen, E.M., Wu, Y.M., Schultz, N., Lonigro, R.J., Mosquera, J.M., Montgomery, B., Taplin, M.E., Pritchard, C.C., Attard, G.*, et al.* (2015). Integrative clinical genomics of advanced prostate cancer. Cell *161*, 1215-1228.

Rodrigues, L.U., Rider, L., Nieto, C., Romero, L., Karimpour-Fard, A., Loda, M., Lucia, M.S., Wu, M., Shi, L., Cimic, A.*, et al.* (2015). Coordinate loss of MAP3K7 and CHD1 promotes aggressive prostate cancer. Cancer Res *75*, 1021-1034.

Rouleau, M., Patel, A., Hendzel, M.J., Kaufmann, S.H., and Poirier, G.G. (2010). PARP inhibition: PARP1 and beyond. Nature Reviews Cancer *10*, 293-301.

Rubin, M.A. (2012). ETS rearrangements in prostate cancer. Asian J Androl *14*, 393-399.

Ruscetti, M., Dadashian, E.L., Guo, W., Quach, B., Mulholland, D.J., Park, J.W., Tran, L.M., Kobayashi, N., Bianchi-Frias, D., Xing, Y.*, et al.* (2016). HDAC inhibition impedes epithelial-mesenchymal plasticity and suppresses metastatic, castration-resistant prostate cancer. Oncogene *35*, 3781-3795.

Sancar, A. (1999). Excision repair invades the territory of mismatch repair. Nat Genet *21*, 247-249.

Scher, H.I., Morris, M.J., Stadler, W.M., Higano, C., Basch, E., Fizazi, K., Antonarakis, E.S., Beer, T.M., Carducci, M.A., Chi, K.N.*, et al.* (2016). Trial Design and Objectives for Castration-Resistant Prostate Cancer: Updated Recommendations From the Prostate Cancer Clinical Trials Working Group 3. J Clin Oncol *34*, 1402-1418.

Shenoy, T.R., Boysen, G., Wang, M.Y., Xu, Q.Z., Guo, W., Koh, F.M., Wang, C., Zhang, L.Z., Wang, Y., Gil, V.*, et al.* (2017). CHD1 loss sensitizes prostate cancer to DNA damaging therapy by promoting error-prone double-strand break repair. Ann Oncol *28*, 1495-1507.

Siegel, R.L., Miller, K.D., and Jemal, A. (2017). Cancer Statistics, 2017. CA Cancer J Clin *67*, 7-30.

Siggens, L., Cordeddu, L., Ronnerblad, M., Lennartsson, A., and Ekwall, K. (2015). Transcription-coupled recruitment of human CHD1 and CHD2 influences chromatin accessibility and histone H3 and H3.3 occupancy at active chromatin regions. Epigenetics Chromatin *8*, 4.

Simic, R., Lindstrom, D.L., Tran, H.G., Roinick, K.L., Costa, P.J., Johnson, A.D., Hartzog, G.A., and Arndt, K.M. (2003a). Chromatin remodeling protein Chd1 interacts with transcription elongation factors and localizes to transcribed genes. Embo Journal *22*, 1846-1856.

Simic, R., Lindstrom, D.L., Tran, H.G., Roinick, K.L., Costa, P.J., Johnson, A.D., Hartzog, G.A., and Arndt, K.M. (2003b). Chromatin remodeling protein Chd1 interacts with transcription elongation factors and localizes to transcribed genes. EMBO J *22*, 1846-1856.

Sims, R.J., 3rd, Chen, C.F., Santos-Rosa, H., Kouzarides, T., Patel, S.S., and Reinberg, D. (2005). Human but not yeast CHD1 binds directly and selectively to histone H3 methylated at lysine 4 via its tandem chromodomains. J Biol Chem *280*, 41789-41792.

Sims, R.J., Millhouse, S., Chen, C.F., Lewis, B.A., Erdjument-Bromage, H., Tempst, P., Manley, J.L., and Reinberg, D. (2007). Recognition of trimethylated histone h3 lysine 4 facilitates the recruitment of transcription postinitiation factors and pre-mRNA splicing. Molecular cell *28*, 665-676.

Srivastava, D.K., Husain, I., Arteaga, C.L., and Wilson, S.H. (1999). DNA polymerase beta expression differences in selected human tumors and cell lines. Carcinogenesis *20*, 1049-1054.

Starcevic, D., Dalal, S., and Sweasy, J.B. (2004). Is there a link between DNA polymerase beta and cancer? Cell Cycle *3*, 998-1001.

Stokes, D.G., Tartof, K.D., and Perry, R.P. (1996). CHD1 is concentrated in interbands and puffed regions of Drosophila polytene chromosomes. Proc Natl Acad Sci U S A *93*, 7137-7142.

Sulli, G., Di Micco, R., and d'Adda di Fagagna, F. (2012). Crosstalk between chromatin state and DNA damage response in cellular senescence and cancer. Nat Rev Cancer *12*, 709-720.

Sung, P., and Klein, H. (2006). Mechanism of homologous recombination: mediators and helicases take on regulatory functions. Nat Rev Mol Cell Bio *7*, 739-750.

Tan, Y., Ci, Y., Dai, X., Wu, F., Guo, J., Liu, D., North, B.J., Huo, J., and Zhang, J. (2017). Cullin 3SPOP ubiquitin E3 ligase promotes the poly-ubiquitination and degradation of HDAC6. Oncotarget *8*, 47890-47901.

Tarish, F.L., Schultz, N., Tanoglidi, A., Hamberg, H., Letocha, H., Karaszi, K., Hamdy, F.C., Granfors, T., and Helleday, T. (2015). Castration radiosensitizes prostate cancer tissue by impairing DNA double-strand break repair. Sci Transl Med *7*, 312re311.

Tavtigian, S.V., Simard, J., Rommens, J., Couch, F., ShattuckEidens, D., Neuhausen, S., Merajver, S., Thorlacius, S., Offit, K., StoppaLyonnet, D.*, et al.* (1996). The complete BRCA2 gene and mutations in chromosome 13q-linked kindreds. Nature Genetics *12*, 333-337.

Taylor, B.S., Schultz, N., Hieronymus, H., Gopalan, A., Xiao, Y., Carver, B.S., Arora, V.K., Kaushik, P., Cerami, E., Reva, B.*, et al.* (2010a). Integrative genomic profiling of human prostate cancer. Cancer Cell *18*, 11-22.

Taylor, B.S., Schultz, N., Hieronymus, H., Gopalan, A., Xiao, Y.H., Carver, B.S., Arora, V.K., Kaushik, P., Cerami, E., Reva, B.*, et al.* (2010b). Integrative Genomic Profiling of Human Prostate Cancer. Cancer cell *18*, 11-22.

Tereshchenko, I.V., Zhong, H., Chekmareva, M.A., Kane-Goldsmith, N., Santanam, U., Petrosky, W., Stein, M.N., Ganesan, S., Singer, E.A., Moore, D.*, et al.* (2014). ERG and CHD1 heterogeneity in prostate cancer: use of confocal microscopy in assessment of microscopic foci. Prostate *74*, 1551-1559.

Thomsen, F.B., Brasso, K., Klotz, L.H., Roder, M.A., Berg, K.D., and Iversen, P. (2014). Active surveillance for clinically localized prostate cancer--a systematic review. J Surg Oncol *109*, 830-835.

Tomlins, S.A., Bjartell, A., Chinnaiyan, A.M., Jenster, G., Nam, R.K., Rubin, M.A., and Schalken, J.A. (2009). ETS gene fusions in prostate cancer: from discovery to daily clinical practice. Eur Urol *56*, 275-286.

Tomlins, S.A., Laxman, B., Dhanasekaran, S.M., Helgeson, B.E., Cao, X., Morris, D.S., Menon, A., Jing, X., Cao, Q., Han, B.*, et al.* (2007). Distinct classes of chromosomal rearrangements create oncogenic ETS gene fusions in prostate cancer. Nature *448*, 595-599.

Tomlins, S.A., Rhodes, D.R., Perner, S., Dhanasekaran, S.M., Mehra, R., Sun, X.W., Varambally, S., Cao, X., Tchinda, J., Kuefer, R.*, et al.* (2005). Recurrent fusion of TMPRSS2 and ETS transcription factor genes in prostate cancer. Science *310*, 644-648.

Trapnell, C., Pachter, L., and Salzberg, S.L. (2009). TopHat: discovering splice junctions with RNA-Seq. Bioinformatics *25*, 1105-1111.

Trapnell, C., Roberts, A., Goff, L., Pertea, G., Kim, D., Kelley, D.R., Pimentel, H., Salzberg, S.L., Rinn, J.L., and Pachter, L. (2012). Differential gene and transcript expression analysis of RNA-seq experiments with TopHat and Cufflinks. Nat Protoc *7*, 562-578.

Truett, G.E., Heeger, P., Mynatt, R.L., Truett, A.A., Walker, J.A., and Warman, M.L. (2000). Preparation of PCR-quality mouse genomic DNA with hot sodium hydroxide and tris (HotSHOT). Biotechniques *29*, 52, 54.

Turner, N., Tutt, A., and Ashworth, A. (2004). Hallmarks of 'BRCAness' in sporadic cancers. Nature Reviews Cancer *4*, 814-819.

Tutt, A., Bertwistle, D., Valentine, J., Gabriel, A., Swift, S., Ross, G., Griffin, C., Thacker, J., and Ashworth, A. (2001). Mutation in Brca2 stimulates error-prone homology-directed repair of DNA double-strand breaks occurring between repeated sequences. Embo Journal *20*, 4704-4716.

Vanhaesebroeck, B., and Khwaja, A. (2014). PI3Kdelta inhibition hits a sensitive spot in B cell malignancies. Cancer Cell *25*, 269-271.

Waddell, N., Pajic, M., Patch, A.M., Chang, D.K., Kassahn, K.S., Bailey, P., Johns, A.L., Miller, D., Nones, K., Quek, K.*, et al.* (2015). Whole genomes redefine the mutational landscape of pancreatic cancer. Nature *518*, 495-501.

Wallace, S.S., Murphy, D.L., and Sweasy, J.B. (2012). Base excision repair and cancer. Cancer Lett *327*, 73-89.

Wang, S., Gao, J., Lei, Q., Rozengurt, N., Pritchard, C., Jiao, J., Thomas, G.V., Li, G., Roy-Burman, P., Nelson, P.S.*, et al.* (2003). Prostate-specific deletion of the murine Pten tumor suppressor gene leads to metastatic prostate cancer. Cancer Cell *4*, 209-221.

Wang, X.S., Shankar, S., Dhanasekaran, S.M., Ateeq, B., Sasaki, A.T., Jing, X., Robinson, D., Cao, Q., Prensner, J.R., Yocum, A.K.*, et al.* (2011). Characterization of KRAS rearrangements in metastatic prostate cancer. Cancer Discov *1*, 35-43.

Watson, P.A., Arora, V.K., and Sawyers, C.L. (2015). Emerging mechanisms of resistance to androgen receptor inhibitors in prostate cancer. Nat Rev Cancer *15*, 701-711.

Weinstock, D.M., Nakanishi, K., Helgadottir, H.R., and Jasin, M. (2006). Assaying double-strand break repair pathway choice in mammalian cells using a targeted endonuclease or the RAG recombinase. Methods in enzymology *409*, 524-540.

Wu, X., Wu, J., Huang, J., Powell, W.C., Zhang, J., Matusik, R.J., Sangiorgi, F.O., Maxson, R.E., Sucov, H.M., and Roy-Burman, P. (2001). Generation of a prostate epithelial cell-specific Cre transgenic mouse model for tissue-specific gene ablation. Mechanisms of development *101*, 61-69.

Yang, H., Ye, D., Guan, K.L., and Xiong, Y. (2012). IDH1 and IDH2 mutations in tumorigenesis: mechanistic insights and clinical perspectives. Clin Cancer Res *18*, 5562-5571.

Zeng, L., Morinibu, A., Kobayashi, M., Zhu, Y., Wang, X., Goto, Y., Yeom, C.J., Zhao, T., Hirota, K., Shinomiya, K.*, et al.* (2015). Aberrant IDH3alpha expression promotes malignant tumor growth by inducing HIF-1-mediated metabolic reprogramming and angiogenesis. Oncogene *34*, 4758-4766.

Zhao, D., Lu, X., Wang, G., Lan, Z., Liao, W., Li, J., Liang, X., Chen, J.R., Shah, S., Shang, X.*, et al.* (2017). Synthetic essentiality of chromatin remodelling factor CHD1 in PTEN-deficient cancer. Nature *542*, 484-488.

Zhou, Z., Flesken-Nikitin, A., Corney, D.C., Wang, W., Goodrich, D.W., Roy-Burman, P., and Nikitin, A.Y. (2006). Synergy of p53 and Rb deficiency in a conditional mouse model for metastatic prostate cancer. Cancer Res *66*, 7889-7898.

Zhuang, M., Calabrese, M.F., Liu, J., Waddell, M.B., Nourse, A., Hammel, M., Miller, D.J., Walden, H., Duda, D.M., Seyedin, S.N.*, et al.* (2009). Structures of SPOP-substrate complexes: insights into molecular architectures of BTB-Cul3 ubiquitin ligases. Mol Cell *36*, 39-50.